Strathclyde Institute of Pharmacy and Biomedical Sciences

High Pressure Polymer Science; Routes to Drug Delivery

A thesis presented for the degree of

Doctor of Philosophy

in the Faculty of Science of the

University of Strathclyde

Abdullah Ali Al Balushi

July 2019

Declaration

This thesis is the result of the author's original research. It has been composed by the author and has not been previously submitted for examination which has led to the award of a degree.

Signed: 

Date: 3rd July 2019

Abstract

The area of high pressure is receiving great attention and being used to study a range of materials including metals, minerals, energetic materials and pharmaceuticals. Polymers are being increasingly used in pharmaceutical and biomedical applications. The main reason behind this is their physico-chemical characteristics that can be tuned to suit different applications. These characteristics can differ in different forms of the same compound. These forms can be obtained by different techniques including high pressure (Chapter 1). The work presented in this thesis has used high pressure techniques, including diamond anvil cells (DACs) and large volume press cell, to investigate pharmaceutical polymers and a model active pharmaceutical ingredient (ibuprofen). The change of materials under pressure was studied by *in-situ* Raman spectroscopy (Chapter 2). The first challenge faced in this project was fluorescence, which hinders Raman spectroscopy. Surface enhanced Raman spectroscopy (SERS) technique was adopted to improve the signal and overcome fluorescence. This was achieved successfully on weak Raman scattering amino acids and fluorescent polymers (Chapter 3). A range of commonly used polymers were studied under high pressure in DAC. Poly glycolic acid (PGA) and poly lactic acid (PLA) exhibited a similar phenomenon of moving from crystalline or semi-crystalline into a less ordered form between 4-5 GPa. Ethylcellulose (EC) and hydroxypropyl methylcellulose (HPMC) demonstrated a similar change at about 2-3 GPa (Chapter 4).

Both EC and HPMC were used as a platform for sustained release dosage forms in different ratios with ibuprofen. These formulations were mixed using resonant acoustic mixing technique and subjected to high pressure (0.8 GPa) before being tested for drug

release. The change in release patterns was mainly caused by the pressure transmitting medium (PTM) rather than the application of pressure (Chapter 5). Individual formulation components were used as received powders, treated by PTM at ambient pressure and subjected to 0.8 GPa before exploring their flowability. The PTM treatment and pressure has increased the flow function of polymers but not ibuprofen. The formulation blends were tested for flowability in powder and ambient pressure forms. Unlike individual components, the treated blends exhibited a decrease in flow function and increase in cohesion (Chapter 6).

Overall, this thesis demonstrates that the application of pressure, using DACs, on commonly used polymers in pharmaceutical applications does help in inducing phase transitions at different pressures. Adapting SERS technique has been successful in overcoming fluorescence in polymers and improving Raman signal in weakly scattering amino acids. The application of pressure, using large volume press, did not have a significant effect on release pattern of APIs from the tested formulations. The change was mainly due to the pressure transmitting medium. The effect of pressure was tested on powder flowability and found to increase polymers flowability but not ibuprofen.

Research outputs

1. Poster presentation. “Enhancing Raman Signalling Under High Pressure”. Presented at SciX 2016: The 43rd Annual North American Meeting of the Federation of Analytical Chemistry and Spectroscopy Societies (FACSS). Minneapolis, Minnesota, USA. 18-23 September 2016
2. Oral presentation. “Enhancing Raman Signalling under High Pressure”. Presented at the Research Day in SIPBS. 11th November 2016
3. Poster presentation. “The impact of high pressure on the release profile of ibuprofen from polymeric formulations”. Presented at SIPBS mini-conference. 10th May 2018

Acknowledgments

I would like to express my sincere gratitude to my first supervisor, Dr Iain Oswald, for giving me the chance to join his group. His supervision, guidance, support and encouragement throughout the project duration has been invaluable. This thesis would not have been possible without his support and advice on writing tactics.

I am highly indebted to my second supervisor, Professor Alexander Mullen, for his support and productive discussions around the formulation side of the project. I would like to thank the CMAC National Facility for allowing access to Raman microscopes, powder rheometer and other equipment when required. Special thanks are due to Professor Moustafa Fahmy, for his continuous supervision and professional mentorship throughout my career in hospital practice and academia. Special thanks to Dr Colin Hare of the University of Surrey for the discussions on powder flowability.

Special thanks to Dr Oswald's group members; Dr Martin Ward, Dr Ian Hutchison, Dr Lauren Connor, Suse Bebiano, Metinee Hemaprasertsuk (Bow) and Lloyd Farquhar for the help and advice in the lab and discussions around day-to-day issues. Other colleagues in 501R, especially John Totten, Dr Waleed Al Tuwayan, Dr Mohammed Obaid, Abiy Desta, Taufiq, Rachel and Natalie; thank you for the great company.

My deepest gratitude goes to my father, mother, brothers and sisters for their emotional support and encouragement to do my best in this course as well as supporting my family. Special thanks to my lovely wife, Rania, and my kids Renaad, Noor, Mohammed and Yousuf for their patience and their support during my PhD journey.

Finally, I would like to thank the Ministry of Health (Oman) for funding this PhD.

Contents

List of Figures

List of Tables

List of Abbreviations

µm	micrometre
AgNPs	Silver nanoparticles
AP	Ambient pressure
API	Active pharmaceutical ingredient
cm^{-1}	Wavenumber
DAC	Diamond anvil cell
EC	Ethylcellulose
ER	Extended release
FWHM	Full width half maximum
GPa	Giga Pascal
HME	Hot-melt extrusion
HP	High pressure
HPMC	Hydroxypropyl methylcellulose
IBP	Ibuprofen
LVP	Large volume press
meOH:etOH	Methanol : ethanol
mg	milligram
mm	millimetre
MR	Modified release
NSAID	Non-steroidal anti-inflammatory drug
P	Powder
PGA	Poly glycolic acid

PLA	Poly lactic acid
PLGA	Poly lactic-co-glycolic acid
PTM	Pressure transmitting medium
RAM	Resodyn acoustic mixer
SEM	Scanning electron microscopy
SERS	Surface enhanced Raman spectroscopy
UV	Ultraviolet

Chapter One: General Introduction

1.1 Introduction

The word “polymer” is a Greek word that means many parts and in chemistry, it is a molecular structure built from similar subunits called monomers and joined together by covalent bonds. A polymer is scientifically defined as “a molecule of high relative molecular mass, the structure of which essentially comprises the multiple repetitions of units derived, actually or conceptually, from molecules of low relative molecular mass” and the process of converting a monomer or a mixture of monomers into a polymer is defined as polymerization.[1] Polymers consisting of one type of subunits are called homopolymers whereas the ones consisting of several types of repeating units are called copolymers.

Polymers are classified as ‘macromolecules’ as they contain a large number of monomers i.e. thousands or tens of thousands. There are natural and synthetic polymers. The best known examples of natural ones are cotton, wool and silk and they are widely used in clothing materials. Collagen, lignin, proteins and deoxyribonucleic acid (DNA) are natural polymers as well and they are essential parts of living tissues.[2] Moreover, cellulose is the most abundant polymer of vegetal origin and basically it is a polysaccharide composed of cellobiose repeated units.[3] Natural rubber has been considered as a prehistoric polymer and has been in use since 1600 BC by Manati Indians to make balls and later to make waterproof garments and shoes.[3] On the other hand, there are many synthetic polymers like polyimides, polyamides, polyesters and rubber where the latter duplicates natural substances. They are used in daily life and that is mainly due to their physical properties, which is due to their low density and high strength.

1.1.1 Morphology of polymers

Polymers exist in different architectures and this gives an initial indication about their physico-chemical properties. Such architectures include linear, branched or cross-linked polymers. Linear polymers are regarded as water-soluble polymers and they can be either homopolymers or copolymers which also exist in different patterns like diblock, triblock, random or alternating copolymers (Figure 1.1). The name linear does not necessitate that the polymer is absolutely linear but it indicates the successive chemical bonds that hold the monomers together. Furthermore, they are the simplest architectural form and they have two main advantages, which are the formation of random coil structures and their ability to tailor multivalency, which is achieved by the introduction of functional co-monomers along their backbone.[4] Those advantages make them good candidates for drug-polymer conjugations.

Branched polymers also exist in different shapes, as they can be either hyper-branched, star-shaped, graft, dendrimer or a combination of more than one shape and this means that they have more than two end groups. Finally, the cross-linked polymers can be basically linear polymers but cross-linked, interpenetrating polymer networks or semi-interpenetrating polymer networks (Figure 1.1).

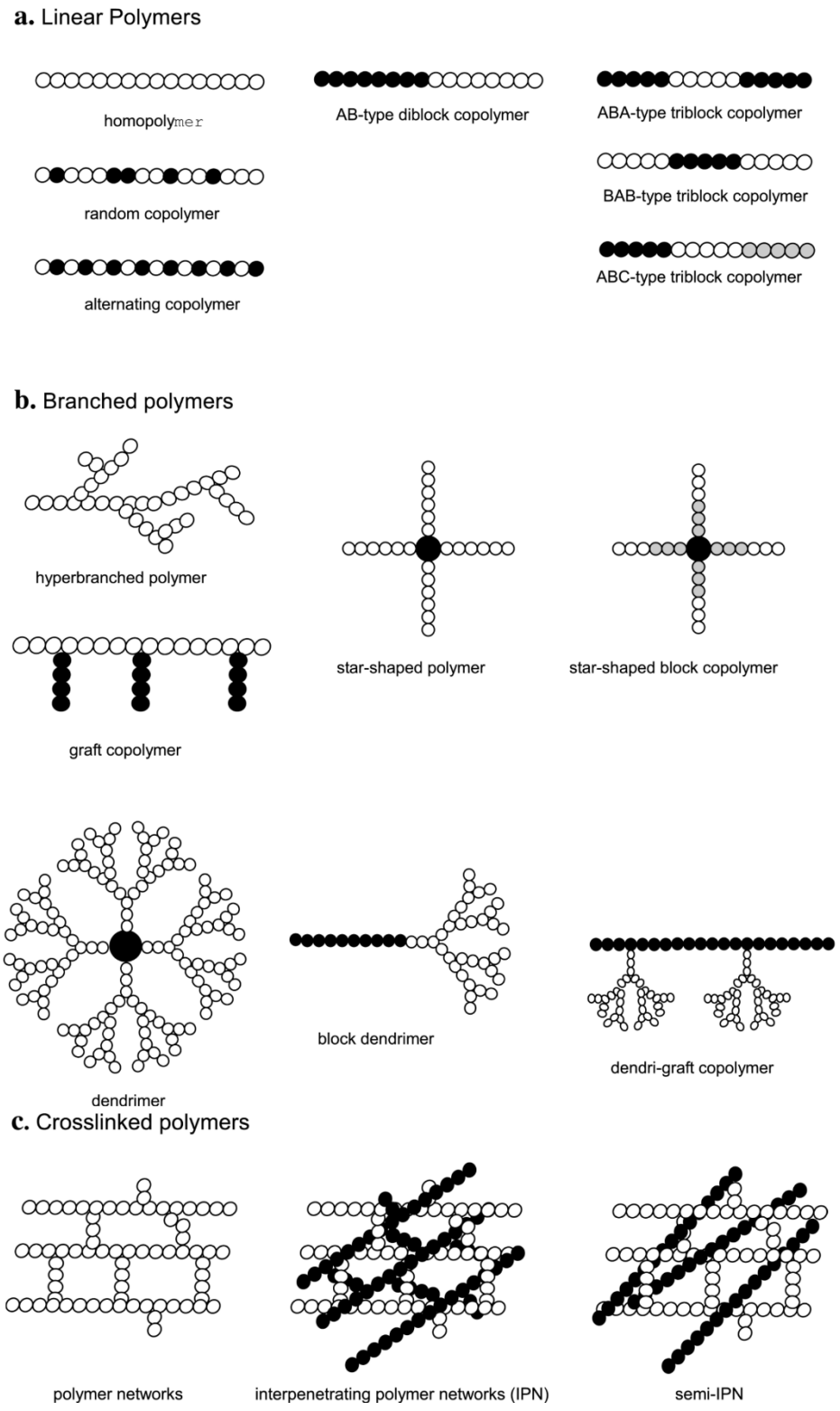

Figure 1.1 Architecture of polymers: (a) linear polymers, (b) branched polymers and (c) cross-linked polymers[4]

1.1.2 Nomenclature of polymers

There are three main ways of nomenclature of polymers. As with other chemicals, the official nomenclature is the one published by the International Union of Pure and Applied Chemistry (IUPAC) that uses the simplest repeating unit available in the polymer. Another way of nomenclature, which is the most common, is based on the name of repeating unit yielded from the monomer. Finally, generic names are also available and registered for commercial polymers e.g. aliphatic polyamides are called nylons. The commonly used nomenclature is poly (the repeating monomer) and an abbreviation is given to each (Table 1.1).[3]

Table 1.1 Examples of polymers nomenclature

Monomer unit	Name	Abbreviation
$(CH_2\text{-}CH_2)_n$	Polyethylene	PE
$[CH_2CH(CH_3)]_n$	Polypropylene	PP
$(CH_2\text{-}CHCl)_n$	Polyvinyl chloride	PVC
$(C_2H_2O_2)_n$	Polyglycolic acid	PGA
$(C_3H_4O_2)_n$	Polylactic acid	PLA

1.1.3 Pharmaceutical polymers

Proteins and peptides are known to be susceptible to enzymatic degradation as well as rapid clearance. This necessitates multiple drug administration which is inconvenient and risky in some instances where unexpected higher levels are attained. The concept of pegylation has optimised protein therapeutics. One of the best known examples for polymer-protein conjugates is Pegasys® that uses polyethylene glycol (PEG) as a polymer and interferon alfa-2a as the API. This development solved issues related to plasma half-life, immunogenicity and stability. Pegasys® contains pegylated interferon

alfa-2a used for the treatment of chronic hepatitis C. The active ingredient, interferon alfa-2a, is conjugated to a 40 kDa branched moiety of poly ethylene glycol. This combination is given once a week as it demonstrates enhanced solubility, increased resistance to enzymatic degradation, reduced immunogenicity, reduced clearance and sustained absorption, hence better clinical outcomes and improved patient compliance.[5]

1.1.4 Evolution of polymers as therapeutics

There has been an increased interest in polymers as therapeutics since the 1940s. In the early stages, the clinical interest was in polyvinylpyrolidone (PVP) as a plasma expander as well as dextran, whereas PVP-iodine as an antiseptic.[6] In the 1960s, the interest grew to include polymers in drug formulation i.e. polymer-drug conjugates and polymer-based drugs. The first polymeric formulation used PEG, where a protein conjugate was formulated. Research kept growing into lysosomotropic polymer-drug conjugates and block copolymer micelles. Some of these examples which progressed to the market are illustrated in Table 1.2.

Table 1.2 Examples of polymer therapeutics in the market

Class	Example	Composition
Polymeric drugs	Copaxone	Glu, Ala, Tyr copolymer
Polymeric sequestrants	Renagel	Phosphate binding polymer cholesterol binding
Polymer-protein conjugates	Zinostatin Stimaler	Styrene maleic anhydride-neocarzinostatin (SMANCS)
PEGylated proteins	Pegasys	PEG-Interferone α 2a
PEGylated-aptamer	Macugen	PEG-aptamer (apatanib)

When dendrimers appeared, in 1980s, they were expected to be more promising because of the theoretical advantages over linear and branched polymers i.e. multi-functionality, three dimensional structure and better control of composition but they faced difficulty to proceed to clinical development stage. One parenteral product, Gadomer-17, made its way to clinical stage and used as blood pool MRI agent but has been discontinued.[6] Moreover, a topical virocide formulation, Vivagel®, based on lysine dendrimer was developed as a preventive agent for human immuno-deficiency virus infection.

Research is on-going in this field and the regulatory authorities' requirements are being satisfied and more complex technologies including ligand targeting, multiple combination therapies and imaging agents are evolving. It is important for polymer therapeutics quality control to monitor their characteristics like size, architecture, molecular weight, polydispersity and charge density as variation may alter biological activity as well as other required physico-chemical properties including stability and release properties.

Although PEG & hydroxypropyl methacrylamide (HPMA) are non-biodegradable polymers, they are commonly used as polymeric platforms for many formulations. Despite the ability to tailor their molecular weight to make their elimination easier, they possess a risk of lysosomal storage syndrome (LSS) especially in patients who require high doses and chronic parenteral administration. On the other hand, the currently available PEGylated formulations are considered to be safe as they contain much less than the expected concentration that causes PEG toxicity i.e. the therapeutic window is very large and is approximately 600 folds.[7] This low possibility of toxicity has generated new trends of manufacturing for example, quality by design which

focuses on quality, safety and efficacy. It also encouraged chemists and scientists to look at different polymers as well as different architectural structures like star polymers, block copolymers, dendrimers and complex dendritic architectures and how they interact with biologicals and human body organs.[8]

Natural and synthetic biodegradable polymers like PGA, dextrin and hyaluronic acid, which are degraded by lysosomal cathepsin B, α-amylase and aluronidase respectively, have been explored clinically for various indications. Additionally, hydroxyethyl starch (HES) and dextran are approved for human use and they are currently used as a plasma expander and peritoneal dialysis solution. A study by Duncan et al.[9] aimed to explore a novel approach for polymer-protein modification called polymer-masking-unmasking-protein therapy (PUMPT) using a biodegradable polymer like dextrin in different molecular weights i.e. 7700 and 47200 g/mol. The group hypothesised that conjugating a protein with a biodegradable polymer would protect the protein and mask its activity until it reaches the required site of action where the activity will be reinstated by triggered degradation of the polymeric component. It will also protect it against premature proteolytic inactivation. The natural polymer, dextrin, was conjugated to either a model enzyme or a model receptor-binding ligand namely trypsin or melanocyte stimulating hormone (MSH). The dextrin used had a degree of succinoylation (9-32 mol %). The group found that the conjugate has reduced enzyme activity by 34-69% considering the molecular weight as well as the degree of succinoylation, the highest the better. Moreover, incubation with α-amylase, which is responsible for polymer degradation, has led to activity reinstatement.

Polymers have also been successfully used in oral drug delivery platforms as release extenders. This property is vital in drugs susceptible to degradation in the stomach or

fast clearance from the body. Many disease conditions including asthma, epilepsy and pain require a constant level of the API in the blood, so a better control of the disease is achieved hence better quality of life. Polypharmacy in patients with chronic conditions is becoming a big concern to healthcare professionals. Compliance and adherence to therapeutic regimens is decreasing in a number of patients either due to intolerance to side effects or due to the number of medicines taken and this issue may negatively impact therapeutic outcomes and in some diseases resistance to therapy or disease progression. The most currently available combinations of drugs to overcome this issue are for the treatment of cardiovascular diseases, cancer, diabetes mellitus, chronic infections like hepatitis C, immunological disease etc. The main aim of such combinations is to reduce or prevent resistance, improve compliance and to reach as many different targets as possible. The number of such formulations is on the rise and the following are examples PEG α-interferon & ribavirin which is used for the management of hepatitis C. Opaxio™ is another combination, which is in clinical trials for non-small cell lung cancer and glioma in combination with carboplatin and temozolamide respectively.

Opaxio™ is an example of polymer-drug conjugate and such formulations are expected to have several advantages compared to free drug. Some of these advantages are passive tumour targeting by enhanced permeability and retention (EPR) effect, improved solubility in biological fluids, reduced toxicity and a better ability to combat resistance.[10] There are four different types of combinations of polymer-drug conjugates (Figure 1.2). The first one is polymer-drug conjugate plus free drug, where a polymer carrying a single drug is administered with a low molecular weight drug or radiotherapy. The second type is polymer-drug conjugate plus polymer-drug

conjugate, where each polymer carries a single drug but administered together. In type three, a single polymeric carrier carries two drugs or more as this will assure that both drugs will undergo the same distribution. Finally, in type four, the system contains polymer-directed enzyme prodrug therapy (PDEPT) and polymer enzyme liposome therapy (PELT), where a single drug is carried in a polymer-drug conjugate combined with a polymer-enzyme conjugate (PDEPT) or the combination of a polymer-phospholipase conjugate (PELT) with a liposomal system. "The polymer–enzyme conjugate is responsible for drug release following cleavage of the drug–polymer linker (in PDEPT) or disruption of the liposomal system (in PELT)."[10]

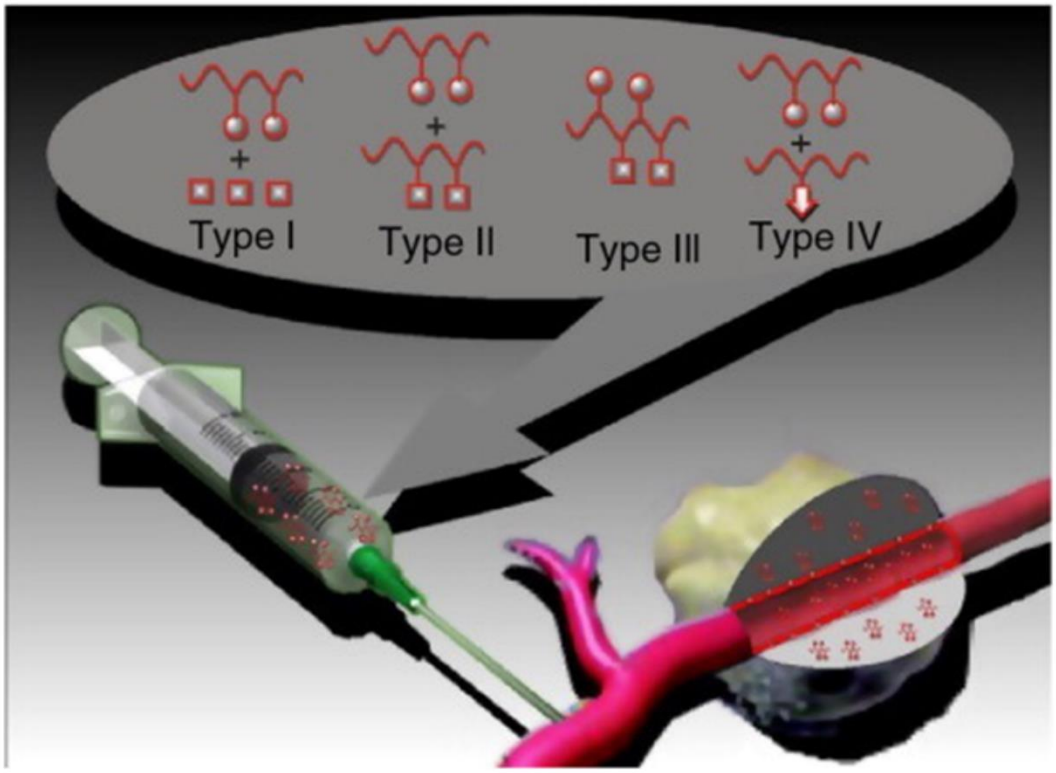

Figure 1.2 Schematic representation of the different types of polymer-based combination therapy for targeted drug delivery by the EPR effect (reproduced from reference 10)

There has been an increase in the number of approved polymeric therapeutics as well as the number of declined applications. It is not easy to predict the future but there is rapid progress in scientific advances in the area of medicines development and once a

product makes it to the market other products will start to follow. Advances in chemistry like reversible addition-fragmentation chain transfer polymerisation (RAFT) and atom transfer radical polymerisation (ATRP) in linear synthetic polymers and "one-pot" synthesis technique in hyper branched polymers are expected to move the polymers' industry forward as RAFT and ATRP technologies are known to have control over average molecular weight, reduce heterogeneity and to have better control over polydispersity.[6] Development in this field is on-going and new novel techniques like peptidyl linkers, which are designed to be cleaved by the tumour-associated protease legumain, bioresponsive coiled-coil peptide linkers, self-immolative linkers and bioreductive linkers were launched.[6]

1.1.5 The pharmacokinetics of polymers

The main aim of polymer therapeutics, polymer conjugates, is to improve the delivery of certain drugs as well as their bioavailability. The concept of polymer therapeutics is to protect the body form the drug i.e. protecting the stomach from irritant drugs, and to protect the drug from the body as well as improving therapeutic index of drugs in therapeutic areas including cancer, pain, inflammation and infections.[11] The use of polymers as drug carriers has been encouraged especially in low molecular weight drugs, which are administered via parenteral routes and consequently exhibit non-specific pharmacokinetic profile i.e. not the wanted distribution, shorter circulation and faster elimination, which in turn leads to side effects and sub-therapeutic levels and subsequently resistance and treatment failure.

Therapeutic polymers systems usually contain three main groups, namely material, excipient and molecule. The material group, such as polyesters, polyorthoesters and

polyanhydrides, is used for the site-specific drug delivery and release modification of drugs i.e. continuous or prolonged release whereas the excipient group contains coatings (methylcellulose), adhesion enhancers (Hydroxyethylcellulose) and formulation stabilizers (PEG). Moreover, the molecule group contains physiologically soluble drug or protein-polymer conjugates.[12] Enhanced permeability and retention (EPR) is one of the most wanted advantages of polymer-drug conjugates and this property is very useful especially in cancer as angiogenic tumours have vasculature that is disorganized with discontinuous endothelium. This causes macromolecules to permeate easily and reach their target and this is known as passive targeting.[11] Nevertheless, there are limitations to this approach like variable permeability in different tissue, different heterogeneity of cancerous tissues and low cellular uptake after extravasation. However, these limitations can be overcome by the involvement of receptor-ligand moiety and this is known as active targeting.[13]

1.1.6 The use of polymers in biomedical applications

Polymers have been used for different biomedical applications and that is mainly due to the different physico-chemical properties they possess including possessing a degradation time coinciding with their function, having appropriate mechanical properties for their intended use and having appropriate processability and permeability properties. These properties depend on polymer's molecular weight, glass transition temperature, crystallinity etc.

1.1.6.1 Gene transfection

Extensive research is on-going for more than two decades about the potential use of polymers as non-viral vectors to correct genetic disorders by designing safe vectors

for efficient gene delivery. Poly-cations, which form the majority of non-viral vectors for gene delivery, have some issues that hamper their use like difficulty to synthesize, sophisticated purification, lack of responsiveness, low efficiency and high toxicity.[14] Dendrimers and hyperbranched polymers are considered as better vectors for gene delivery than linear polymers because of their branching nature but that is still argued. A study using hyperbranched poly amido amines (PAA), with the same repeating units but different branched architecture, as vectors found a dramatic improvement in buffering capacity, DNA condensation capability, gene transfection and reduced cytotoxicity.[15]

1.1.6.2 Protein delivery

Replacement of dysfunctional proteins, in some diseases, is a modern concept in treating such diseases. Nonetheless, proteins are very unstable as they are prone to proteases and have low bioavailability profile in the digestive and circulatory systems. Drug delivery systems like hydrogels, nanotubes, nanocapsules etc. have been used to overcome those issues and details about such systems are beyond the scope of this review.

Hydrogels have advantages of wider availability, easy to prepare and their mechanical properties are tuneable. A study using high-water content cellulose based supramolecular hydrogels including polyvinyl alcohol as a polymer was conducted to evaluate the release proteins like lysozyme and bovine serum albumin from hydrogels as well as the effect of protein molecular weight and polymer loading on the release rate.[16] A burst release, which lasted shortly (1 week), was found followed by a very sustained release for up to 160 days from the hydrogel containing 1.5% polymer. This

finding is a good driving reason for further studies in protein delivery using polymeric constituents.

1.1.6.3 Tissue engineering

Tissue engineering is a very promising concept in modern medicine as it has the potential to regenerate malfunctioning tissues and organs.[14] Polymers are considered as the backbone of tissue engineering as cells are cultured on polymeric matrices. Polymers are usually selected based on their properties like chemistry, shape, solubility, molecular weight, hydrophilicity/hydrophobicity, structure and erosion. Many polymers are prepared by different methods for different applications like poly lactide-co-glycolide (PLGA), that is prepared as a biodegradable porous scaffold fabrication to be used for bone and cartilage tissue engineering. On the other hand, PLGA prepared using fibrous scaffold fabrication is used in drug delivery (Lupron Depot used in prostate cancer), wound healing and soft tissue synthetic skin.[17]

1.2 High pressure

Pressure is defined as the force applied to an object per unit area (p=F/A) and it reduces the volume of systems applied to especially liquids and soft solids. Size reduction occurs because the intermolecular distance decreases and subsequently electronic structure changes. The area of high pressure was mainly the interest of geoscientists, who were interested in minerals and rocks formation, and physicists who were looking into the matter of Earth and the Solar System.[18] Later, it became a major interest for chemists and pharmaceutical scientists when they realized polymorphism and phase transition of compounds when being exposed to high pressure and sometimes the development of new crystal structures. The application of pressure also facilitates the

entry of solvents into porous materials as found by Moggach et al. in their work on metal-organic frameworks at 0.78 GPa.[19] They also found that further increase in pressure (1.35 GPa) has decreased the volume of metal-organic frameworks.

1.2.1 Diamond anvil cells (DAC)

Diamond is not only known for compression strength but also for its transparency properties to electromagnetic spectrum. The first DAC (Figure 1.3) was made by Charlie Weir in 1958 in the National Bureau of Standards laboratory (NBS) in Washington.[20] The idea of DAC emerged when AlvinVan Valkenburg was trying to look at his compressed sample between two diamond cells using infrared beam, and was not sure if diamond faces were parallel. He had to check this by a microscope. He found that diamond faces were not parallel and importantly he spotted the area of high pressure as sample looked different. This discovery made it possible to observe phase and colour changes and recrystallization. Nonetheless, the science of high pressure has been in practice prior to the invention of DAC using Be cylinders and diamond in a piston-cylinder arrangement.[21]

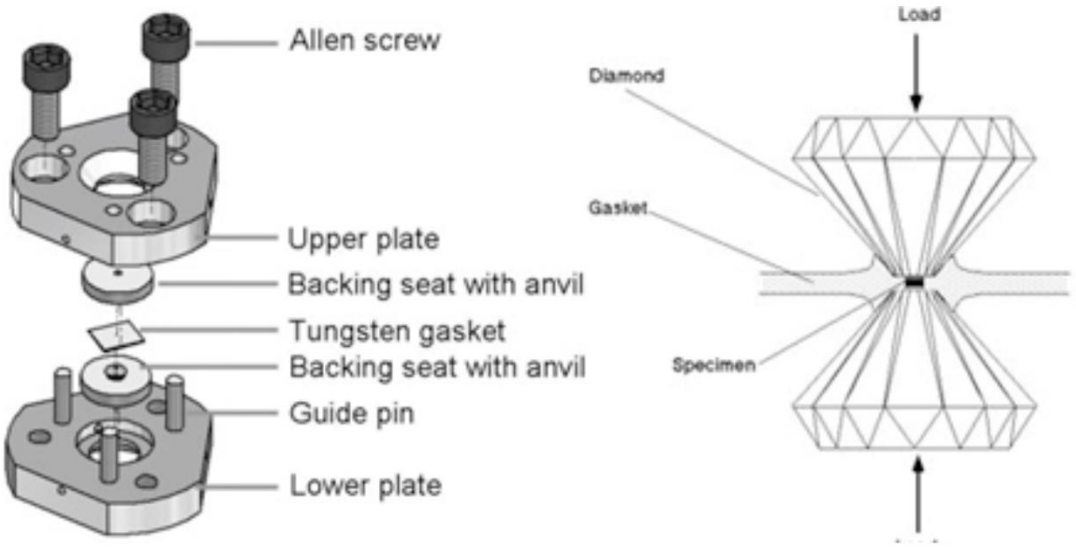

Figure 1.3 Schematic diagram of a diamond anvil cell (DAC)[22]

Initially, pressure was measured using calibrated crystalline materials parameters, which was mixed with the studied sample. This was NaCl which was suitable for X-ray diffraction users but not for others. In 1971, scientists at NBS decided to use ruby, which could fluoresce and its fluorescence wavelength emission could be calibrated. Ruby has an additional advantage of having two peaks in its spectrum and this helps in determining if the pressure is hydrostatic. One disadvantage of ruby is that it is not a good option for measuring pressure at high temperature as temperature causes fluorescence i.e. fluorescence peaks broaden and have a weaker intensity. Gold is preferred for those using X-ray diffraction as pressure and temperature effects on its lattice parameters are well documented. It is also chemically inert and scatters X-rays.[20]

DACs and large volume presses are widely used devices for subjecting materials to high pressure. DACs, in their beginning, used to induce pressure up-to 3 GPa whereas today it can induce up-to 100 GPa or more[23] while the large volume press can induce

up-to 0.8 GPa. Despite the small sample volume that a DAC can accommodate (10^{-3}-10^{-5} mm^3), it remains the most reliable technique to induce high pressure especially when temperature becomes an issue.[24] High pressure is one of the most important ways in detecting drug polymorphism and this is mainly due to hydrogen bonds dynamics, squeezing and stretching. Moreover, the following facts should be considered when using high pressure to form polymorphs:[25]

- Different forms are obtained from different polymorphs at same conditions such as polymorphs of glycine.[26]
- Different forms are formed on compressions and on decompression and such transformations may not necessarily be reversible (paracetamol).[27]
- Powder samples and single crystals are affected differently by high pressure (L-serine).[28]
- The speed of compression and decompression yields different forms and the time the sample was held at certain pressure (β-alanine).[29]
- Pressure transmitting medium also affects transformation (chlorpropamide).[30]

In this thesis, pressure is defined using the unit gigapascals (GPa), as 1 GPa is equivalent to 9869.2 standard atmosphere (atm).

1.2.2 The importance of polymorphism

Polymorphism is the ability of a compound to exist in different structures and it is inevitable. The International Conference on Harmonisation (ICH) defined polymorphic form as some new drug substances exist in different crystalline forms, which differ in their physical properties. Polymorphism may also include solvation or hydration products (also known as pseudo-polymorphs) and amorphous forms.[31] This is a very important issue in pharmaceutical industry as different polymorphs may exhibit different physicochemical properties such as density, stability, solubility, melting point and dissolution rate, which are important for pharmaceutical compounds. Changes in these properties may hinder pharmaceutical compounds from reaching the market and that is mainly due to safety and efficacy concerns.[32] The production of different polymorphs can be achieved using different techniques and the following are some examples:[32]

- Crystallisation from single/mixed solvents (acetaminophen).[33]
- Crystallisation from the melt (nifedipine).[34]
- Solid state polymorphic transformation (flufenamic acid and mefenamic acid).[35]
- Mechanical activation of solid substances (famotidine).[36]
- Crystallisation in the presence of tailor-made additive (tolfenamic acid).[37]
- Laser induced crystallisation (urea).[38]
- Exposure to vapour or humidity (acyclovir).[39]
- Structure prediction (dihydroxybenzoic acid).[40]

Polymorphs and solvates may have different important properties, like bioavailability, hence very important to differentiate. For example, a new form of piracetam (form V) was formed by the recrystallization of methanolic and aqueous solutions of piracetam (form II) under high pressure in a DAC at pressures of 0.07-0.40 GPa.[41] Another example of high pressure crystallization is the formation of paracetamol II from paracetamol I and shown to be the a thermodynamically stable phase at high pressure.[25] Oswald et al. worked on obtaining elusive crystalline forms of maleic acid, malonamide and paracetamol in a reproducible manner using high pressure. They found that high pressure formed significantly higher crystal density for the three compounds at similar temperatures and this was calculated using X-ray diffraction. For instance, they found that form II of maleic acid is thermodynamically stable at high pressure. Although the molecules used are not as complex as many modern pharmaceutical compounds, they proved that high pressure has the potential to improve our control on elusive polymorphs as well as solvates.[42]

One of the important polymorphism problems faced the already marketed pharmaceutical formulations is the case of ritonavir. It was produced as Norvir® Capsules by Abbott. The production was brought to a halt after producing 240 lots. This was due to the sudden change in the physical properties of the product. The main problem was the change in the crystal form of ritonavir. This change affected the solubility and as a result reduced the bioavailability to less than 5%. [43,44]

The development of new chemical entities (NCE) is ongoing but poor water solubility is becoming a big concern to the pharmaceutical industry as about 40% of those have poor water solubility hence will have a poor oral bioavailability.[45] There are certain formulation techniques to overcome this problem like the use of solvent mixtures but

limited to other physicochemical properties of the chemical entities. Micronisation is another approach used to reduce particle size to µm scale thus increasing surface area, but again it does not overcome the problem in all cases. Moreover, nanonisation is also used to produce particle size below 1µm i.e. ideally range between 200 – 500 nm. The most widely available and preferable dosage form is tablet. The preparation of tablets involves many steps like milling and compressing. Those two processes involve the use of pressure, within the range of 40 – 200 MPa for less than a second, and temperature, which may alter the crystal structure of such compounds and subsequently yield different polymorphs that may be required or not. From that, high pressure is considered an important tool for identifying new polymorphs and for understanding the interactions and processes involved in changing from one form to another.[23]

1.3 Research Hypothesis and Aims

The hypothesis to be tested in this thesis is that the application of high pressure to pharmaceutical polymers and API leads to changes in their physico-chemical properties.

The application of pressure is another potential tool for obtaining novel polymorphs of pharmaceutical compounds. The main aim of this research is to investigate the effect of high pressure application, using DACs and LVP, on commonly used pharmaceutical and biomedical polymers using Raman spectroscopy, which is an important analytical tool in determining crystallinity of compounds especially lattice vibrations in low energy phonon region. Some polymers are fluorescent and this hinders Raman

spectroscopy as fluorescence emission competes with Raman scattering. The adoption of surface enhanced Raman spectroscopy (SERS) technique under high pressure will be explored for fluorescent materials and weak Raman scaterers (Chapter 3).

The application of high pressure on pharmaceutical polymers including PLA, PGA, EC and HPMC and an API (ibuprofen) will be tested by monitoring changes in their Raman spectra as pressure increased (Chapter 4).

Formulations containing different ratios of commonly used pharmaceutical polymers like ethylcellulose and hydroxypropyl methylcellulose and a model API (ibuprofen) will be subjected to high pressure (0.8 GPa) and the impact of high pressure on their release profile will be explored (Chapter 5).

Finally, the impact of pressure on polymers and ibuprofen powder flowability, using 1 mL shear cell module, will be explored as stand-alone compounds and within formulations with different ratios (Chapter 6).

1.4 References

[1] Jenkins AD, Kratochvil P, Stepto R, Suter U. Glossary of basic terms in polymer science. Pure and Applied Chemistry, 1996 Dec, Vol68(12), 2287-2311.

[2] Brauman JI. Polymers. Science (New York, NY), 22 1991, Vol251(4996), 853.

[3] Denis JPL. Biomedical and pharmaceutical polymers. Gilles P, Christine V, editors. London: London: Pharmaceutical Press; 2011.

[4] Qiu L, Bae Y. Polymer Architecture and Drug Delivery. Pharmaceutical Research, 2006, Vol23(1), 1-30.

[5] Rajender Reddy K, Modi MW, Pedder S. Use of peginterferon alfa- 2a (40 KD) (Pegasys ®) for the treatment of hepatitis C. Advanced Drug Delivery Reviews. 2002;54(4):571-86.

[6] Duncan R, Vicent MJ. Polymer therapeutics-prospects for 21st century: the end of the beginning. Advanced drug delivery reviews 2013, Vol65(1), 60-70.

[7] PEGylated Protein Drugs: Basic Science and Clinical Applications. Veronese F, editor. Basel: Birkhäuser Basel, Basel; 2009.

[8] Barz M, Luxenhofer R, Zentel R, Vicent MJ. Overcoming the PEG-addiction: well-defined alternatives to PEG, from structure property relationships to better defined therapeutics. Polymer Chemistry, 2011, Vol2(9), 1900-1918.

[9] Duncan R, Gilbert H, Carbajo R, Vicent M. Polymer masked- unmasked protein therapy. 1. Bioresponsive dextrin-trypsin and -melanocyte stimulating hormone conjugates designed for alpha-amylase activation. Biomacromolecules, 2008 Apr, Vol9(4), 1146-1154.

[10] Greco F, Vicent MJ. Combination therapy: Opportunities and challenges for polymer–drug conjugates as anticancer nanomedicines. Advanced Drug Delivery Reviews, 2009, Vol61(13), 1203-1213.

[11] Haag R, Kratz F. Polymer therapeutics: concepts and applications. Angewandte Chemie International Edition. 2006 Feb 13;45(8):1198-215.

[12] Godwin A, Bolina K, Clochard M, Dinand E, Rankin S, Simic S, et al. New strategies for polymer development in pharmaceutical science--a short review. The Journal of pharmacy and pharmacology 2001, Vol53(9), 1175-84.

[13] Markovsky E, Baabur-Cohen H, Eldar-Boock A, Omer L, Tiram G, Ferber S, et al. Administration, distribution, metabolism and elimination of polymer therapeutics. Journal of controlled release: official journal of the Controlled Release Society, 20 2012, Vol161(2), 446-60.

[14] Dong R, Zhou Y, Zhu X, Lu Y, Huang X, Shen J. Functional supramolecular polymers for biomedical applications. Advanced Materials, 21 January 2015, Vol27(3), 498-526.

[15] Wang R, Zhou L, Zhou Y, Li G, Zhu X, Gu HC, et al. Synthesis and Gene Delivery of Poly (amido amine) s with Different Branched Architecture. Biomacromolecules, 2010 Feb, Vol11(2), 489-495.

[16] Appel EA, Loh XJ, Jones ST, Dreiss CA, Scherman OA. Sustained release of proteins from high water content supramolecular polymer hydrogels. Biomaterials, 2012, Vol33(18), 4646-4652.

[17] Brahatheeswaran D, Yasuhiko Y, Toru M, Kumar DS. Polymeric Scaffolds in Tissue Engineering Application: A Review. International Journal of Polymer Science, Vol 2011 (2011).

[18] Katrusiak A. High-pressure crystallography. Acta crystallographica Section A, Foundations of crystallography 2008, Vol64(Pt 1), 135-48.

[19] Graham AJ, Allan DR, Muszkiewicz A, Morrison CA, Moggach SA. The Effect of High Pressure on MOF- 5: Guest- Induced Modification of Pore Size and Content at High Pressure. Angewandte Chemie International Edition. 2011;50(47):11138-41.

[20] Bassett W. Diamond anvil cell, 50th birthday. High Pressure Research, 2009, Vol29(2), CP5-186.

[21] McMahon MI. High-pressure crystallography. Topics in current chemistry, 2012, Vol315, 69-109.

[22] Crystal.chem.ed.ac.uk. (2019). High Pressure Crystallography | Crystal Chemistry. [online] Available at:http://www.crystal.chem.ed.ac.uk/research-themes/high-pressure-crystallography [Accessed 1 Mar. 2015].

[23] Fabbiani FPA, Pulham CR. High-pressure studies of pharmaceutical compounds and energetic materials. Chem. Soc. Rev., 2006,35, 932-942

[24] Schettino V, Bini R. Molecules under extreme conditions: Chemical reactions at high pressure. Physical Chemistry Chemical Physics, 2003, Vol5(10), 1951-1965.

[25] Boldyreva E. High-pressure polymorphs of molecular solids: When are they formed, and when are they not? Some examples of the role of kinetic control. Crystal Growth & Design, 2007 Sep, Vol7(9), 1662-1668.

[26] Perlovich GL, Hansen LK, Bauer-Brandl A. The polymorphism of glycine. Thermochemical and structural aspects. Journal of thermal analysis and calorimetry. 2001 Dec 1;66(3):699-715.

[27] Boldyreva E, Shakhtshneider T, Ahsbahs H, Sowa H, Uchtmann H. Effect of high pressure on the polymorphs of paracetamol. Journal of thermal analysis and calorimetry. 2002 May 1;68(2):437-52.

[28] Kolesnik EN, Goryainov SV, Boldyreva EV. Different behavior of L-and DL-serine crystals at high pressures: phase transitions in L-serine and stability of the DL-serine structure. In Doklady Physical Chemistry 2005 Sep 1; Vol. 404, No. 1-3, 169-172. Nauka/Interperiodica.

[29] Boldyreva, E.V., Goryainov, S.V., Seryotkin, Yu.V., Ahsbhas, H., Dmitriev, V.P. Pressure-induced phase transitions in the crystals of *β*-alanine, Vestnik NGU, Ser. Fizika (Proceed. NSU, Series Physics), 2(2) (2007) 30–35.

[30] Boldyreva EV, Dmitriev V, Hancock BC. Effect of pressure up to 5.5 GPa on dry powder samples of chlorpropamide form-A. International journal of pharmaceutics. 2006 Dec 11;327(1-2):51-7.

[31] Specification: Test procedures and acceptance criteria for new drug substances and new drug products: chemical substances Q6A, part of U. S. Food and Drug Administration. [Online] http://www.ich.org/fileadmin/Public_Web_Site/ICH_Products/Guidelines/Quality/Q6A/Step4/Q6Astep4.pdf (accessed 03.10.17).

[32] Lee EH. A practical guide to pharmaceutical polymorph screening & selection. Asian Journal of Pharmaceutical Sciences. 2014;9(4):163-75.

[33] Peterson ML, Morissette SL, McNulty C, Goldsweig A, Shaw P, LeQuesne M, Monagle J, Encina N, Marchionna J, Johnson A, Gonzalez-Zugasti J. Iterative high-throughput polymorphism studies on acetaminophen and an experimentally derived

structure for form III. Journal of the American Chemical Society. 2002 Sep 18;124(37):10958-9.

[34] Zhu L, Wong L, Yu L. Surface- enhanced crystallization of amorphous nifedipine. Molecular pharmaceutics. 2008;5(6):921-6.

[35] Lee EH, Byrn SR. Stabilization of metastable flufenamic acid by inclusion of mefenamic acid: Solid solution or epilayer? Journal of Pharmaceutical Sciences. 2010;99(9):4013-22.

[36] Lin SY. An overview of famotidine polymorphs: solid-state characteristics, thermodynamics, polymorphic transformation and quality control. Pharmaceutical research. 2014 Jul 1;31(7):1619-31.

[37] Mattei A, Li T. Polymorph formation and nucleation mechanism of tolfenamic acid in solution: an investigation of pre-nucleation solute association. Pharmaceutical research. 2012 Feb 1;29(2):460-70.

[38] Zaccaro J, Matic J, Myerson AS, Garetz BA. Nonphotochemical, laser-induced nucleation of supersaturated aqueous glycine produces unexpected γ-polymorph. Crystal Growth & Design. 2001 Jan 1;1(1):5-8.

[39] Terada K, Kurobe H, Ito M, Yoshihashi Y, Yonemochi E, Fujii K, et al. Polymorphic and pseudomorphic transformation behavior of acyclovir based on thermodynamics and crystallography. Journal of Thermal Analysis and Calorimetry. 2013;113(3):1261-7.

[40] Braun DE, Karamertzanis PG, Price SL. Which, if any, hydrates will crystallise? Predicting hydrate formation of two dihydroxybenzoic acids. Chemical communications (Cambridge, England). 2011;47(19):5443-5.

[41] Fabbiani FPA, Allan D, David W, Davidson A, Lennie A, Parsons S, et al. High-pressure studies of pharmaceuticals: An exploration of the behavior of piracetam. Crystal Growth & Design, 2007 Jun, Vol7(6), 1115-1124.

[42] Oswald I, Chataigner I, Elphick S, Fabbiani FPA, Lennie A, Maddaluno J, et al. Putting pressure on elusive polymorphs and solvates. Crystengcomm, 2009, Vol11(2), 359-366.

[43] Bauer J, Spanton S, Henry R, Quick J, Dziki W, Porter W, et al. Ritonavir: an extraordinary example of conformational polymorphism. Pharmaceutical research. 2001;18(6):859-66.

[44] Bauer JF. Polymorphism--a critical consideration in pharmaceutical development, manufacturing, and stability. (Pharmaceutical Solids). Journal of Validation Technology. 2008;14(5):15.

[45] Keck CM, Müller RH. Drug nanocrystals of poorly soluble drugs produced by high pressure homogenisation. European Journal of Pharmaceutics and Biopharmaceutics, 2006, Vol62(1), 3-16.

Chapter Two: General Methods

2.1 Diamond anvil cell

The studies in this thesis made use of Merrill-Basset diamond anvil cells (DACs). Merrill-Basset DACs are a self-contained, convenient method to apply pressure to materials as they are small and do not require the use of further equipment, for example, a gas supply is required to drive a membrane-driven DACs. The basis of the DAC is the same despite the different methods of pressure generation. They are used to maintain materials at high hydrostatic pressure. DACs contain two opposed gem quality diamonds, which are securely glued into backing seats placed within upper and lower plates (Figure 2.1). The backing seats were traditionally made of beryllium due to the relatively low scatter of X-ray radiation. However, the toxicity of the beryllium was a hindrance and new backing seats and shape of diamonds has allowed the use of tungsten carbide as the backing seat material.

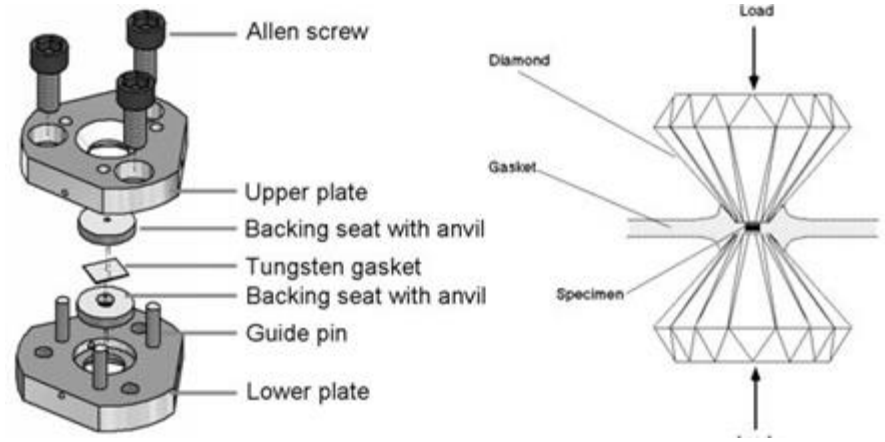

Figure 2.1 Schematic diagram of a diamond anvil cell. Two opposing diamonds compress a metallic gasket between the culets of the diamonds. The gasket contains a hole that hosts the sample, pressure transmitting medium and ruby chips to measure pressure. [1]

Diamond is used for two main reasons: 1) it is one of the hardest known materials; and 2) it is transparent to a wide range of electromagnetic radiation. The range of electromagnetic radiations permitted by the transparent diamonds allows many

techniques to be used to study materials under high pressure conditions. Raman, infra-red spectroscopy and X-ray diffraction can all be performed, making it easier to study phase transformations and vibrational excitations of the studied compounds.

Another component that is required is the gasket, which is placed between the diamond culets. The gasket is an essential part of the assembly as it provides an encapsulated chamber to house the compound under study. This gasket usually comes in a width of 200 – 250 µm. Prior to drilling, the gasket is pre-indented by pushing the diamonds against each other to ~ 90 - 100µm. The thickness is usually measured using a micrometre with small measuring tips. Pre-indentation is an important step for high pressure studies, as it gives better support to the diamond tips during the high pressure experiment. By reducing the thickness of the gasket the material hardens which will subsequently increase the pressure obtainable for the experiment. This step also allows the gasket to deform plastically and extrude outwards as this will later form a ring around the anvils to support the flank region. At the centre of the indentation, a hole of 300 µm is drilled by an electro-discharge-machine Boehler microDriller®. Electro discharge drillers are preferred in such applications as they produce clean boreholes with no burrs. Moreover, the hole size should be in the range of 1/3 to 1/2 of the culet diameter in order the gasket remains stable during high pressure.[2] Parameters like indent depth and hole size play an important role in high pressure studies. Thick gaskets are known to give larger sample space whereas thin gaskets give less space but allow higher pressures to be reached, so it is recommended to pre-indent gaskets to a thickness such that there will be a minimum of further thinning during the experiment.[3] The assembly of the gasket between the diamond anvils and the principle of generating pressure is presented in Figure 2.2.

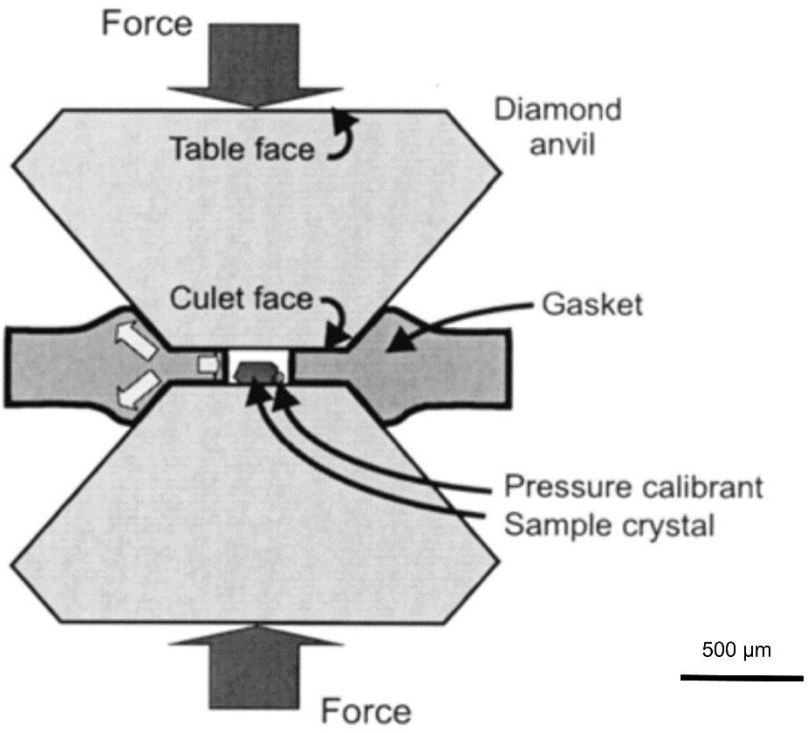

Figure 2.2 The assembly of the gasket between the opposed diamonds. The sample chamber is in the middle of the gasket where the sample, pressure transmitting medium ruby chips are placed. (Figure reproduced from reference 2).

The gasket is placed on the lower diamond and the position of the gasket should be known to the user by having marks on both the gasket and the backing plate. The DAC is assembled by placing the upper plate in the correct orientation and securing it with Allen screws. The screws are tightened equally until felt secured. It is then placed under the microscope, where the gasket can be seen through the upper diamond as a dark ring, which can be used to estimate the depth of the indentation. The screws are equally tightened in order to maintain a uniform indentation. The DAC is disassembled and the gasket is removed. The indentation is measured using a micrometre and the height should be between 90 and 100 µm.

After that, the gasket is placed in the drilling well of the micro-driller, where it is secured by the well cap. The space between the indent and the previously marked corner should be in the centre of the crosshairs in the well cap. Propanol, which is a dielectric fluid, is used to fill the well. Then, the drill well is moved carefully under the drill while taking care not to touch the drill bit. A pilot hole is drilled initially to ensure that that the drill is aligned to the crosshairs of the eyepiece so as to avoid misalignment, which will cause further issues i.e. indentation off-centre drilling. Once satisfied with the accuracy of the pilot hole, the gasket is moved until the indent is in the centre of the crosshairs and a hole is drilled. It is very important for the hole to be drilled at the centre of the indentation as off-centre holes may not remain stable for the study and extrude asymmetrically because of the differential stress.[2] Then, the gasket is removed and remounted on the lower diamond. The user should make sure that the hole is on the centre of the diamond's culet by moving the gasket to see the facets of the diamond around the culet. Using the correct orientation, the upper plate should be fixed over the lower one and checked under the microscope for transparency. Once the light is seen through the centrally positioned hole, the upper plate is removed. One or two ruby chips are placed at the side of the hole. Ruby chips are used to measure *in-situ* pressure by the ruby fluorescence method.[4] A single crystal or powdered sample is loaded into the sample chamber depending on the experiment. The upper plate is placed in position with Allen screws on while leaving a space to for the user to add the pressure-transmitting medium (PTM). It is imperative to make sure the sample is fully surrounded by PTM and in case of powders, there should be a space for the PTM and the sample should be totally wetted in order to maintain hydrostasticity. This can be done by making an indent in the powder sample using a fine needle. Finally, the upper

plate is closed and screws tightened in order to seal the system. The cell is checked again under the microscope for the presence of the added components, which can be done optically as the PTM will have higher refractive index than air. There is a common risk of having a bubble in the sample chamber trapped either between crystals or between the sample and the hole wall. Depending on the size of the bubble pressure can be applied to dissolve the gas into the medium or if it is too large reloading is required.

2.2 Large volume press

The large volume press (LVP) is a pressure cell that can hold a larger quantity of sample than the DAC (i.e. 500 mg, depending on particle size); however, there is the limitation of the maximum pressure that can be achieved. Pressure up to 10-100 GPa can be applied to samples using a Diamond anvil cell but the large volume press is limited to 0.8 GPa. It was designed at the Centre for Science at Extreme Conditions at the University of Edinburgh. The main body of the cell is a thick walled cylinder made of BeCu alloy (BERYLCO-25) with inner diameter of 10 mm, external diameter of 35 mm and height of 127 mm. The cell body contains two M22x1 threaded seat at the top and at the bottoms with depths of 35 mm and 14 mm respectively. The bottom thread is for the bottom nut which closes the cell whereas the top thread is for the retaining nut which clamps and holds the piston in place. The components of the LVP cell and a schematic diagram are presented in Figure 2.3 and Figure 2.4 respectively.

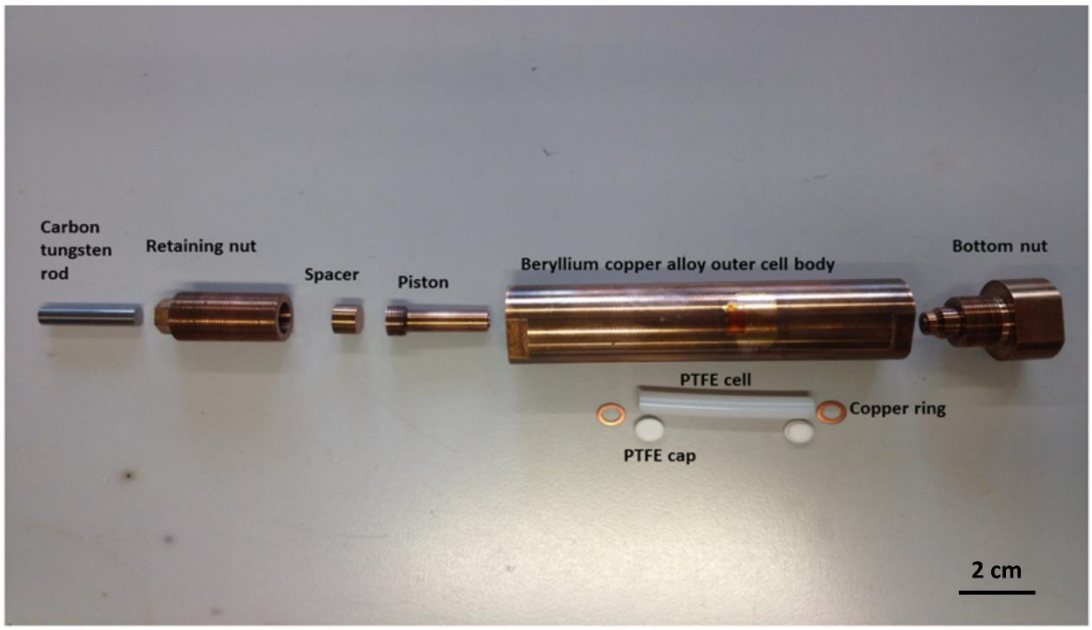

Figure 2.3 Large volume press cell and its components

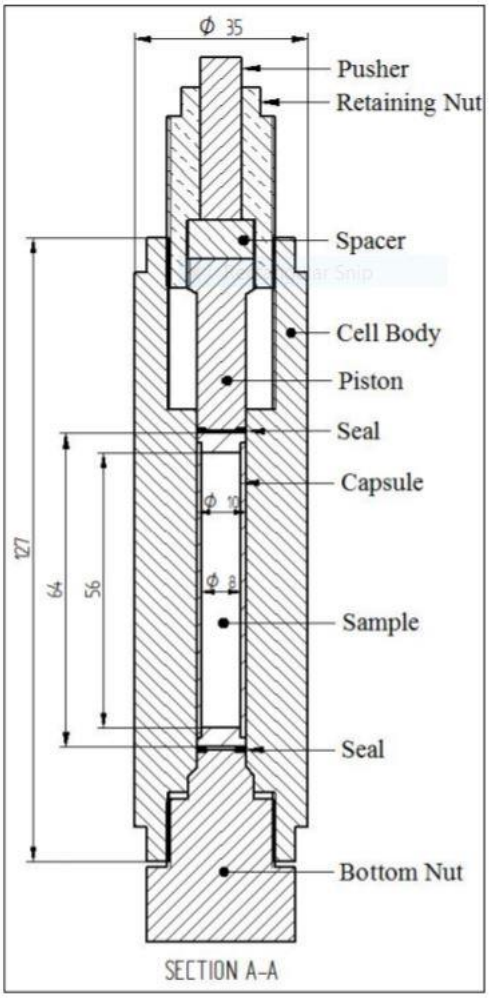

Figure 2.4 Schematic diagram of the large volume press cell including the dimensions of the components. Designed at the Centre for Science at Extreme Conditions at the University of Edinburgh.

The sample is held in a commercially available 60 mm long polytetrafluoroethylene (PTFE) tube with internal diameter of 8 mm and outer diameter of 10 mm. PTFE is used due to its chemical inertness and robustness. It is also known to withstand pressure as well as temperature.[5] The tube is sealed by PTFE caps at both ends. Those caps are wound with PTFE tape to ensure appropriate sealing of the capsule by filling the gap between the tube and the caps. The capsule is opened by removing one cap and filled with the compound to be examined while considering the volume in ratio to

the PTM. The capsule is then filled with the appropriate PTM ensuring that it is bubble-free. Filling with PTM is crucial in order to maintain the pressure and avoid crushing the capsule; there is limited travel on compression due to the geometry of the cell and its components. The capsule is closed and inserted in the cell from the bottom. The bottom nut is used to ensure the capsule is pushed fully into the bore. The bottom nut is removed and a copper ring seal with inner diameter of 6 mm, outer diameter of 10 mm and height of 1 mm is placed onto the bottom of the capsule that will help to seal the cell under pressure. The bottom nut is closed using a spanner by applying reasonable force. Another copper ring seal is also placed on the top of the capsule. A piston is then inserted in the bore and a small amount of vacuum grease is applied on it for lubrication purpose and to prevent the rotation of the piston when the retaining nut is turned. The spacer is placed on the top of the piston (to separate the pusher from the piston) and the retaining nut is locked over the spacer using a size 14 mm spanner. The tungsten carbide made pusher is inserted through the retaining nut. The assembled cell is placed in a protective steel shield before being transferred for loading. A hydraulic press is used to induce pressure (Figure 2.5), where the cell is placed into and load applied slowly by stopping after every 0.5 ton. The retaining nut is tightened by a spanner after every pressure increment until the required pressure is achieved. The pressure reading of the press gauge is noted for verification purpose and the pressure is released to zero by opening the valve gently. The cell is taken out of the press, tungsten pusher removed and the cell is covered with the shield cap and kept for 24 hours.

Figure 2.5 Hydraulic press used to induce pressure into the large volume press cell

To release the pressure and recover the sample, the pusher is inserted back into the cell and placed into the press. The pressure is increased in small increments to the initial pressure. At each increment the retaining nut is tested to observe whether the nut can be unlocked as this will indicate the true pressure in the cell in case the cell has lost pressure. Once the pressure has been verified, the retaining nut is unscrewed for one or two turns only and the valve of the pump is opened gently. This step is important in terms of safety of the user. The final step is repeated until ambient pressure is achieved, where the cell can be removed out of the press to recover the sample. The latter can be done by removing the pusher, retaining nut and spacer. The piston puller, which has internally threaded head that matches the threads on the piston, is used to pull the piston. The cell is then clamped to unscrew the bottom nut. Finally, the long pusher is used to push the capsule from the top of the cell. Decompressing the cell and sample extraction takes about 10 minutes. Each of the internal components, PTFE cell and copper seals can only be used once.

2.3 Pressure transmitting medium

Pressure transmitting medium (PTM) is an essential part of high pressure experiments. Whether in single crystals or powder sample, the PTM should surround the sample to ensure homogenous and hydrostatic pressure across the sample. There are certain features required in the selection of the PTM. These features include pressure regime, hydrostasticity, compressibility and being chemically inert. Frequently used PTMs and their maximum pressure of (quasi) hydrostasticity is presented in Table 2.1.[2]

Table 2.1 Commonly used pressure transmitting media and their relevant maximum GPa of (quasi) hydrostasticity[2]

Medium	Maximum GPa of (quasi) hydrostasticity
silicon oil	< 2.0
isopropyl alcohol	4.3
petroleum ether	6
Water	2.5
methanol:ethanol (4:1)	10.4

Hydrostatic conditions exist until the point at which the PTM can no longer support shear stress. If a PTM is used beyond the hydrostatic limit, pressure gradients are expected in the cell. The sample may be affected by shear and this can impact data collection.[6] Klotz et al.[7] have studied pressure-induced solidification commonly used PTMs in high pressure studies including methanol:ethanol (4:1). Multiple ruby spheres were used to measure pressure during compression until the point where pressure was inhomogeneous across the chamber. At that point, they knew that the PTM has solidified. They have also used the width of R1 line or R1-R2 splitting, which was similar to the reported alcohol mixtures but different in other PTMs.

2.4 Powder rheometer

The majority of oral pharmaceutical compounds come in powder form so their flow properties should be considered as it affects their processing during transport, handling, storage, manufacturing and in their final dosage form either individually or when blended with others. One of the important properties to look at is shear properties as they give an understanding on how consolidated powder will flow and for that to happen, the yield point of powder should be overcome. Moreover, flow is largely affected by physical properties like size, shape and surface characteristics of powders. In this project, an FT4 powder rheometer and 1 mL shear cell module (Figure 2.6 (a)

& (b)) were used because it allows the measurement of shear properties for a very limited amount of powder especially for expensive pharmaceutical compounds or those subjected to high pressure using the large volume press.

Compared to larger shear cells, the 1 mL shear cell, shown in Figure 2.7, uses same principles and methodologies and provides same yield loci output and other parameters like cohesion and unconfined yield strength. The module used in this project is constructed of polymer and stainless steel parts that can be disassembled and cleaned after every run.

Initially, a metal base is firmly fitted into the bottom of the shear cell module. The slide is then put on the splitting shim and both inserted into the shear cell module. This is then pushed into the module until comes to a stop, where the holes in the slide and splitting shim line up with the base and form a groove to host the studied powder. The assembled module is mounted on the table of the rheometer whilst keeping the spring plate towards the front. The test program is selected and test information, for example, sample name and run are entered into the system and the balance is tared. Enough powder of the studied sample is placed into the module, so the sample height is slightly greater than the sample chamber and this is an important step to maintain a flat surface of the sample before the shear test begins. The sample is initially conditioned using the 1 ml conditioning module. This is done to ensure uniformity of packing of the sample. This step is important before any test as it helps in establishing a uniform stress in the sample bed and eradicates air pockets and possible agglomerations which could occur due to handling or during previous storage or when the powder is placed into the vessel. After that, the condition module is replaced with 24.0 mm flat surface vented piston to do the pre-consolidation. Once pre-consolidation is over, the splitting shim

and the slide are pulled together carefully and removed from the shear cell module to remove excess powder. The flat surface vented piston is then replaced with 24 mm shear cell, which induces vertical and rotational stresses. Once the test is started, the shear head moves downwards until reaches the sample, where blades go into the powder and induces normal stress. After that, the shear head starts to rotate slowly to induce shear stress. The shear stress increases as the powder bed resists the rotation of the head until the bed fails or shears, where the maximum shear stress is observed, whereas the normal stress is maintained throughout the shear step.

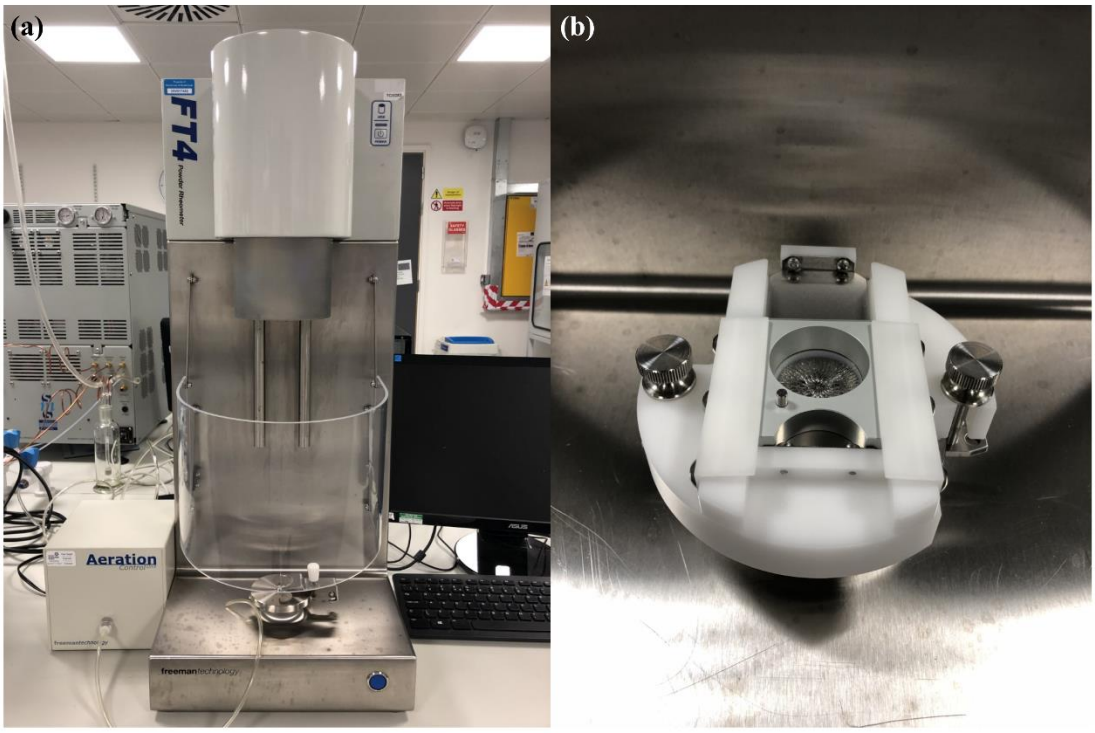

Figure 2.6 (a) FT4 powder rheometer, (b) assembled 1 mL shear cell module fitted in the rheometer

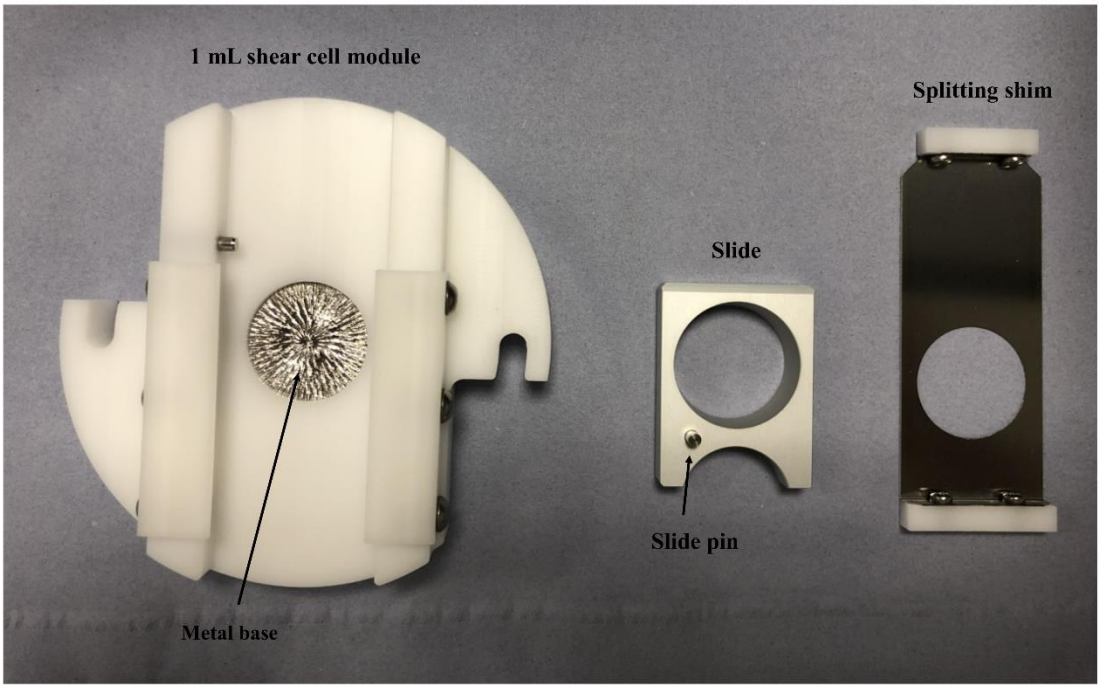

Figure 2.7 1 mL shear cell module and its components. The metal base is fitted in the bottom of the module. The slide is fitted over the splitting shim and both inserted into the module. They are used to remove excess powder before running the shear test.

2.5 Resonant acoustic® mixer

Resonant acoustic® mixer (RAM) offers a novel way of mixing powders, slurries, liquids and pastes including cosmetics, resins, composites, adhesives, pastes, polymers and pharmaceuticals without the use of impellers (Figure 2.8 (a)).[8,9,10] The technology of mixing relies on the application of a low-frequency acoustic field, which creates micro-mixing zones throughout the mixing vessel, hence does not require impellers or specific vessel design. The mixing occurs by the propagation of an acoustic pressure wave in the vessel. In solid-solid mixing, specifically, the process relies on particle collision as particles get excited by collision with the vessel walls and other particles in the vessel. This is all dependant on the vibration amplitude, frequency and acceleration that particles undergo. In various locations of the container holding the

sample, longitudinal vibration and vortexes are generated. The sample container is securely fixed by a clamp. Once the equipment is run, the vibrational motion moves the container up and down. Consequently, multiple mixing zones are generated and bulk mixing flow occur (Figure 2.8 (b)).[8]

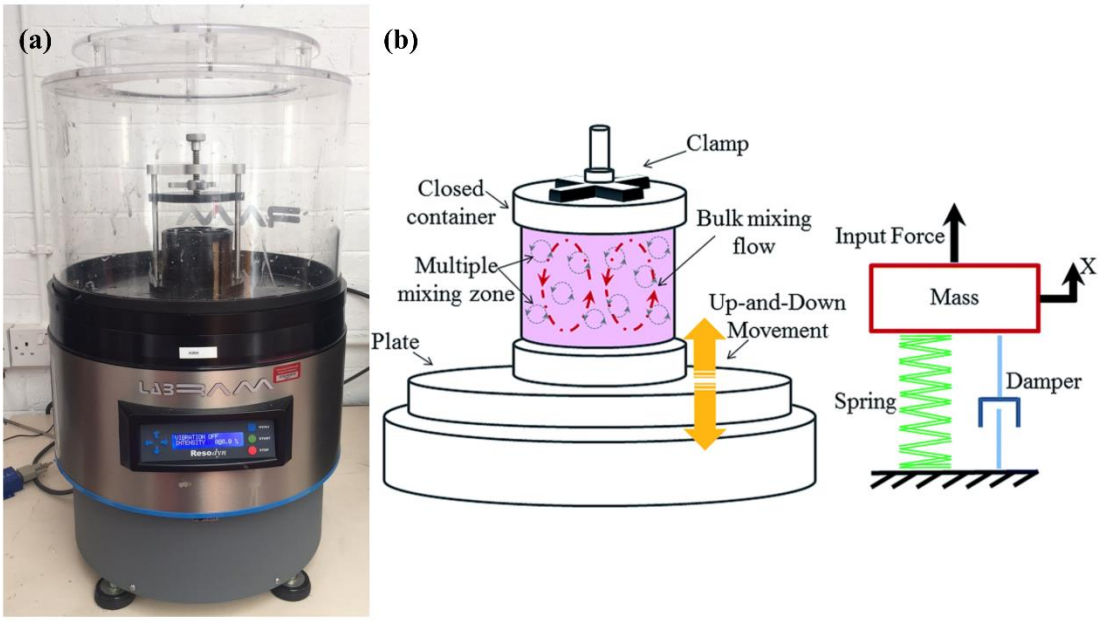

Figure 2.8 (a) LabRAM at the University of Edinburgh, (b) Schematic diagram of mixing mechanism in RAM (reproduced from reference 8)

Unlike mechanical mixers, one of the key advantages of RAM is that it does not generate heat because it uses low frequency (60 Hz), high intensity energy so it has low hydrodynamic shear stress. Other advantages include time saving, mixing materials in their shipping containers due to the adjustability of vessel holder, rapid mixing for high viscosity materials, safe mixing of hazardous and abrasive materials and fast and simple clean up. The powder formulation blends were mixed using the force 40G for 30 minutes as per the guidelines developed and validated at the University of Edinburgh (Table 2.2).

Table 2.2 RAM mixing guidelines developed at the University of Edinburgh - Standard configuration

Procedure	Recommended vessel	Recommended parameters
Mixing unreactive powders (similar particle size)	Glass or plastic. As little head space as possible	10-30 G 5-15 minutes
Mixing unreactive powders (disparate particle sizes)	Glass or plastic. As little head space as possible	20-40 G 10-30 minutes

2.6 Dissolution study

Dissolution is simply defined as the process by which a solid compound, from tablet or capsule dosage forms, dissolves into a solvent to give a solution.[11] It is considered as an important tool in formulation development as well as the process of quality control. Moreover, dissolution is used sometimes for in vitro/in vivo correlation studies, but the complexity of the gastro-intestinal system remains a barrier. However, it is still used as a qualitative tool to obtain information about release patterns and batch-to-batch consistency. It aims to obtain drug-release characteristics of pharmaceutical formulations under standardised test conditions.

There are different dissolution methods used for different dosage forms but some of the key components are the same. Those methods are specified by the United States Pharmacopoeia (USP) or National Formulary (NF)[12]:

1. USP/NF Method 1 (Rotating Basket Method)
2. USP/NF Method 2 (Rotating Paddle Method)
3. USP/NF Method 3 (Reciprocating Cylinder)

4. USP Apparatus 4 (Flow-Through cell)

5. USP Apparatus 5 (Paddle Over Disk)

6. USP Apparatus 6 (Rotating Cylinder)

7. USP Apparatus 7 (Reciprocating Cylinder)

In this study, USP/NF Method 2 (Rotating Paddle Method) apparatus was used for both tablet and capsule dosage forms. For this method, the formulations were immersed in 900 ml of dissolution medium in 1000 ml capacity vessels. The temperature of the dissolution medium was maintained at 37 ± 0.5°C by the water bath containing the vessels. Each vessel was also covered with a fitted cover to prevent the evaporation of dissolution medium. The rotating paddle, running at 100 revolutions per minute (RPM), comprises of metallic or inert rigid blade and shaft (Figure 2.9). Small variations to the test are allowed like the use of helix sinkers for floating dosage forms; these were used in our experiments. Experimental details are specified in relevant chapters (Chapter Six).

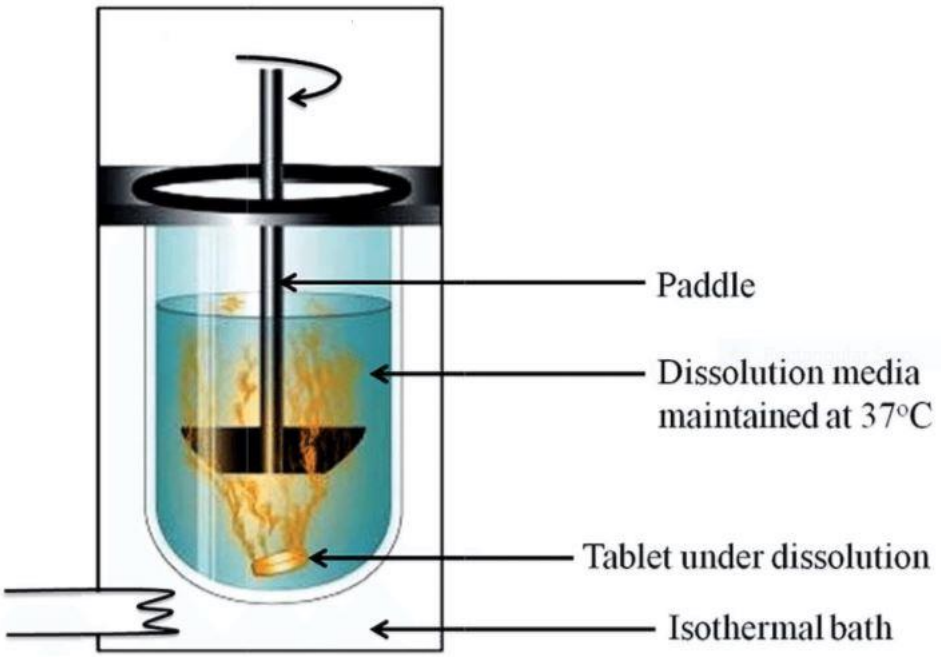

Figure 2.9 Dissolution vessel as part of USP method 2 (Rotating Paddle method)

2.7 Raman Spectroscopy

Vibrational spectroscopy was an integral part of this project especially Raman spectroscopy. Due to advancements in the field of Raman spectroscopy and instrument simplification, it made it easier to use in different forms of physical states of the examined compounds like solids, liquids or vapours.[13] Once the studied compound is irradiated with light, this will result in two types of scattering, namely, elastic (Rayleigh scattering, in which the incident light interacts with the molecule but the frequency of the scattered light is same as the frequency of incident light and the net exchange of energy is zero) and inelastic scattering.[14] In elastic scattering, there is no change in photon frequency. On the other hand, inelastic scattering is accompanied with shift in photon frequency, where it can be either, anti-stokes or stokes Raman scattering. In anti-Stokes scattering, the frequency of the scattered light is higher than

that of the incident light as the light photon gains energy from the molecule as shown in Figure 2.10, whereas in the Stokes Raman scattering, the molecule gains energy from the photon causing the frequency of the scattered light to be lower than that of the incident light so molecules move from the ground vibrational state *m* to a higher energy excited vibrational level *n* and that is all governed by the polarizability of electron clouds around the molecule. The anti-Stokes Raman lines are less intense than the Stokes Raman lines as the majority of atoms are in the ground states, hence more intense stokes Raman lines. The Raman intensity is proportional to the number of molecules in the relevant energy state.

Fluorescence is one the issues that hinder Raman spectroscopy.[15] It could be originating from the material itself or from by-products during manufacturing process. In fluorescence, the molecule absorbs energy and gets excited to a higher level, but upon de-excitation, the photons are emitted with a different energy than the incident one. A major difference between Raman effect and fluorescence is the time involved as fluorescence is resonant while Raman is instant. As Raman scattering is a weak effect, the use of visible excitation wavelengths is recommended, but fluorescence may occur for some samples. Changing to UV or NIR lasers may overcome fluorescence, as the laser photon does not have the energy to excite fluorescence, but the signal will be much weaker.

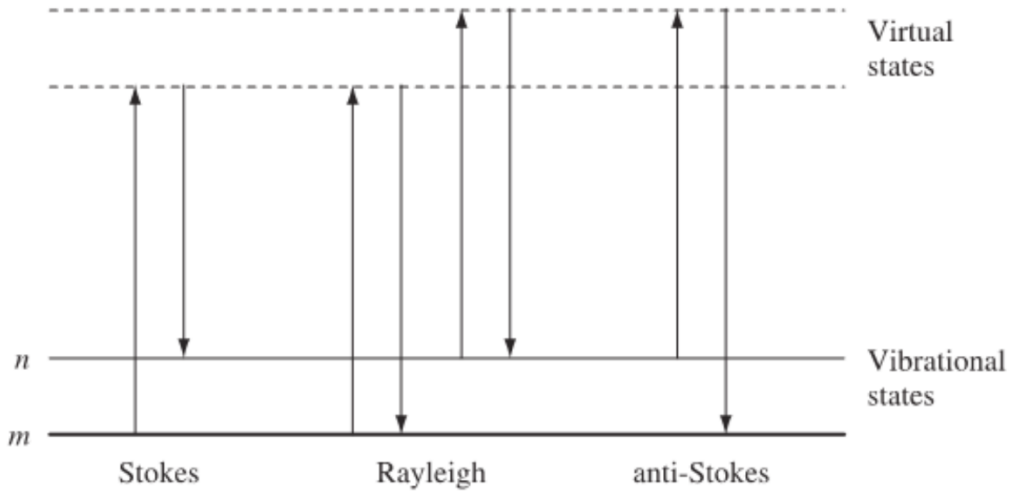

Figure 2.10 Schematic of Rayleigh, Stokes-Raman and anti-Stokes Raman (Reproduced from reference 14)

2.8 Ultraviolet (UV) and visible spectroscopy

UV visible spectroscopy is one of the most robust methods used for the quantification of drugs in formulations as most drug molecules absorb radiation in the UV region, while some of them have colours and thus absorbed in the visible range of the spectrum. The absorption happens due to the promotion of electrons, involved in the bonds between the atoms of the molecules, from a lower to a higher energy state (Figure 2.11).

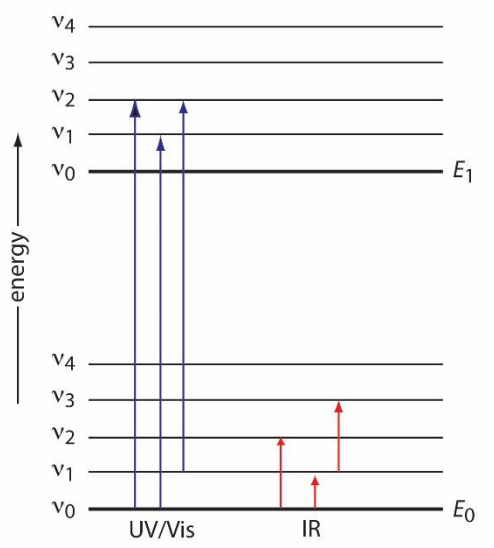

Figure 2.11 Electronic excitation in UV / visible spectroscopy

The UV-visible spectrophotometer is composed of a light source (deuterium lamp for UV region and tungsten lamp for visible), monochromator, optics, sample holder and a detector. The optics are responsible for splitting the beam so it passes through the control and the sample. Light is emitted from the light source with a wavelength range of 190 – 750 nm, where UV region is between 190 – 350 nm and the visible region is between 350 – 750 nm. This emitted light goes through the monochromator and exits with an intensity I_0 and some of it is absorbed by the sample. The light leaves the sample with an intensity of I, which then goes through the detector that analyses the data and gives the spectrum (Figure 2.12).

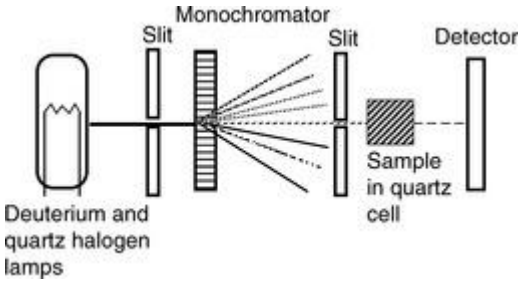

Figure 2.12 Schematic diagram of UV-visible spectrophotometer (Reproduced from reference 16)

The process of measuring absorption of light by molecules is governed by Beer-Lambert Law;[16]

$$\log I_0/I_1 = A = \varepsilon bc$$

where I_0 is the intensity of incident light, I_1 is the intensity of transmitted light, A is the amount of light absorbed by the sample known as absorbance, ε is a constant, b is the pathlength, usually 1 cm and c is the concentration of the analyte in moles/litre. As pharmaceuticals concentrations' are measured in grams or milligrams, Beer-Lambert Law is rewritten as:

$$A = A\,(1\%, 1\text{ cm})\,bc$$

Where A is absorbance, A (1%,1 cm) is the absorbance of a 1% w/v solution in 1 cm cell, b is the pathlength in cm and c is the concentration of the sample expressed as g/100 ml. A cuvettes used have a pathlength of 1 cm, the equation is further simplified to:

$$\left[c = \frac{A}{A(1\%, 1\ cm)}\right]$$

To be able to utilise this technique in drug release studies, a standard stock solution of the sample is prepared. From the stock solution, different dilutions are prepared including the lowest possible concentration of the detected sample to the highest concentration expected from the release study. These dilutions are scanned against a blank to detect the λ_{max} of the sample. A calibration curve is then plotted against these concentrations to determine the linearity. R^2 value gives an indication of curve linearity and the equation is utilised to obtain drug concentrations from the absorbance.

2.9 References

[1] Crystal.chem.ed.ac.uk. (2016). High Pressure Crystallography | Crystal Chemistry. [online] Available at:http://www.crystal.chem.ed.ac.uk/research-themes/high-pressure-crystallography [Accessed 1 Apr. 2016].

[2] Miletich R, Allan DR, Kuhs WF. High-pressure single-crystal techniques. Reviews in mineralogy and geochemistry. 2000 Jan 1;41(1):445-519.

[3] Dunstan DJ, Spain IL. Technology of diamond anvil high-pressure cells: I. Principles, design and construction. Journal of Physics E: Scientific Instruments. 1989 Nov;22(11):913.

[4] Forman RA, Piermarini GJ, Barnett JD, Block S. Pressure measurement made by the utilization of ruby sharp- line luminescence. Science (New York, NY). 1972;176(4032):284-5.

[5] Likhacheva AY, Chanyshev AD, Goryainov SV, Rashchenko SV, Litasov KD. High-Pressure– High Temperature (HP- HT) Stability of Polytetrafluoroethylene: Raman Spectroscopic Study Up to 10 GPa and 600 ℃. Applied Spectroscopy. 2017;71(8):1842-8.

[6] Piermarini GJ, Block S, Barnett JD. Hydrostatic limits in liquids and solids to 100 kbar. Journal of Applied Physics. 1973;44(12):5377-82.

[7] Klotz S, Chervin JC, Munsch P, Le Marchand G. Hydrostatic limits of 11 pressure transmitting media. Journal of Physics D: Applied Physics. 2009;42(7):075413.

[8] Tanaka R, Takahashi N, Nakamura Y, Hattori Y, Ashizawa K, Otsuka M. Verification of the mixing processes of the active pharmaceutical ingredient, excipient

and lubricant in a pharmaceutical formulation using a resonant acoustic mixing technology. RSC Advances. 2016;6(90):87049-57.

[9] Osorio JG, Sowrirajan K, Muzzio FJ. Effect of resonant acoustic mixing on pharmaceutical powder blends and tablets. Advanced Powder Technology. 2016;27(4):1141-8.

[10] Vanarase A, Coguill S, Lucon P. ResonantAcoustic® mixing; uniform distribution of minor materials during powder mixing. InProceedings of the JANNAF 36th Propellant and Explosives Development and Characterization Joint Subcommittee Meeting 2010.

[11] Felton LA. Remington: essentials of pharmaceutics. Philadelphia: Philadelphia College of Pharmacy; London: Philadelphia: Philadelphia College of Pharmacy; London: Pharmaceutical Press; 2013.

[12] Usp.org. (2016). <711> Dissolution. [online] Available at: http://www.usp.org/sites/default/files/usp/document/harmonization/gen-method/stage_6_monograph_25_feb_2011.pdf [Accessed 1 Mar. 2017].

[13] Vandenabeele P. Raman spectroscopy. Analytical and Bioanalytical Chemistry, 2010 Aug, Vol397(7), pp2629-2630.397(7).

[14] Ewen S. Modern Raman spectroscopy: a practical approach. Geoffrey D, editor. Hoboken, NJ: Hoboken, NJ: J. Wiley; 2005.

[15] Peter V. Practical Raman spectroscopy: an introduction. Chichester, West Sussex, United Kingdom: Chichester, West Sussex, United Kingdom: Wiley; 2013.

[16] Watson DG. Pharmaceutical Analysis [internet resource]: A Textbook for Pharmacy Students and Pharmaceutical Chemists. 4th edition. ed: Edinburgh: Elsevier; 2017.

Chapter Three: Enhancing Raman Signalling under High Pressure

This work was done in collaboration with Karen Faulds, Duncan Graham, Hayleigh May and Kirsten Gracie of the Nanobiotechnolgy team at the Chemistry department at the University of Strathclyde. The silver nanoparticles were prepared and supplied by them.

3.1 Introduction

Raman spectroscopy is one of the important techniques in studying materials in all states. The recent advancements in Raman microscopes and technical improvements enabled multidisciplinary research of materials.[1] It is used to study a materials' molecular and crystalline structure as well as their chemical composition but is sometimes hindered by the phenomenon of fluorescence, which dominates Raman signalling. Fluorescence may be caused by impurities or sample degradation by laser light.[2] It is a well-known competitor to Raman scattering and is a particular problem in the area of high pressure where small quantities of pharmaceutically relevant materials may exhibit fluorescence. Fluorescence can be avoided by working in the UV region but a change in the wavelength of the probe may not be suitable for all compounds. For example, absorption of UV radiation by the molecule can cause sample degradation or burning.[3]

Surface enhanced Raman spectroscopy (SERS) technique is recognized as a promising technique in chemical and biological molecular analysis due to its high sensitivity. SERS was first observed and interpreted in the 1970s using pyridine on roughened silver (Ag) electrode.[4,5,6] In 1997, single molecules were observed using SERS and the issue of fluorescence was overcame[7] and this sparked the use of SERS by scientists from different disciplines like physics, chemistry, biology and material science as it is known to enhance Raman signalling to about 10^6-10^8 over normal Raman spectroscopy.[2,3] The ease of using SERS has initiated an increased use in the area of chemical sensing and biological imaging.[8] The presence of metal nanostructures is a prerequisite for SERS, so an interaction should be expected between light and

molecules as well as between molecules and the nanostructures, hence dipoles are induced in both the metal surface and the molecules.[9,2]

SERS requires the presence of a metallic surface. Silver (Ag) and gold (Au) are the most commonly used nanostructures[10], where silver is plasmonically more active than gold and mostly used for single molecule detection. That is to say that the laser excites localised surface plasmons on the metal, which in turn creates a strong localised electromagnetic field. This leads to a great enhancement of Raman scattering of the molecules within the proximity of nanometres of the substrate. Gold, on the other hand, is known to be chemically more inert and used in cases where chemical stability is more important than signal enhancement. It is worth noting that they both have similar enhancement in the red to near-infrared region.[2] Enhancement of Raman signalling caused by SERS is thought to be due to two processes: chemical enhancement and electro-magnetic enhancement. Through the chemically–enhanced route the resonant excitation of the plasmons in the nanostructures of substrate surface are altered and provide increase in the intensity of the spectrum. This route involves the induction of charge transfer between the analyte and the substrate, which in turn will increase the polarizability. Through electromagnetic enhancement it is thought that there is increased polarizability of the adsorbed molecules on the nanostructures.[2,11,12,13,14,15] On the other hand, it is highly debated that the electromagnetic effect is more predominant than the charge transfer effect and is responsible for the signal enhancement.[16] When the incident laser light hits the analyte and the substrate, a localised plasmon is oscillated and that increases the local field around the analyte and the substrate leading to greater polarisation.

The process is explained in the following steps:[16]

1. Adsorption of the analyte on the roughened or patterned surface of the substrate so that the excitation frequency of the laser will excite a plasmon on the metal surface causing the polarisation. The way of adsorption depends on the nature of the substrate surface and the analyte.

2. The energy is transferred from the plasmon to the adsorbed molecule and adds to the Raman process that is already occurring from incident light exciting the molecule.

3. The energy is transferred back to the plasmon less the amount transferred to the nuclei and scattered from the surface as wavelength shifted light.

The signal enhancement in SERS depends on the surface plasmon of individual nanoparticles, which may not lead to large Raman enhancement. The aggregation of nanoparticles causes additional electromagnetic field enhancement and creation of hot spots in closer proximity to the analyte (Figure 3.1). The distance of the analyte from the metallic nanoparticles and the hot spots created between these particles play a major role in the intensity of Raman spectrum.[17] One way of achieving this is the use of aggregating agents. These agents are used to aggregate colloid particles together to create more hot spots, hence lead to larger Raman enhancement. The role of aggregating agents in two different colloidal systems was investigated by Blanch et al.[18] and they found that highly intense anomalous Raman bands appeared in both systems. This study indicates that colloidal systems must be characterised before being used to differentiate between peaks from analytes and the ones from the colloids.

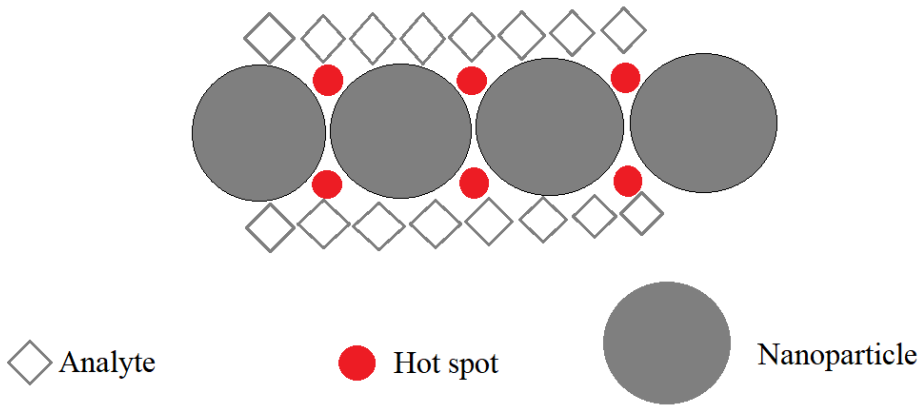

Figure 3.1 Schematic representation of hot spots between nanoparticles

Another important factor is the orientation of the analyte on the surface of the metallic substrate. The scattering comes from the component of the plasmon perpendicular to the surface, which in turn relates to the molecular polarisation vertical to the surface.

Raman spectroscopy is a commonly used technique in the area of high pressure research.[1] Pressure is defined as the force applied to an object per unit area (p=F/A) and it tends to reduce the volume of systems applied to especially liquids and soft solids.[19] Size reduction occurs because the intermolecular distance decreases and subsequently electronic structure changes.[20]

The application of high pressure experimental methods has increased among different disciplines like physics, geology, chemistry and biology as it is known to induce structural changes, phase transition and polymerization of organic compounds. The availability and ease of use of diamond anvil cells (DACs) has revolutionised the science of high pressure.[21] Additionally, the use of diamond due to its strength and

transparency to electromagnetic spectrum facilitated the use of DACs in different analytical techniques including X-ray, infrared and Raman spectroscopy.

The application and success of SERS technique in high pressure research has opened opportunities for further use. It has been used in different ways for the enhancement of Raman signal under high pressure. Wang et al.[22] have assembled the SERS substrate, silver nanoparticles (AgNPs), on an ultra-thin allylamine hydrochloride wafer to detect 4- chlorothiophenol. They found that the detection limit could reach up to 1 x 10^{-10} mol/L and this technique could be used for detecting low molecular concentration at high pressure (0.06-0.978 GPa). The signal enhancement they found was from 11700 (a.u.) at ambient pressure to about 40000 (a.u.) at 0.06 GPa. After pressure was released, the intensity dropped down to about 20000 (a.u). This increase was justified by the creation of shorter distances between the substrates, hence better signal. The decrease of intensity after decompression was due to incomplete recovery of pressure induced active hot spots destruction. Another study by Brown et al.[23] also explored the use of SERS under high pressure. They used benzenethiol and benzenemethylthiol as analytes in a self-assembled monolayer on silver film over nano-spheres. Similarly, they found Raman signal enhancements. SERS technique could be utilised in monitoring the behaviour of weak Raman scaterers as well as fluorescent materials.

The aim of the chapter was to investigate the enhancement in the Raman signal (if any) rather that how the samples responded to pressure. In this study, we explored the use of two different batches of AgNPs to enhance Raman signalling from a range of fluorescent polymers and weakly scattering amino acids including poly glycolic acid

(PGA), poly lactide-co-glycolide (PLGA), DL-valine, L-leucine and L-isoleucine (Figure 3.2).

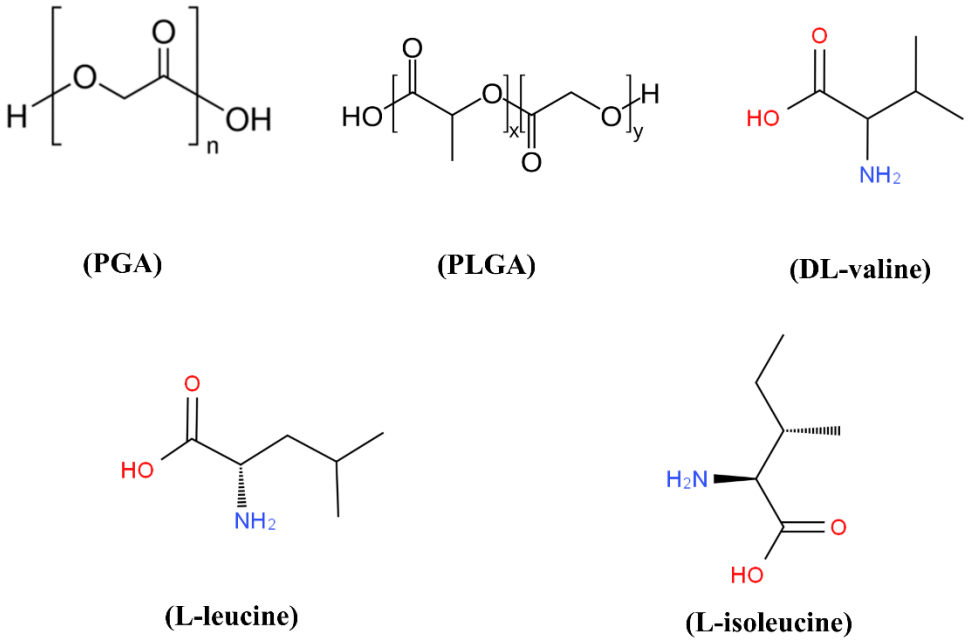

Figure 3.2 Chemical structures of polymers : PGA and PLGA, amino acids: DL-valine, L-leucine and L-isoleucine used in this study

3.2 Materials and Methods

3.2.1 Materials

Poly (D,L-lactide-co-glycolide) (50:50 lactide:glycolide), PGA, L-leucine and L-isoleucine were purchased from Sigma-Aldrich (Irvine, UK) and were of reagent grade. DL-valine was purchased from Alfa Aesar (Lancashire, UK). Methanol (analytical reagent grade) and Ethanol (analytical reagent grade) were purchased from VWR (Leicestershire, UK).

3.2.2 Methods

3.2.2.1 Sample preparation

Samples were ground individually for 10 minutes using an agate mortar and pestle, as shown in Table 3.1, unless otherwise specified. PGA was received as pellets which were difficult to break into smaller particles. 300 mg of PGA was ball-milled with few (4) drops of (methanol:ethanol (4:1)) for 90 minutes at 30 Hz/second. The powder produced via this method was used for the study.

Table 3.1 Summary of samples and quantities used

Sample	PLGA	PGA	DL-Valine	L-leucine	L-isoleucine
Quantity used	50 mg	300 mg	300 mg	300 mg	300 mg

3.2.2.2 High pressure

High pressure studies were conducted using Merrill-Basset DAC containing two opposed gem-quality diamonds with 600 µm culets supported by tungsten carbide backing discs. Tungsten was used as a gasket material with a thickness of 230 µm and pre-indented to ~ 90 - 100 µm thick. The gaskets were drilled in the centre of the indent using Boehler microDriller®, an electro-discharge-machine, using a tungsten carbide electrode (250 µm). The hole was used as the sample chamber. The sample was added to the sample chamber and packed into the hole using the opposed diamond to ensure that enough material was in the hole for analysis. Using a fine needle, a small indent in the sample was made to allow space for the pressure transmitting medium (PTM). Methanol:ethanol (4:1) was used as PTM to ensure that the samples were compressed isotropically and no shear was introduced; ruby chips were added to the sample chamber to measure the *in-situ* pressure.[24]

3.2.2.3 Synthesis of silver nanoparticles

Silver nanoparticles (AgNPs) were prepared using a modified Lee and Meisel method.[25] Silver nitrate (90 mg) was dissolved in 500 mL distilled water and heated rapidly with continuous stirring to boiling. A 10 mL aqueous solution of sodium citrate (1%) was added quickly to the boiling solution. The heat was reduced and the solution was left to boil for 90 minutes with stirring. The colloid was analysed by UV-vis spectroscopy and the λ_{max} was 406 nm. The concentration of the colloid was calculated to be 0.57 nM and the size of the NPs was 85.13 ± 0.73 nm.

A second batch of AgNPs was prepared using the same method. This was done to examine the difference in signal enhancement between batches. The analysis showed that λ_{max} was 394 nm. The concentration of the colloid was calculated to be 0.488 nM and the size of the NPs was 76.8 nm. The AgNP solutions were centrifuged for 20 minutes at 6000 rpm then were suspended in the PTM (4:1) methanol:ethanol.

3.2.2.4 Raman spectroscopy

Raman spectra were acquired using Raman XplorA Microscope by Horiba Scientific John Yvon Technology with an excitation wavelength of 532 nm. Spectra were summed using 2 accumulations and a grating of 1200-gr/mm, which was found to be the best suitable to yield good peak resolution.[26] Diamond has a strong peak between 1330 and 1380 cm^{-1} hence this region is not shown in the Raman spectra of high pressure data sets. Data analysis and graph production was done using OriginPro® 2017 software (OriginLab, Northampton, MA).[27]

3.3 Results and Discussion

In this study, 2 batches of AgNPs were tested to explore the level of Raman signal enhancement, in fluorescent polymers and weakly scattering amino acids, obtained by adopting SERS technique. The SERS substrates were suspended in the PTM and no further chemical bonding with the analyte was attempted. As an initial experiment the Raman spectrum of AgNPs suspended in the PTM (methanol:ethanol (4:1)) was acquired to check if there are Raman active bands that may appear when acquiring the Raman spectra of the samples (Figure 3.3 (a)). The spectrum shows fluorescence but also Raman bands in the CH region, which could be a SERS signal enhancement of the PTM. The AgNPs suspended in the PTM formed a cloudy solution filling the gasket hole is shown in Figure 3.3 (b); the small spheres are ruby spheres to measure the *in-situ* pressure.

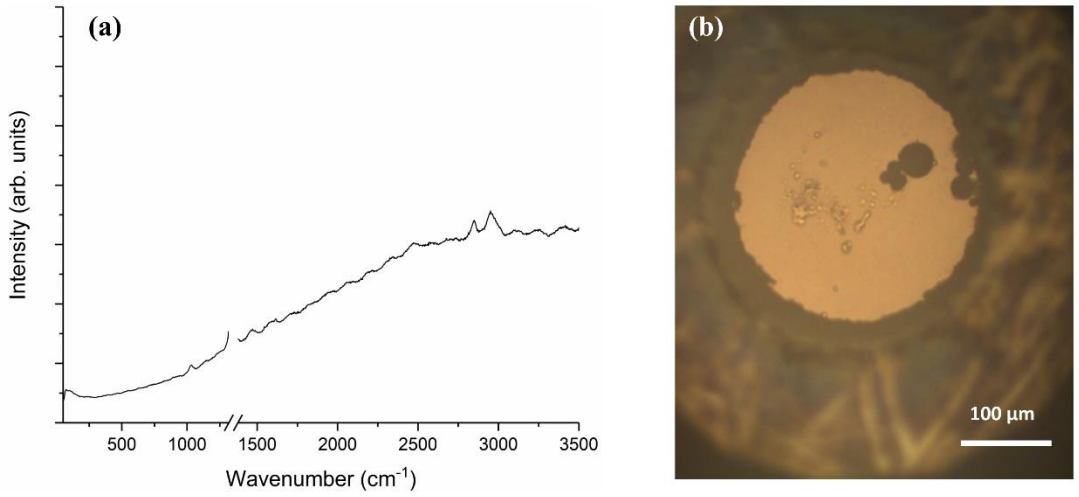

Figure 3.3 (a) Raman spectrum of AgNPs used to enhance Raman signal. (b) AgNPs suspended in PTM filling the hole with few ruby spheres

3.3.1 Raman signalling from batch 1

In this set of experiments, comparative studies of selected samples of weak Raman scattering amino acids using plain PTM and PTM with AgNPs, the first batch, at a pressure point around ±1 GPa. The colloid prepared for this set of experiments was analysed and found to have λ_{max} of 406 nm. The concentration of the colloid was calculated to be 0.57 nM and the size of the NPs was 85.13 ± 0.73 nm. In this set of experiments, it is evident that the Raman signal improvement was of better quality and higher clarity than the other batch.

3.3.1.1 DL-valine

The enhancement seen in DL-valine set of experiment using the SERS technique showed a clear Raman spectrum without the need for baseline treatment as shown in (Figure 3.4), which presents a comparative Raman spectrum in the range of 50-3500 cm^{-1} of DL-valine using AgNPs in the PTM and without AgNPs at ~ 1 GPa. It is clearly seen that the use of AgNPs has significantly improved the Raman signal and the peaks can be easily distinguished.

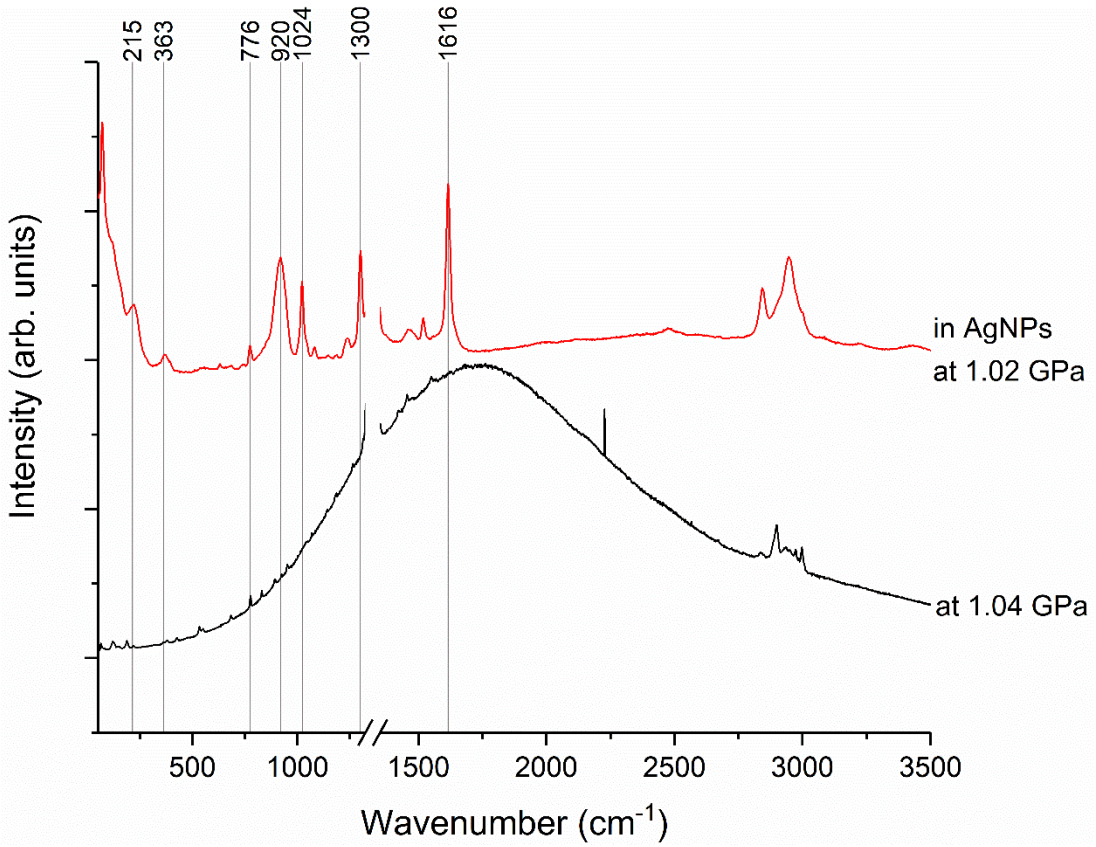

Figure 3.4 Comparative Raman spectra of DL-valine at ca. 1 GPa using AgNPs and without AgNPs. The spectrum in red was recorded using AgNPs in the PTM and it shows distinguishable peaks compared to the spectrum recorded without using AgNPs, in which fluorescence overcomes Raman signal and peaks can be barely seen.

Characteristic Raman peaks in the spectral region between 50 and 1800 cm^{-1} are clearly identified when compared with the non-SERS spectrum (Figure 3.5 (a)). In the lattice spectral range, which is known to be below 200 cm^{-1}, we have seen an improvement in peak intensity at 71 and 119 cm^{-1}. The peak at 215 cm^{-1} also has an increased intensity when compared with the non-SERS. This peak can be assigned as a deformation of CH unit.[28] The peak at 363 cm^{-1} is relatively clearer in the AgNPs set of experiment and it is assigned to skeletal deformation mode.[28] The peak at 776 cm^{-1} is classified as wagging CO_2 and it is more intense when we used AgNPs. Generally, CC and CN stretching are observed in the 850-1100 cm^{-1} spectral range. One of the

most intense peaks at 920 cm^{-1} has not been identified in previous works but it can be assigned as v(CC) deformation.[29] Similarly for the peaks at 1024 and 1063 cm^{-1}, they are considered as contributions from the (CC) and (CN) vibrations. Bands between 1300 – 1400 cm^{-1} are generally assigned as bending of CH and CH_3 units as occurs in other amino acids like l-alanine and l-asparagine.[29] The peak at 1300 cm^{-1} is seen highly intense when using AgNPs whereas it was seen as shoulder present just before the diamond peak without the AgNPs. The peak observed at 1460 cm^{-1} is classified as deformation of CH_3 unit and the same was seen experimentally at 1454 cm^{-1}.[30] The intense peak at 1616 cm^{-1} has been assigned as deformation of NH_3.

The Raman spectrum of DL-valine powder in the spectral region between 2750 and 3150 cm^{-1} using AgNPs in the PTM is presented in Figure 3.5 (b). There are two distinct peaks namely at 2842 and 2947 cm^{-1}. The peaks appear in this region are associated mainly with CH and CH_3 stretching vibrations and they are assigned as CH and CH_3 vibrations respectively.[36]

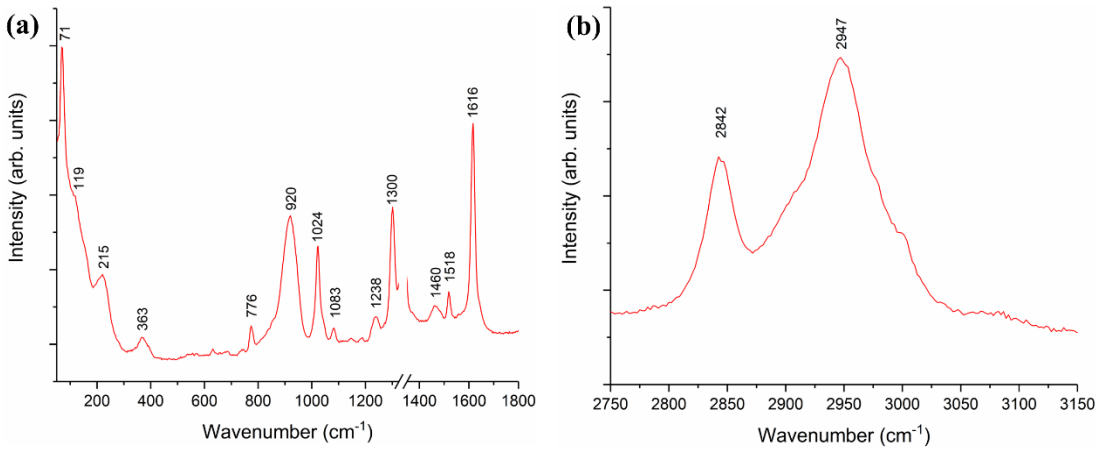

Figure 3.5 Raman spectrum of DL-valine using AgNPs in the PTM with peaks numbered in the spectral region (a) 50-1800 cm^{-1} (b) 2750-3150 cm^{-1}

3.3.1.2 L-leucine

Similar to other samples, L-leucine powdered sample was subjected to ~ 1 GPa of pressure using DAC. Comparative Raman spectra of the l-leucine with and without the use of AgNPs in the range of 50-3500 cm^{-1} are presented in Figure 3.6. It is clearly seen that the Raman spectrum of l-leucine in AgNPs has more clear and distinct peaks than the one with no AgNPs. Both spectra were produced without any modification or treatment.

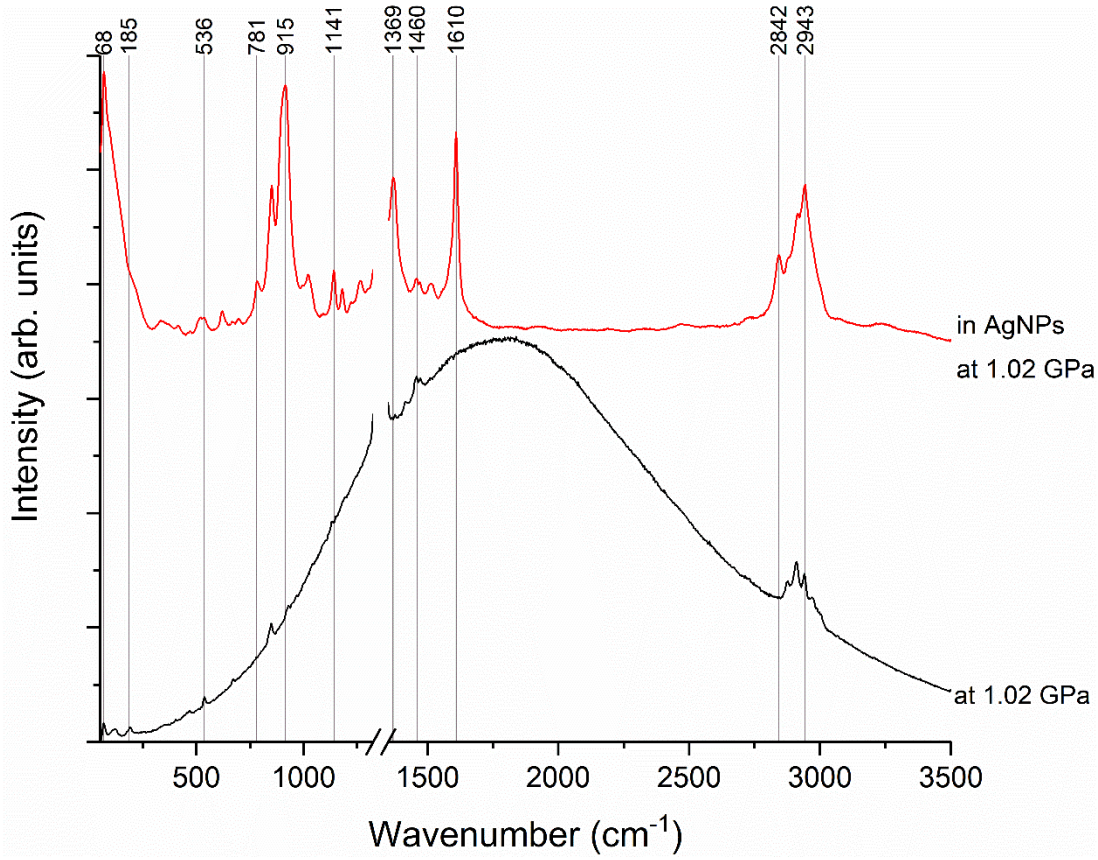

Figure 3.6 Comparative Raman spectra of L-leucine at ca 1 GPa using AgNPs and without AgNPs. The spectrum in red was recorded using AgNPs in the PTM and it shows distinguishable peaks compared to the spectrum recorded without using AgNPs, in which fluorescence overcomes Raman signal and peaks can be barely seen.

The spectral range of 50-1800 cm^{-1} of l-leucine is presented in Figure 3.7 (a). Two Raman peaks were identified for the lattice mode below 200 cm^{-1} and they are at 68

and 185 cm^{-1}. The band observed at 245 cm^{-1} is assigned as out-of-plane vibration of CH unit.[31] The low intensity peak at 332 cm^{-1}, which higher in intensity when using AgNPs, is assigned as NCC deformation.[36] Other low intensity peaks at 415 and 461 cm^{-1} are assigned as skeletal structure deformation.[36] The peak at 536 cm^{-1} was assigned as the rocking of CO^{-}_{2}. The peak at 781 cm^{-1} was not observed in the non-AgNPs spectrum and assigned as CO^{-}_{2} deformation. Moreover, the peak at 850 cm^{-1} was seen in both spectra but with very low intensity in the non-AgNPs one. This peak is assigned as rocking of CH_3. The bands in the spectral region between 900 and 1100 cm^{-1} are associated with CC and CN vibrations.[37] A highly intense peak was clearly evident at 915 cm^{-1} and is assigned as C-C stretching vibration. The peaks observed at 1141 and 1180 cm^{-1} are tentatively assigned as rocking of NH^{+}_{3}.[36] Another intense peak just after the blanked diamond peak at 1369 cm^{-1} is assigned as deformation of CH unit. Peaks with relatively low intensity at 1460 and 1475 cm^{-1} are assigned as asymmetric bending of CH_3. The highly intense peak at 1610 cm^{-1} has not been observed in the spectrum without AgNPs and can be associated to stretching vibration of CO^{-}_{2} or to bending vibration of NH^{+}_{3}.[32]

The Raman spectra of l-leucine in the spectral region 2750 – 3150 cm^{-1} is presented in Figure 3.7 (b). We have observed four distinct peaks in this region with higher intensity than the spectrum recorded without AgNPs. The peaks observed at 2842 and 2880 cm^{-1} are assigned as symmetrical stretch of CH_2 whereas the peaks observed at 2913 and 2943 cm^{-1} are associated with stretching of CH_2 and CH respectively.

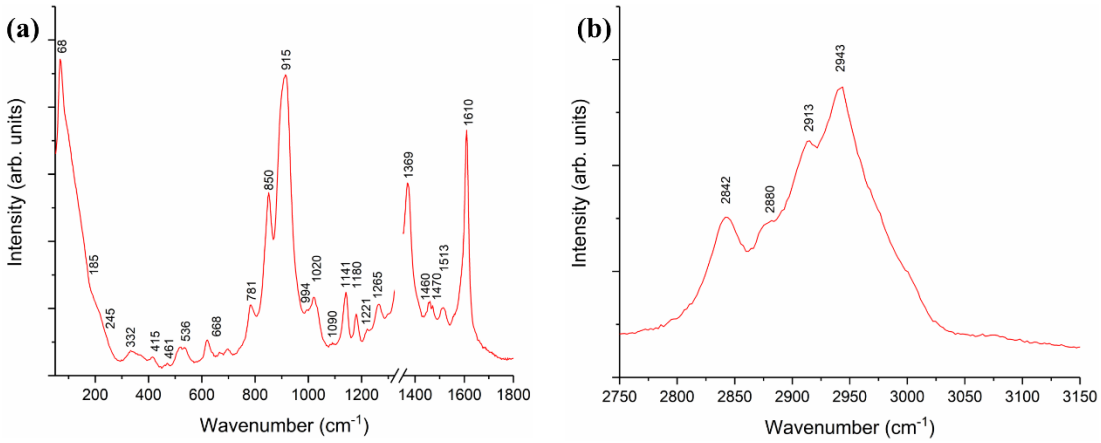

Figure 3.7 Raman spectrum of L-leucine using AgNPs in the PTM with peaks numbered in the spectral region (a) 50-1800 cm^{-1} (b) 2750-3150 cm^{-1}

3.3.1.3 L-isoleucine

L-isoleucine was subjected to ~ 1 GPa in DAC. The Raman spectra in the spectral region 50-3500 cm^{-1} with and without the use of AgNPs was recorded (Figure 3.8). It is evident that there are more distinguishable peaks observed in the spectrum where AgNPs were suspended in the PTM. Both spectra were plotted without any modification or baseline correction.

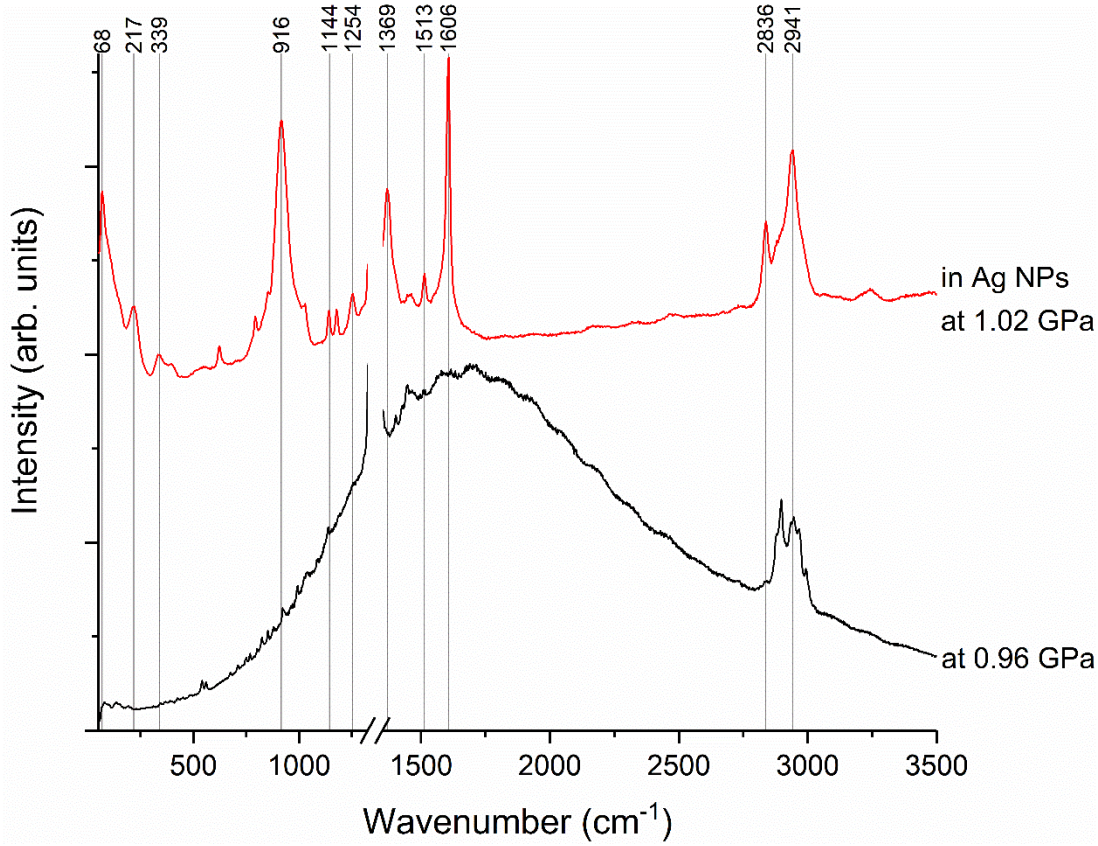

Figure 3.8 Comparative Raman spectra of L-isoleucine at ca 1 GPa using AgNPs and without AgNPs. The spectrum in red was recorded using AgNPs in the PTM and it shows distinguishable peaks compared to the spectrum recorded without using AgNPs in which fluorescence overcomes Raman signal and peaks can be barely seen.

The Raman spectrum of L-isoleucine at 1.02 GPa in the spectral region of 50-1800 cm^{-1} is presented in Figure 3.9 (a). In this region, we have observed one peak as a lattice representation at 68 cm^{-1}. Another peak at 217 cm^{-1} was observed and assigned as torsion of CH unit.[37] Low intensity peaks at 339 and 392 cm^{-1} are associated with bending of NCC and CCC. Two low intensity peaks were observed at 622 and 793 cm^{-1} but have not been assigned. The peak at 851 cm^{-1} appears as a shoulder and is assigned as CH_3 unit rocking. A high intensity peak observed at 916 cm^{-1} is assigned as a stretching vibration of CC unit.[35] The peaks appearing at 1144 and 1177 cm^{-1} are associated with rocking of NH^{+}_3 while the peak at 1254 cm^{-1} is assigned as CH_2

torsion. An intense peak at 1369 cm^{-1} was assigned as bending of CH unit. An asymmetric bending of CH_3 was observed at 1447 cm^{-1} whereas the peak at 1513 has not been assigned.[37] The most intense peak in this figure was observed at 1606 cm^{-1} and is associated with stretching of CO^{-}_2.

The Raman spectrum of L-isoleucine at 1.02 GPa in the spectral region between 2750 – 3100 cm^{-1} is presented in Figure 3.9 (b). Generally, this region is where the stretching vibrations of CH and CH_3 are observed. We observed two distinct peaks at 2836 and 2941 cm^{-1}. The latter is assigned as a stretching of CH unit.

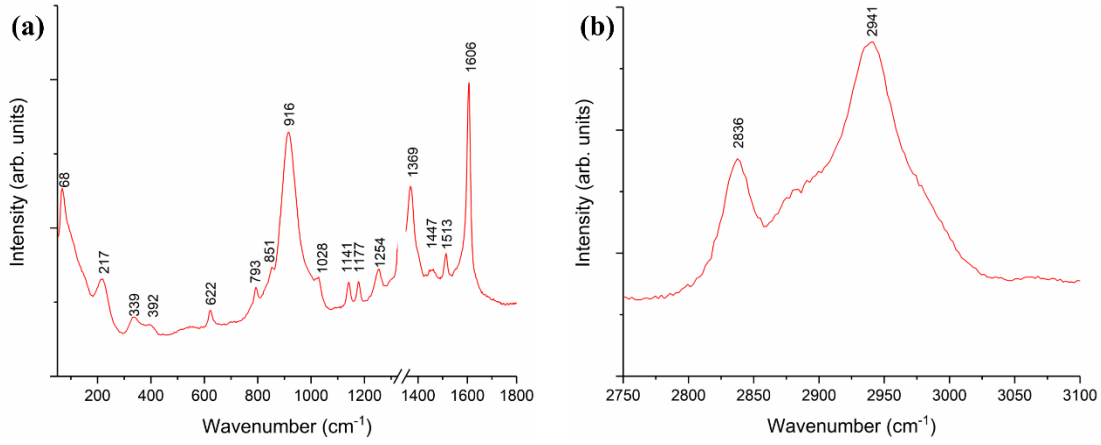

Figure 3.9 Raman spectrum of L-isoleucine using AgNPs in the PTM with peaks numbered in the spectral region (a) 50-1800 cm^{-1} (b) 2750-3100 cm^{-1}

3.3.2 Raman signalling from batch 2

In this experiment, comparative studies of selected samples including fluorescent polymers and weak Raman scattering amino acids using plain PTM and PTM with suspended AgNPs at a pressure point around 1 GPa were performed. The colloid prepared for this set of experiments was analysed and found to have a λ_{max} of 394 nm. The concentration of the colloid was calculated to be 0.488 nM and the size of the NPs was 76.8 nm.

3.3.2.1 DL-valine

The use of SERS was adopted in Raman spectrum acquisition of DL-valine to improve the signalling. DL-valine had a weak Raman spectrum in the diamond anvil cell using pure PTM (no AgNPs). The addition of AgNPs has improved the signal in some peaks and the signal to noise ratio (Figure 3.10). A better peak resolution has been observed when using AgNPs especially in the spectral region between 50-1300 cm^{-1}. The selected Raman peak assignments of DL-valine in the spectral region 50-1300 cm^{-1} presented in Table 3.2 have been assigned by Lima et al.[35] experimentally using valine single crystals grown from an aqueous solution by slow evaporation at 297 K. The Raman peaks in the AgNPs set of experiments are clearer and distinguishable when compared to the one without AgNPs. From our data, it is evident that majority of Raman bands in DL-valine defined in the literature[30] (Figure 3.11) are present in the SERS data set.

Table 3.2 DL-valine selected peak assignments in the spectral region 50-1300 cm^{-1}[33]

Peak Position (cm^{-1})	Assignment	Peak Position (cm^{-1})	Assignment
70	lattice	781	$\delta(CO_2)$
121	lattice	835	$\gamma(CO_2)$
152	lattice	895	ν(C-C)
190	$\tau(CO_2)$	929	ν(C-C)
385	skeletal def.	956	ν(C-C)
476	$\tau(NH_3)$	1186	$r(NH_3)$
537	$r(CO_2^-)$	1247	δ(CH)

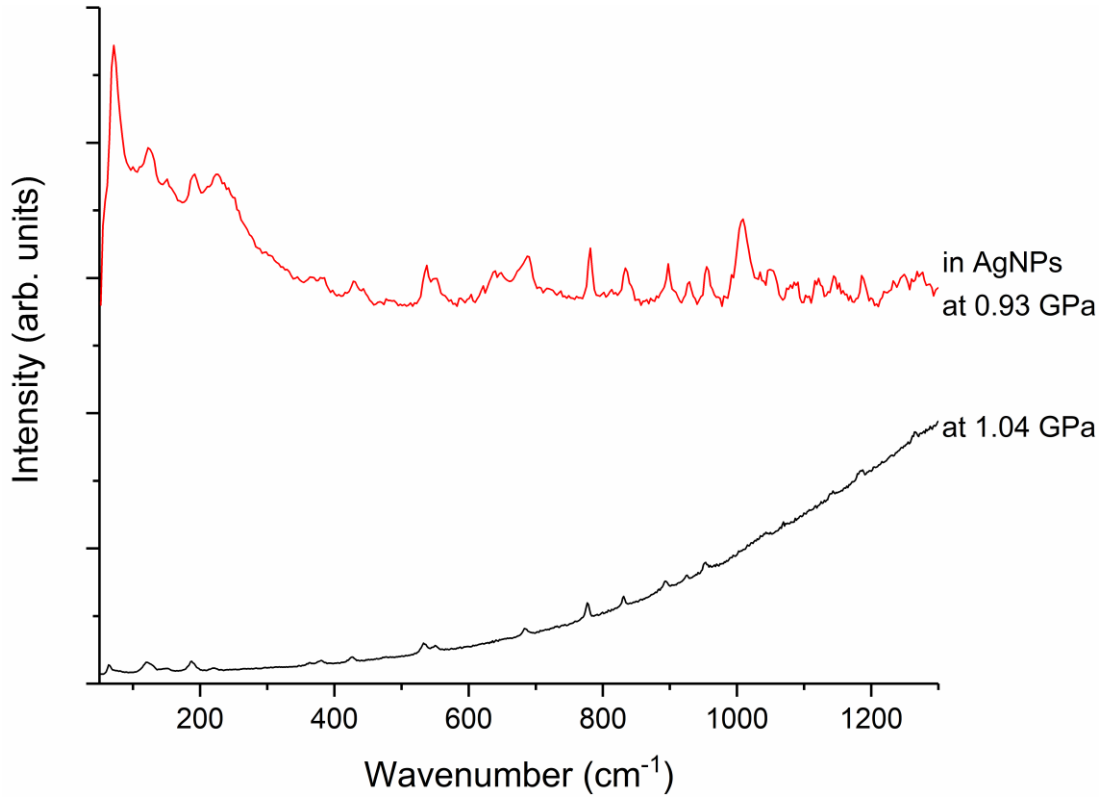

Figure 3.10 Comparative Raman spectra of DL-valine with and without the use of AgNPs. The Raman spectrum in red where AgNPs were suspended in the PTM shows a better Raman signal and distinguishable peaks. Both spectra are untreated.

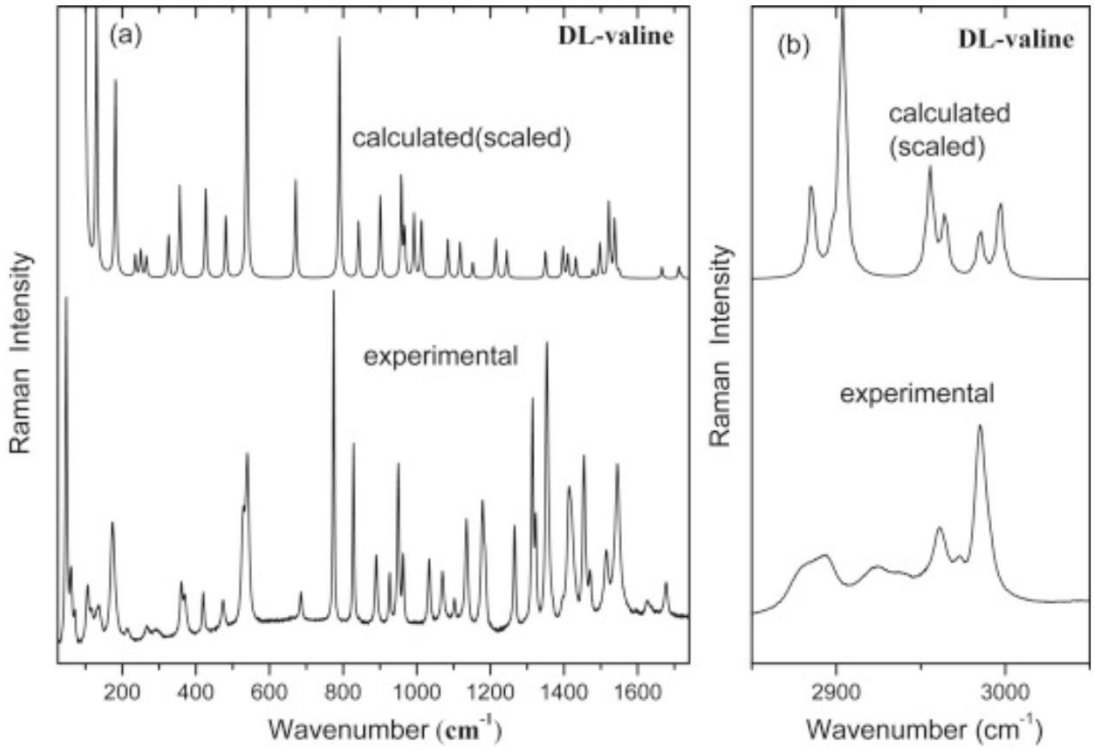

Figure 3.11 Raman spectra of DL-valine (calculated and experimental) in the spectral range 20-1680 cm^{-1} in (a) and 2800-3200 cm^{-1} in (b).Reproduced from reference [30]

3.3.2.2 L-leucine

A similar phenomenon of Raman signal enhancement was observed in L-leucine when using AgNPs in the PTM compared to PTM without AgNPs. In the spectral region 50-1300 cm^{-1}, more distinguishable and clearly defined peaks were observed in the SERS dataset (Figure 3.12). The assignment of these peaks is presented in Table 3.3.

Table 3.3 L-leucine selected peak assignments in the spectral region 50-1300 cm^{-1} [34]

Peak Position (cm^{-1})	Assignment	Peak Position (cm^{-1})	Assignment
73	lattice	772	(CO_2^-)
104	lattice	840	(CO_2^-)
204	τ(CH)	925	v(CC) & v(CN)
346	def (NCC)	966	v(CC) & v(CN)
401	skeletal def	1137	$r(NH_3^+)$
464	skeletal def	1179	$r(NH_3^+)$
544	$r(CO_2^-)$	1247	$\tau(CH_2)$

The selected Raman peak assignments of L-leucine in the spectral region 50-1300 cm^{-1} presented in Table 3.3 have been assigned by Filho et al.[36] experimentally using L-leucine single crystals grown from an aqueous solution containing powder by the slow evaporation method at controlled temperature. Referring to Figure 3.12, it is clearly seen that the majority of Raman bands assigned in Table 3.3 are present when using AgNPs.

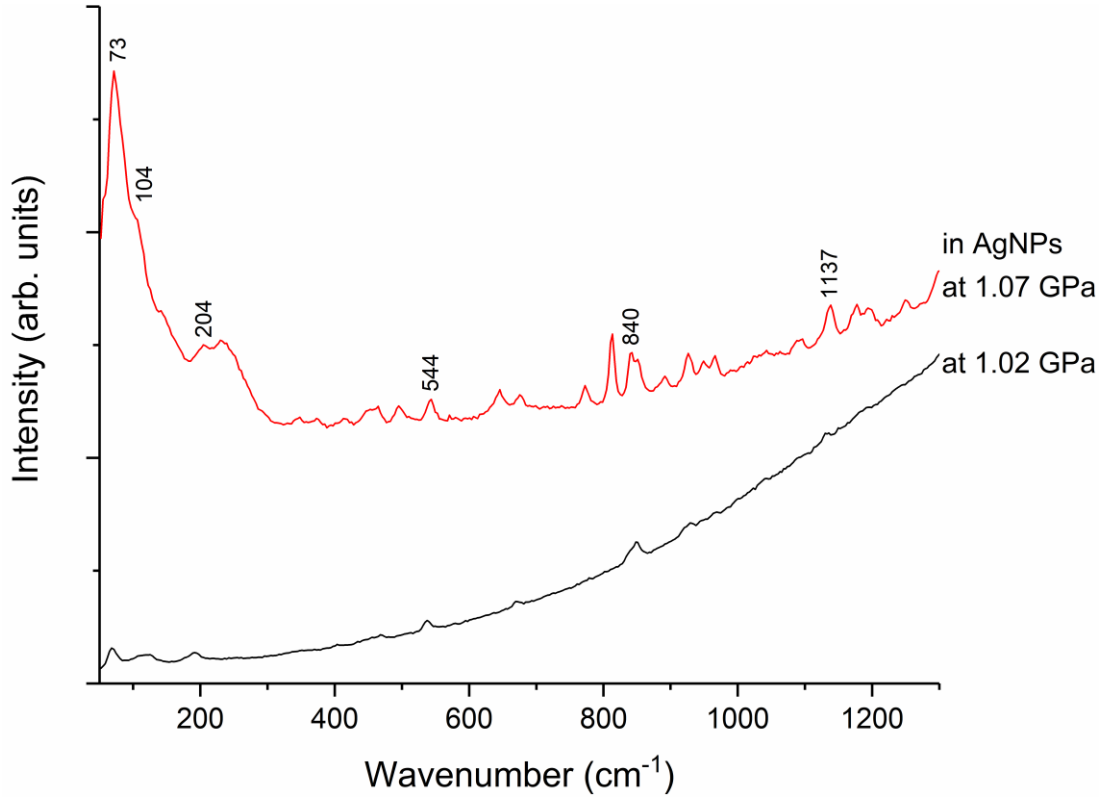

Figure 3.12 Comparative Raman spectra of L-leucine with and without the use of AgNPs. The Raman spectrum in red where AgNPs were suspended in the PTM shows a better Raman signal and distinguishable peaks. Both spectra were untreated.

3.3.2.3 L-isoleucine

L-isoleucine is another amino acid that exhibits weak Raman scattering property. The Raman spectrum acquired by using AgNPs in the PTM shows clearer and distinguishable peaks across the spectrum in comparison with the one recorded using methanol:ethanol (4:1) (Figure 3.13). The assignments of selected peaks is presented in Table 3.4

Table 3.4 L-isoleucine selected peak assignments in the spectral region 50-3500 cm^{-1} [35]

Peak Position (cm^{-1})	Assignment	Peak Position (cm^{-1})	Assignment
71	lattice	1032	ν(CN)
143	lattice	1089	ν(CN)
549	lattice	1141	$r(NH_3^+)$
716	$\omega(CO_2^-)$	1452	$\delta(CH_3)$
830	$\gamma(CO_2^-)$	2849	$\nu_S(CH_3)$
859	$r(CH_3)$	2953	ν(CH)
885	ν(CC)	3001	$\nu_{as}(CH_3)$

The selected Raman peak assignments of L-isoleucine in the spectral region 50-3500 cm^{-1} presented in Table 3.4 have been assigned by Almeida et al.[37] experimentally using L-isoleucine single crystals grown from an aqueous solution with a solute to solvent ratio of 1:30 at a controlled temperature (293 K) for 60 days before spectrum was collected. The Raman spectra collected using the SERS technique shows reasonable Raman bands but the 2 highly intense peaks in the low phonon region at 71 and 250 cm^{-1} are hiding the details of other peaks. The latter peak has not been assigned and it could be a contribution from the AgNPs. Another reason for these peaks could be the orientation of the crystals adjacent to the substrate, hence showing a very high intensity.

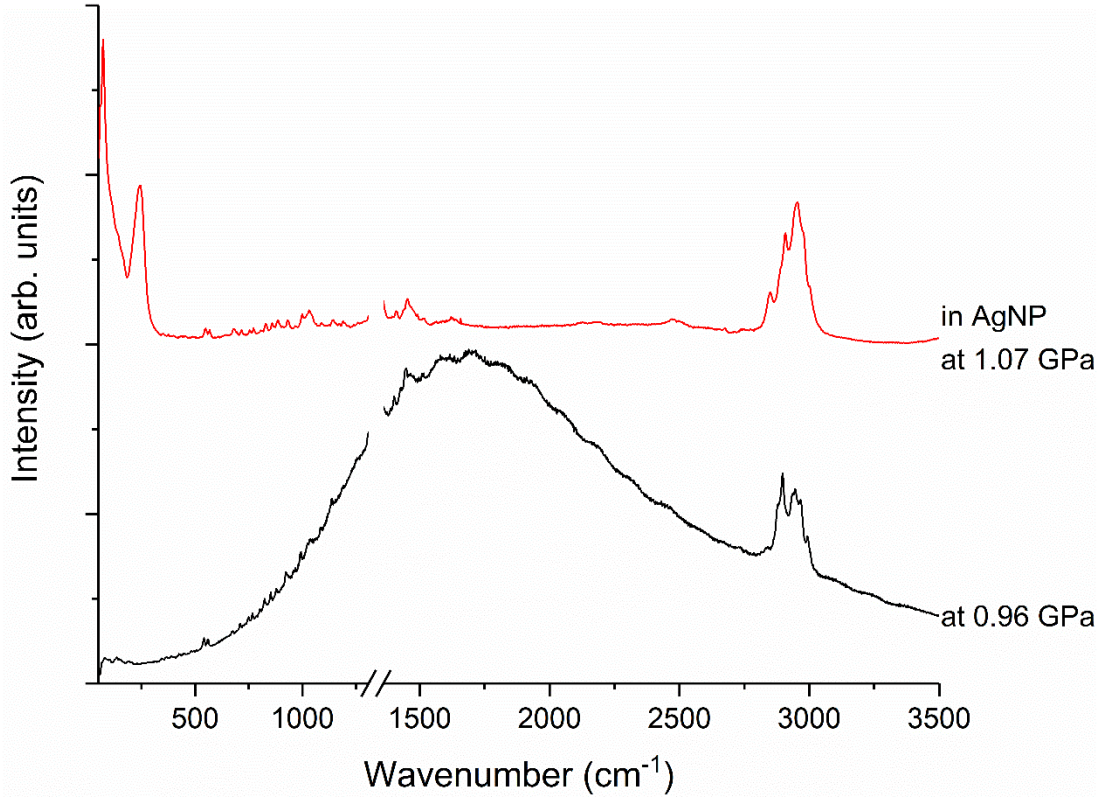

Figure 3.13 Comparative Raman spectra of L-isoleucine with and without the use of AgNPs. The Raman spectrum in red where AgNPs were suspended in the PTM shows a better Raman signal and distinguishable peaks. Both spectra were untreated.

3.3.2.4 Poly glycolic acid

Both the powder and pellets of PGA had the same issue of fluorescence despite trying different techniques like changing the laser and solvent washing. It is clearly seen in Figure 3.14 that there was an enhancement of some Raman bands when using the PTM with AgNPs. The most enhanced peaks were at 72, 239, 619 and 2954 cm^{-1} corresponding to τ(CC), δ(COC), γ(C=O) and $\nu_{as}(CH_2)$ vibrations respectively.[36] Both peaks at 72 and 239 cm^{-1} have the highest intensity enhancement across the spectrum and this could be attributed to the orientation of crystals of the examined sample in relation to the incident laser beam or to the number of hot-spots between the nanoparticles or could be from the nanoparticles.

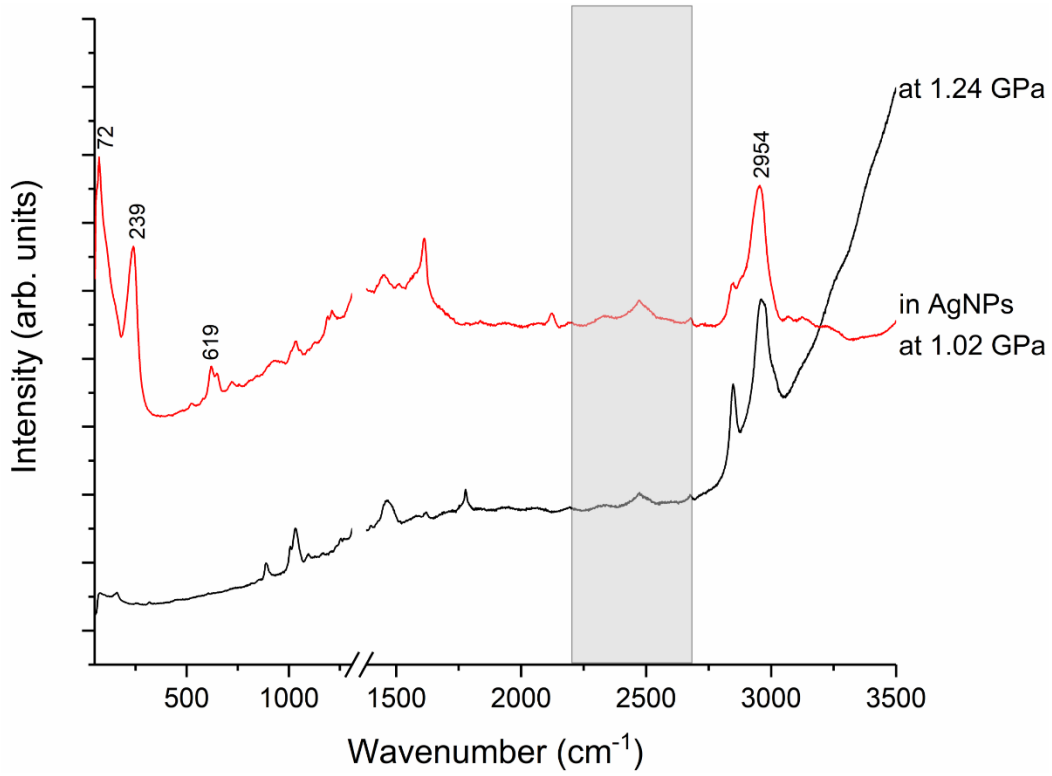

Figure 3.14 Comparative Raman spectra of PGA with and without the use of AgNPs. Numbered Raman peaks are the ones with most enhancement in signal. Both spectra were untreated. The shaded area is background fluorescence of diamond,

3.3.2.5 Poly lactide-co-glycolide

PLGA was received as small yellowish glassy crystals which were difficult to break into smaller particles. These crystals were used as received. It is evident from Figure 3.15 that the use of AgNPs in the PTM has improved the Raman signal dramatically. More distinguishable peaks can be clearly seen especially in the spectral region of 50-1300 cm^{-1} and 1420-1850 cm^{-1} with an improved signal to noise ratio and increased area under the peak. Some selected peaks including peaks at 71, 242, 400, 877, 1769 and 2963 have been assigned as C-C skeletal torsion, CH_3 torsion, CCO deformation, CH_2 rocking, C=O stretch and asymmetric stretch of CH_3 respectively.[33,37]

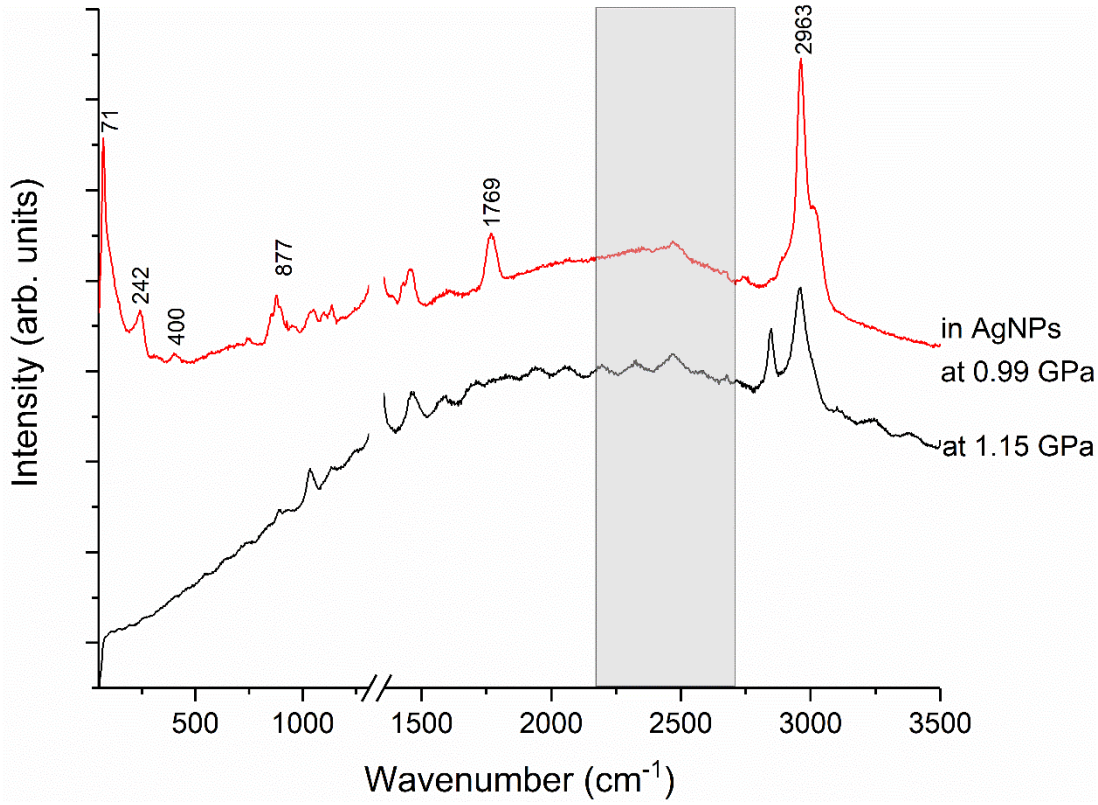

Figure 3.15 Comparative Raman spectra of PLGA with and without the use of AgNPs. Numbered Raman peaks are the ones with most enhancement in signal. Both spectra were untreated. The shaded area is background fluorescence of diamond,

3.4 Evaluation of SERS at high pressure

In this study, we have been able to improve *in situ* Raman signalling by adopting SERS technique. The AgNPs were simply suspended in the PTM with no chemical bonding or alteration. To the best of our knowledge and available literature, this technique is novel and has not been used before. Other studies have used silver nanoparticle layer assembled on poly (allylamine hydrochloride) silicon wafer. Weak scattering amino acids were tested and improvements in their Raman signal was seen. More challenging systems like fluorescent polymers were also tested. Raman signal was enhanced for polymers as well but not as the great enhancement seen in the amino acids. This finding is attributed to the crystalline nature of the examined compounds. The amino acids are

crystalline thus allow the penetration of AgNPs between the crystals, hence a better enhancement is seen. Polymers, on the other hand, are non-crystalline or semi-crystalline and spaces between particles are irregular. PGA was ball-milled beforehand which may render the particles to interact with each other and minimise the entry of AgNPs between them. PLGA was used as a crystal as received from the supplier. For that reason, the attachment of AgNPs was limited to its surface only. This could be the reason why a better enhancement was seen in the amino acids and not in the polymers. SERS technique is believed to enhance Raman signal by electromagnetic enhancement related to rough ended metal surface or by chemical enhancement between the analyte and the substrate.

Another common issue with SERS is the reproducibility. As seen in this chapter, it proved to enhance Raman signalling under high pressure but the level of enhancement was different between batches. This is attributed to the shape, roughness, and other characteristics of the nanostructures. A comparison between both batches is performed for one the samples (l-leucine) to ensure the presence of Raman bands (Figure 3.16). Both Raman spectra show the majority of the peaks of the compound with different resolutions and intensities. This is attributed to the crystal orientation in relation to the nanoparticles and their proximity. Some bands are wider when compared between batches 1 and 2; this may be due to the intensity of other peaks as well as crystal orientation.

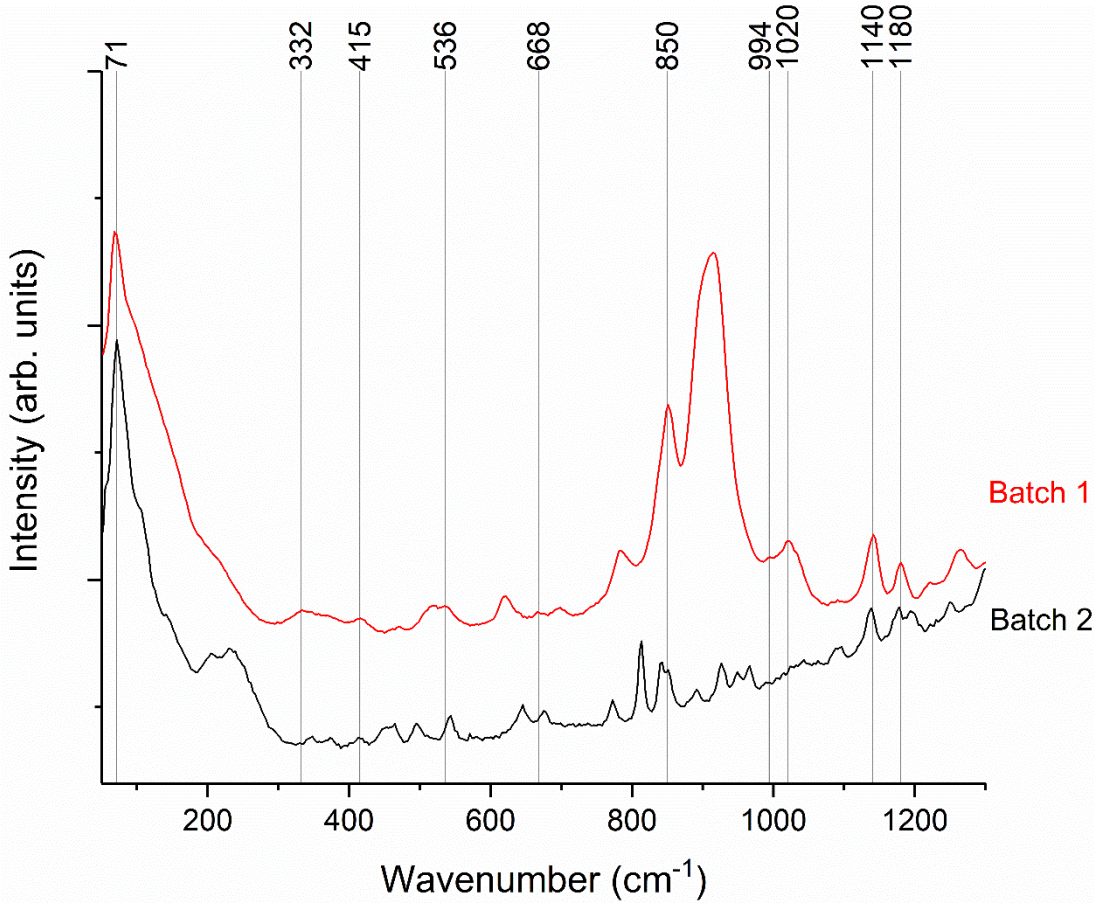

Figure 3.16 Comparative Raman spectra of L-leucine (50-1300 cm-1) at about 1 GPa using different batches of AgNPs in the PTM. Selected peaks are used as reference. Both spectra are untreated.

3.5 Conclusions

In this study, we have obtained the *in situ* SERS of selected fluorescent polymers and weakly scattering amino acids at a pressure point of *ca* 1 GPa in a diamond anvil cell. In the SERS experiments, silver nanoparticles were suspended in the PTM without any chemical binding or modifications. Analysis of the Raman spectra showed signal enhancement and better signal to noise ratio in the AgNPs datasets. In conclusion, we have reported a novel method for improving Raman signalling of fluorescent and weak Raman scaterers under high pressure using SERS technique by simply suspending the

AgNPs in the PTM. This effect is attributed to either electromagnetic enhancement associated with rough ended metal surface or chemical enhancement between examined molecules and AgNPs.

3.6 References

[1] Alexander FG. Raman Spectroscopy at High Pressures. International Journal of Spectroscopy. 2012;2012(2012)

[2] Schlücker S. Surface- Enhanced Raman Spectroscopy: Concepts and Chemical Applications. Weinheim2014. 4756-95.

[3] Smith E. Modern Raman spectroscopy: a practical approach. Dent G, editor. Hoboken, NJ: Hoboken, NJ: J. Wiley; 2005.

[4] Fleischmann M, Hendra PJ, McQuillan AJ. Raman spectra of pyridine adsorbed at a silver electrode. Chemical Physics Letters. 1974 May 15;26(2):163-6.

[5] Albrecht MG, Creighton JA. Anomalously Intense Raman Spectra of Pyridine at a Silver Electrode. Journal of the American Chemical Society. 1977;99(15):5215-7.

[6] Cialla D, März A, Böhme R, Theil F, Weber K, Schmitt M, et al. Surface- enhanced Raman spectroscopy (SERS): progress and trends. Anal Bioanal Chem. 2012;403(1):27-54.

[7] Nie S, Emory SR. Probing Single Molecules and Single Nanoparticles by Surface-Enhanced Raman Scattering. Science. 1997;275(5303):1102-6.

[8] Kneipp J, Kneipp H, Wittig B, Kneipp K. Novel optical nanosensors for probing and imaging live cells. Nanomedicine: Nanotechnology, Biology, and Medicine. 2010;6(2):214-26.

[9] Moskovits M. Surface- enhanced Raman spectroscopy: a brief retrospective. Journal of Raman Spectroscopy. 2005;36(6-7):485-96.

[10] Betz JF, Yu WW, Cheng Y, White IM, Rubloff GW. Physical Chemistry Chemical Physics 2014. 16, 2224.

[11] Moskovits M. Surface- enhanced spectroscopy. Reviews of Modern Physics. 1985;57(3):783-826.

[12] Otto A. The 'chemical' (electronic) contribution to surface- enhanced Raman scattering. Journal of Raman Spectroscopy. 2005;36(6-7):497-509.

[13] Zhao J, Pinchuk A, McMahon J, Li S, Ausman L, Atkinson AL, et al. Methods for Describing the Electromagnetic Properties of Silver and Gold Nanoparticles. Accounts Chem Res2008. 1710-20.

[14] Yamamoto Y, Ishikawa M, Ozaki Y, Itoh T. Fundamental studies on enhancement and blinking mechanism of surface-enhanced Raman scattering (SERS) and basic applications of SERS biological sensing. Front Phys. 2014. 31-46.

[15] Campion A. Surface-enhanced Raman scattering. Chemical Society reviews. 1998;27(4):241.

[16] McNay G, Eustace D, Smith WE, Faulds K, Graham D. Surface-Enhanced Raman Scattering (SERS) and Surface-Enhanced Resonance Raman Scattering (SERRS): A Review of Applications. 2011. 825-37.

[17] Emamian S, Eshkeiti A, Narakathu BB, Avuthu SGR, Atashbar MZ. Gravure printed flexible surface enhanced Raman spectroscopy (SERS) substrate for detection of 2,4-dinitrotoluene (DNT) vapor. Sensors & Actuators: B Chemical. 2015; 217:129-35.

[18] Yaffe NR, Blanch EW. Effects and anomalies that can occur in SERS spectra of biological molecules when using a wide range of aggregating agents for hydroxylamine- reduced and citrate- reduced silver colloids. Vibrational Spectroscopy. 2008;48(2):196-201.

[19] Graham AJ, Allan DR, Muszkiewicz A, Morrison CA, Moggach SA. The Effect of High Pressure on MOF- 5: Guest- Induced Modification of Pore Size and Content at High Pressure. Angewandte Chemie International Edition. 2011;50(47):11138-41.

[20] Fabbiani FPA, Pulham CR. High- pressure studies of pharmaceutical compounds and energetic materials. Chemical Society reviews. 2006;35(10):932-42.

[21] Bassett W. Diamond anvil cell, 50th birthday. High Pressure Research, 2009, Vol29(2), CP5-186.

[22] Wang P, Li H, Cui C, Jiang J. In situ surface enhanced Raman spectroscopy detection in high pressure solution. Applied Surface Science. 2017; 425:833-7.

[23] Brown KE, Dlott DD. High- pressure raman spectroscopy of molecular monolayers adsorbed on a metal surface. Journal of Physical Chemistry C. 2009;113(14):5751-7.

[24] Piermarini GJ, Block S, Barnett JD, Forman RA. Calibration of the pressure dependence of the R 1 ruby fluorescence line to 195 kbar. Journal of Applied Physics. 1975;46(6):2774-80.

[25] Lee PC, Meisel D. Adsorption and surface- enhanced Raman of dyes on silver and gold sols. Journal of Physical Chemistry. 1982;86(17):3391-5.

[26] Adar F. Considerations of Grating Selection in Optimizing a Raman Spectrograph. Spectroscopy (Santa Monica). 2013;28(9)

[27] OriginLab C. OriginPro. b9.4.1.354 (Academic) ed. Northampton, MA 01060 USA2017

[28] Murli C, Vasanthi R, Sharma SM. Raman spectroscopic investigations of dl-serine and dl- valine under pressure. Chemical Physics. 2006;331(1):77-84.

[29] Casado J. Infrared and Raman spectra of l-asparagine and l-asparagine-d5 in the solid state. Journal of Raman spectroscopy. 1995;26(11):1003.

[30] Paiva FM, Batista JC, Rêgo FSC, Lima JA, Freire PTC, Melo FEA, et al. Infrared and Raman spectroscopy and DFT calculations of DL amino acids: Valine and lysine hydrochloride. Journal of Molecular Structure. 2017;1127(C):419-26.

[31] Pawlukojc A, Leciejewicz J, Natkaniec I. The INS spectroscopy of amino acids: l-leucine. Spectrochimica Acta Part A: Molecular and Biomolecular Spectroscopy. 1996;52(1):29-32.

[32] Bougeard D. Phase Transition and Vibrational Spectra of I-Leucine. Berichte der Bunsengesellschaft für physikalische Chemie. 1983 Mar;87(3):279-83.

[33] Lima JA, Freire PTC, Lima RJC, Moreno AJD, Mendes Filho J, Melo FEA. Raman scattering of L - valine crystals. Journal of Raman Spectroscopy. 2005;36(11):1076-81.

[34] Filho PFF, Freire PTC, Lima JMF, Melo FEA. High temperature Raman spectra of L-leucine crystals. Brazilian journal of physics: 2008;38(1):131.

[35] Almeida FM, Freire PTC, Lima RJC, Remédios CMR, Mendes Filho J, Melo FEA. Raman spectra of L - isoleucine crystals. Journal of Raman Spectroscopy. 2006;37(11):1296-301.

[36] G. Cassanas, G. Kister, E. Fabrègue, M. Morssli, L. Bardet, Raman spectra of glycolic acid, l-lactic acid and d,l-lactic acid oligomers, Spectrochimica Acta Part A: Molecular Spectroscopy, Volume 49, Issue 2, 1993, Pages 271-279,

[37] Cassanas G, Vert M, Pauvert B, Terol A. Vibrational analysis of poly (l-lactic acid). J Raman Spectrosc. 1995;26(4):307-11.

Chapter Four: Raman Spectroscopic Investigation of Polymers and Model API under High Pressure

4.1 Introduction

The application of pressure has been easier than before and this is due to the invention of diamond anvil cells (DAC).[1] This made the science of high pressure popular among different disciplines of science including chemistry, physics, geology etc. The application of pressure is used to have a better understanding of how materials respond to the thermodynamic parameter of pressure. Polymorphism, the main drive behind this, is the ability of a compound to exist in multiple crystalline forms.[2] These polymorphs can exhibit different physicochemical properties like solubility, stability and melting point, which makes it very important for pharmaceutical industry as these properties have an impact on the bioavailability, processability and storage of pharmaceuticals.[3] Ritonavir, a protease inhibitor used in the treatment of human immune deficiency syndrome, is one of the exemplary medicines that represent the impact of polymorphism.[4] It was produced as oral liquid and semi-solid capsules dosage forms in ethanol/water based solutions as it was not bioavailable from the solid form. Two years after marketing, several lots failed the dissolution requirements. A new polymorph was identified after further examinations using x-ray powder diffraction and microscopy. This polymorph had greatly reduced solubility and referred to as form II.

Some of the processes involved in pharmaceuticals manufacturing exhibit pressure generation including roller compaction, hot melt extrusion and tabletting. The application of pressure has been studied on hard materials, pharmaceuticals and organic materials. One area that has not been exploited in the area of high pressure is polymers and how they respond to pressure. Polymers are macromolecules that consist

of a set of regularly repeated units and can be natural or synthetic. They are used widely in pharmaceutical and biomedical applications especially in the area of controlled drug delivery.[5] Polyesters and cellulose derivatives are commonly used examples. Poly glycolic acid (PGA) is a polyester that has high mechanical properties and melting point, compared to other aliphatic polyesters. It is used in biomedical applications including sutures, bone fixation and drug delivery systems and that is because of its biocompatibility, biodegradability and non-toxicity.[6,7,8] The high mechanical strength could be explained by the planar zigzag conformation of PGA. Cellulose and its derivatives are extensively used in pharmaceutical and biomedical applications as they can be chemically modified according to the intended use. These modifications are mainly determined by their chemical structures, molecular weight and distribution of substituent groups. Such modifications lead to change in physical/chemical properties of the end-products including stability, solubility and viscosity. Examples of cellulose modifications include microcrystalline cellulose (MCC), ethylcellulose (EC), hydroxypropyl methylcellulose (HPMC) and carboxymethyl cellulose (CMC).

To be able to study these materials under high pressure, Raman spectroscopy was used as the studied samples are semi-crystalline or amorphous. Additionally, it is one of the commonly used vibrational techniques in the area of high pressure as it provides fingerprinting of materials being examined. It provides high selectivity for the phonon region, which determines the state of materials. Moreover, phase transitions and polymorphism of materials can be detected using Raman spectroscopy.[9]

The aim of this chapter was to investigate the behaviour of commonly used pharmaceutical polymers and a model API, ibuprofen (IBP) under high pressure using Raman spectroscopy. Simple polymers like PGA and PLA and their response to

pressure is compared with complex polymer systems like EC and HPMC. The latter will be studied in formulations under high pressure in Chapter Five. The chemical structures of these polymers and IBP are presented in Figure 4.1.

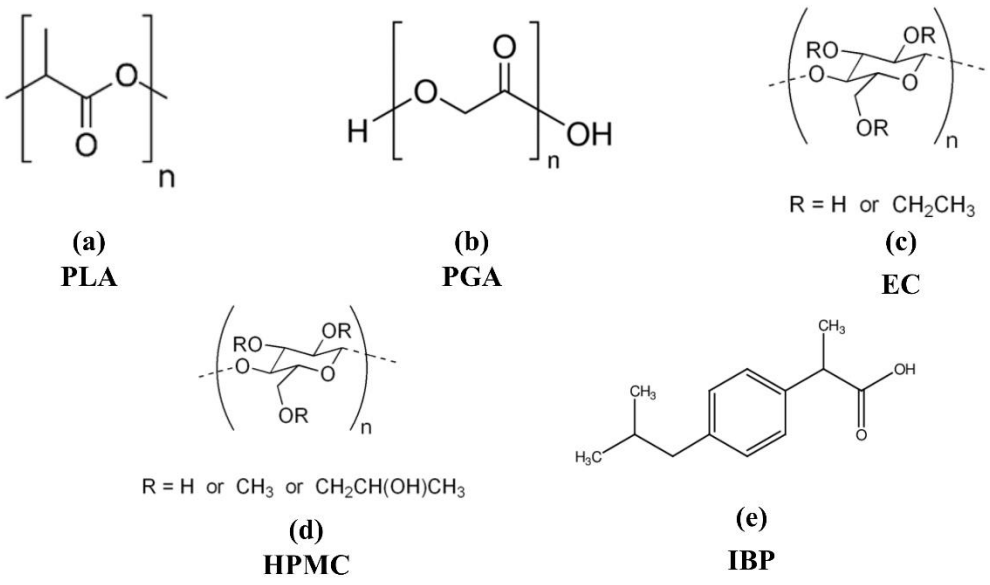

Figure 4.1 Chemical structures of simple polymers (a) poly lactic acid, (b) poly glycolic acid and complex polymers (c) ethylcellulose, (d) hydroxypropyl methylcellulose and (e) ibuprofen used in high pressure studies

4.2 Materials and Methods

4.2.1 Materials

Poly lactic acid (PLA), poly glycolic acid (PGA) and ibuprofen (IBP, ≥98%) were purchased from Sigma Aldrich (Irvine, UK). Ethylcellulose (EC) 10 premium (Ethocel™) and hydroxypropyl methylcellulose (HPMC) E50 premium (Methocel™) were kindly gifted by Colorcon® (Kent, UK). Methanol (analytical reagent grade) and Ethanol (analytical reagent grade) were purchased from VWR (Leicestershire, UK). Petroleum ether 35/60 ACS grade was purchased from Alfa Aesar (Lancashire, UK).

4.2.2 Methods

4.2.2.1 Sample preparation

Samples were ground individually for 10 minutes using an agate mortar and pestle, as shown in Table 4.1, unless otherwise specified.

Table 4.1 Summary of samples and quantities used

Sample	PLA	PGA	EC	HPMC	IBP
Quantity used	100 mg	300 mg	100 mg	100 mg	100 mg

4.2.2.2 High pressure

High pressure studies were conducted using Merrill-Basset DAC containing two opposed gem-quality diamonds with 600 µm culets supported by tungsten carbide backing discs. Tungsten was used as a gasket material with a thickness of 230 µm and it was pre-indented to ~ 90 - 100 µm. The gasket was drilled in the centre of the indent using Boehler microDriller®, an electro-discharge-machine, using a tungsten carbide electrode (250 µm). The hole was used as the sample chamber. The sample was added

to the sample chamber and packed into the hole to ensure that enough material was in the hole for analysis. Methanol:ethanol (4:1) or petroleum ether were used as pressure transmitting medium (PTM) to ensure that the samples were compressed isotropically and no shear was introduced; ruby chips were added to the sample chamber to measure the in-situ pressure.[10] Sample were tested at pressure ranges between ambient pressure and 8.8 GPa as described in relevant sections.

4.2.2.3 Raman spectroscopy

Raman spectra were acquired using Raman XplorA Microscope by Horiba Scientific John Yvon Technology with an excitation wavelength of 532 nm. Spectra were summed using 2 accumulations and a grating of 1200-gr/mm, which was found to be the best suitable to yield good peak resolution.[11] Diamond has a strong peak between 1330 and 1380 cm^{-1} hence this region is not shown in the Raman spectra of high pressure data sets. Data analysis and graph production was done using OriginPro® 2017 software (OriginLab, Northampton, MA).[12]

4.3 Results and Discussion

4.3.1 Poly lactic acid (PLA)

4.3.1.1 Ambient pressure characterisation

To ensure that the starting material received was consistent with literature data, the Raman spectrum (50-3500 cm^{-1}) was acquired for PLA powder at ambient pressure (Figure 4.3). Another reason for that is to ensure that PTM does not interact or alter the sample as both methanol and ethanol are found to induce cold crystallisation at 37 °C.[13] In this study, PLA was exposed to different liquids i.e. water, methanol and

ethanol using thermal analysis to elucidate if these liquids alter the physical structures of PLA. They found that water had no effect on the cold crystallisation and melting peaks of PLA but cold crystallisation peak and glass transition were 10 °C lower than the unexposed sample. On the other hand, samples exposed to methanol for 72 hours and longer had a higher shift in glass transition (20-30 °C) in comparison to the unexposed sample displaying no cold crystallisation peak and a large melting peak. Sample exposed to methanol for 24 hours only showed cold crystallisation peak. Exposure to ethanol had a similar effect on PLA but the peak remained for longer time suggesting that cold crystallisation was slower in ethanol than methanol at 37 °C. Both methanol and ethanol induced cold crystallisation which in turn resulted in fast methanol uptake into the rubbery PLA structure while the second stage highlighted a low uptake of methanol due to the growth of tighter semi-crystalline layers. The peak assignments are consistent with the study of Kister et al. and are presented in Table 4.2 as well as indicated on Figure 4.3.[14] It is clear from the distinct peaks in the low-energy phonon region that the received sample of PLA is crystalline. This region is very sensitive to crystal structure and are attributed to external lattice vibrational modes and bands.[15] External vibrations are a collective motion of molecules as a whole. Low-energy bands arise because of shear or interlayer breathing modes. In the former, shear modes, atoms and molecular layers move antiparallel from each other within their planes. On the other hand, in breathing modes, those layers move away and towards each other.

Table 4.2 Raman peak positions of PLA and their assignments[14]

Peak Position (cm^{-1})	Assignment	Peak Position (cm^{-1})	Assignment
60	skeletal C-C torsion	1042	$\nu C\text{-}CH_3$
77	skeletal C-C torsion	1092	$\nu_s COC$
117	skeletal C-C torsion	1128	$r_{as}CH_3$
158	skeletal C-C torsion	1179	$\nu_{as}COC$
208	CH_3 torsion	1216	$\nu_{as}COC$
238	CH_3 torsion	1293, 1302, 1315	δCH
251	CH_3 torsion	1356	$\delta CH + \delta_s CH_3$
300-308	$\delta C\text{-}CH_3$ bend	1363, 1371	$\delta CH + \delta_s CH_3$
398-411 doublet	CCO deformation	1384, 1388	$\delta_s CH_3$
520	$\delta C\text{-}CH_3$ bend	1452	$\delta_{as}CH_3$
675	$\gamma C{=}O$ out-of-plane bending	1749	$\nu(C{=}O)$
711	$\gamma C{=}O$	1763	$\nu(C{=}O)$
736	$\delta C{=}O$ in-plane bending	1773	$\nu(C{=}O)$
760	$\delta C{=}O$ in-plane bending	2877	νCH
873	$\nu C\text{-}COO$	2901	νCH
923	$rCH_3 + \nu CC$	2943	$\nu_s CH_3$
954	$rCH_3 + \nu CC$	2960, 2970, 2995	$\nu_{as}CH_3$

Raman peaks of PLA were assigned using amorphous and crystalline PLA, while some of them and some infra-red bands have been proposed by comparison with work on other similar compounds with a helical structure such as polypropylene and poly(α-L-alanine).[14] These assignments are also similar to the work done by Qin et al.[16] and Kister et al.[17], in which they determined the crystallinity of PLA exhibiting different crystallinities. Working with compounds under high pressure, it is important to have an idea about what effect pressure can exert on the sample. Torsional angles can be affected by the application of pressure as seen in paracetamol,[18] glycolide[19] and 3-Hydroxy-4,5-dimethyl-1-phenylpyridazin-6-one.[20] The latter transformed from α

phase to γ phase at 0.4 GPa and stayed intact for months after being retrieved to ambient pressure.

At ambient pressure the α form of PLA packs together so that the chains align along the c-axis of the unit cell determined via a combination of wide-angle X-ray and neutron scattering. From their analysis, Wasanasuk et al observed that the chains are closed packed when viewed down the c-axis. The oxygen and methyl side groups of neighbouring chains pack in close proximity to each other (Figure 4.2).[21] This makes it prone to potential torsional angle changes by the application of pressure which will be observed through the Raman modes at X and Y cm^{-1}.

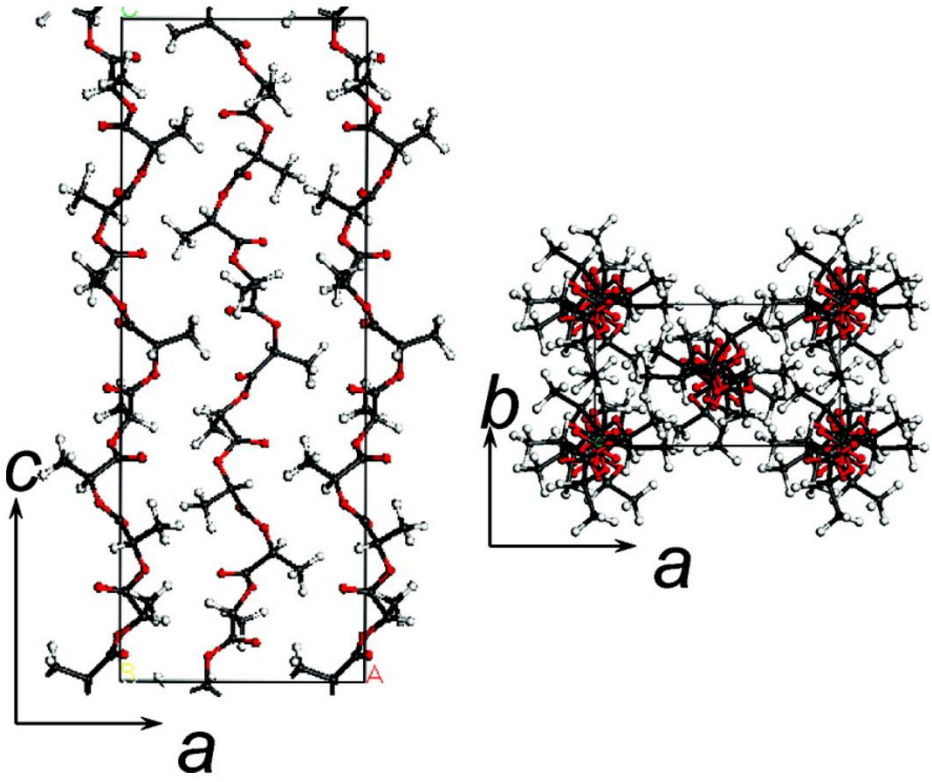

Figure 4.2 Crystal structure of PLLA α form (reproduced from reference 21)

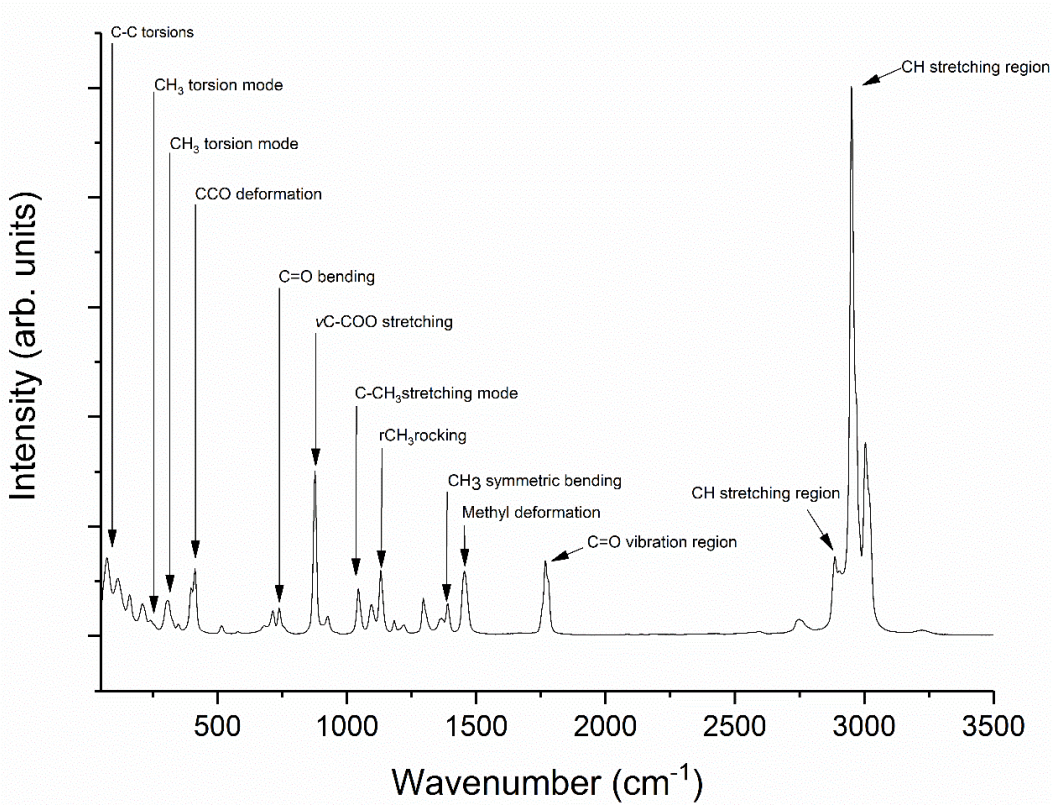

Figure 4.3 PLA Raman spectrum at ambient pressure with peak assignments that can also be found in Table 4.2

4.3.1.2 High pressure characterisation

Raman spectra of PLA powder as a function of pressure up to 8.8 GPa, measured at room temperature, are reported here. The spectra presented in Figure 4.4 (a) show distinct Raman peaks in the low-energy phonon region decreasing in intensity and becoming broader as pressure increases. Those peaks were present and clearly seen until 4.57 GPa. After that pressure point, they started to either disappear or become too broad and difficult to be distinguished. This is an indication that PLA is losing its crystallinity. This is confirmed as other vibrations also broaden and become overlapped with one another at pressure points above 5 GPa. The doublet peaks at 398 and 411 cm^{-1} corresponding to CCO deformation were clearly differentiated at pressures below 4.57 GPa but become broader at pressures beyond this. The peak at

873 cm^{-1} corresponding to ν*C*-COO stretching of the repeating unit of the polymeric chain has turned into a doublet at 2.2 GPa and started to decrease in intensity as pressure increased (Figure 4.4 (b)). This phenomenon of decreased particular peak intensity assists the idea of phase transition. The distance between the doublet peaks increased at 4.57 GPa and they seemed to merge at higher pressures. One of the reasons a peak may become broader and have a reduced intensity is due to the change of the environment surrounding the molecules and the decreased spatial order of molecules. In a crystalline sample the long range order is present due to the fact that the molecules are similarly orientated and the groups have a similar environment. As the molecules change orientation or environment then the molecular vibrations are no longer the same and may have slightly different energies hence a broader peak. A study by Bardet et.al[22] found that the peak at 873 cm^{-1} increased in intensity from 90% concentration solution to viscous state and then to solid state, where molecules in the solution will be less ordered than viscous than solid state. In our experiment, we started with a solid state PLA that exhibited intense sharp peaks at the start. These peaks decreased in intensity and sharpness as pressure increased reaffirming that PLA is moving towards a less order state as pressure increases. Raman peaks at 1042, 1092 and 1128 cm^{-1} were assigned as ν*C*-CH_3 stretching mode, ν_sCOC and $r_{as}CH_3$ rocking respectively. They also exhibited a similar phenomenon of losing the peak sharpness and became broader as pressure increased (Figure 4.4 (b)). In the C=O vibration region, the Raman peak at 1766 cm^{-1} and its shoulder at 1777 cm^{-1} were both assigned as ν(C=O). They have merged and became one broad peak at 5.44 GPa and above. This is better explained by the use of full-width half maximum (FWHM) value of certain peaks (Figure 4.5 (a)). FWHM gives a better representation of peak broadening and the dashed line in

the figure shows the transition point at which many peaks broaden indicating a change of state from a more ordered arrangement of molecules to a less ordered arrangement.

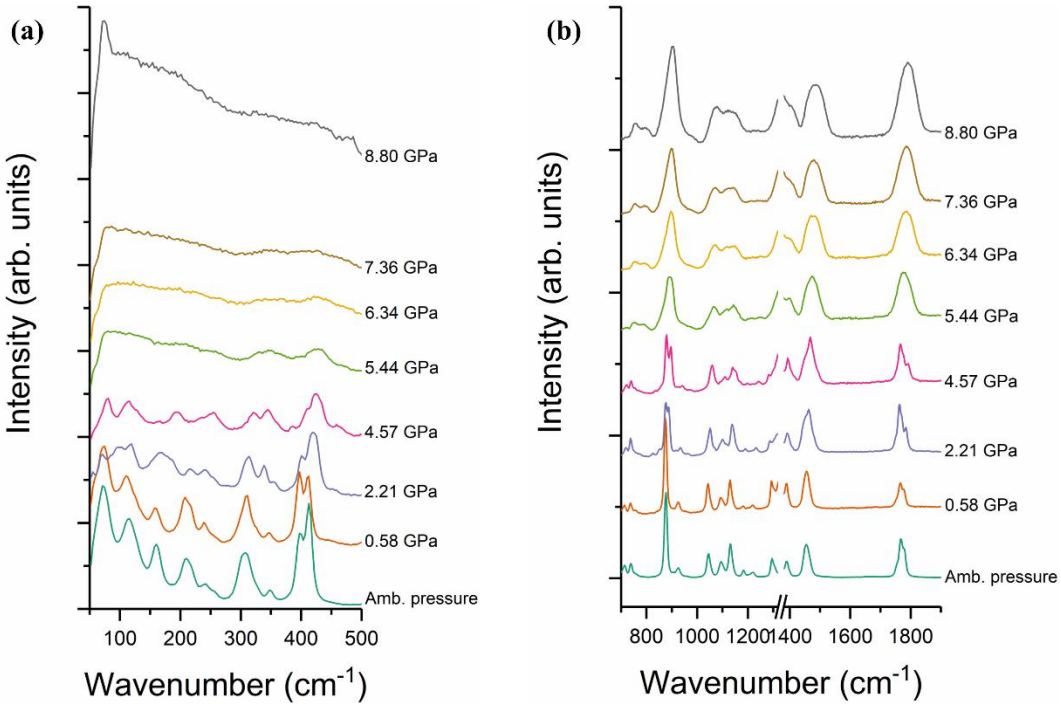

Figure 4.4 Raman spectra of PLA at increasing pressure in spectral region of (a) 50-500 cm^{-1}, (b) 700-1900 cm^{-1}. PLA was compressed in 4:1 meOH:etOH to ensure hydrostatic environment. Note at 2.2 GPa a transition to a possible new polymorph as peaks at 100 and 120 cm^{-1} start to change,the peak at 160 cm^{-1} split and the peak at 873 cm^{-1} split and at 5.44 GPa the broadening of the vibrations indicating transition to a less ordered state

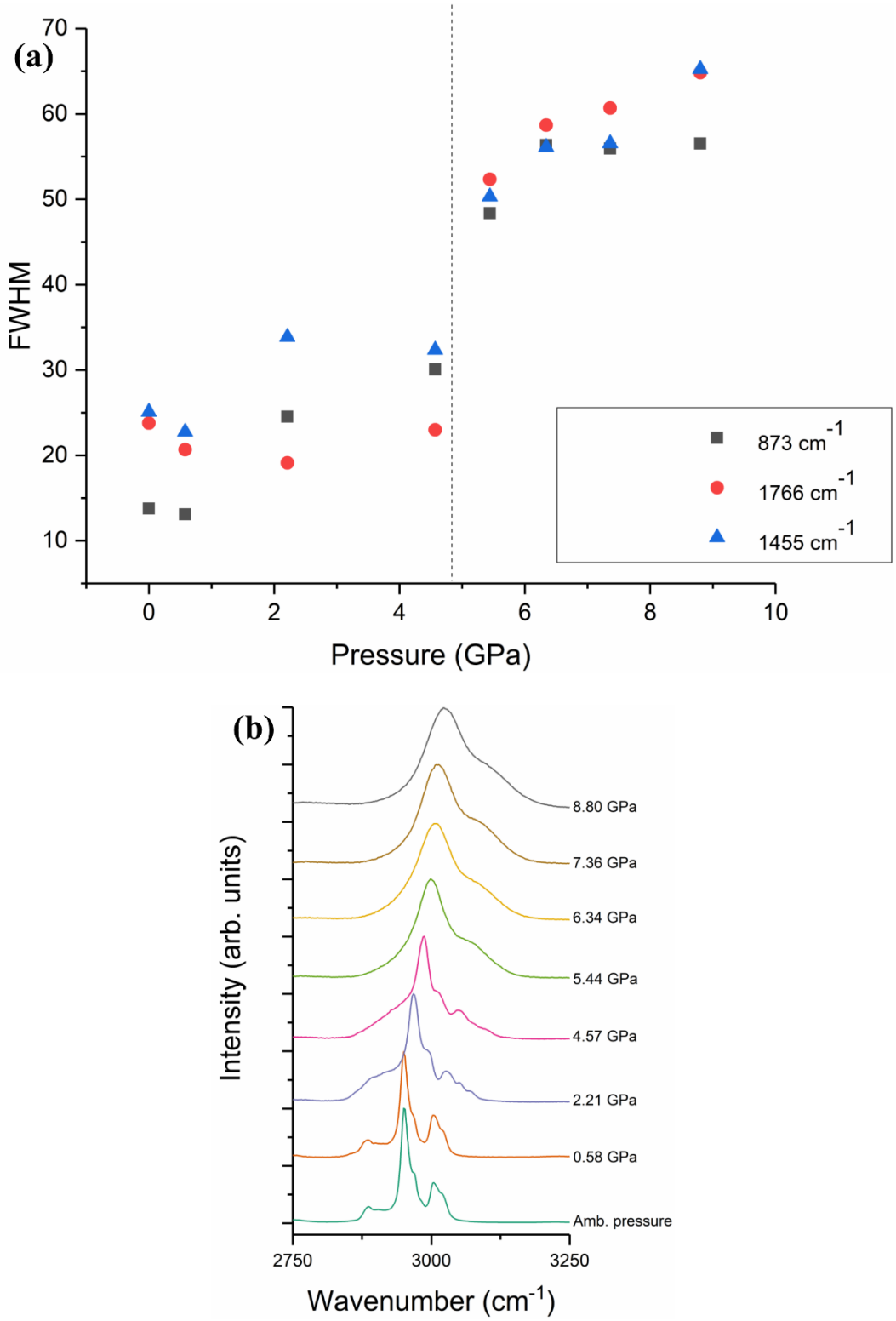

Figure 4.5 (a) Full width half maximum for selected Raman bands with increasing pressure. Note: the dashed line indicates the phase transition point. (b) PLA high wavenumber region with function of pressure

The high-wavenumber stretching region, as shown in Figure 4.5 (b) exhibited distinguished peaks and shoulders corresponding to CH, symmetric and asymmetric stretches of CH_3. The peaks at 2884 and 2901 cm^{-1} merged together at 2.21 GPa and became as a shoulder. Similarly, peaks at 3004 and 3021 cm^{-1} merged together and became wider at pressures higher than 4.57 GPa. On the other hand, the peak at 2950 cm^{-1} assigned as $\nu_s CH_3$ maintained its intensity but broadened as pressure increased.

In general, the application of pressure causes a shift in Raman bands towards higher energies.[23] The shift of bands is approximately linear, as presented in Figure 4.6, for some bands indicating a proportional relationship between pressure and Raman shift. It is notable some peaks i.e. 413, 1131 and 1455 cm^{-1} have shifted dramatically at the 2.21 GPa. This jump supports the idea of phase transition at this pressure. For some wavenumbers, only three points were plotted and this is because at pressure points beyond 4.57 GPa, those peaks were broad.

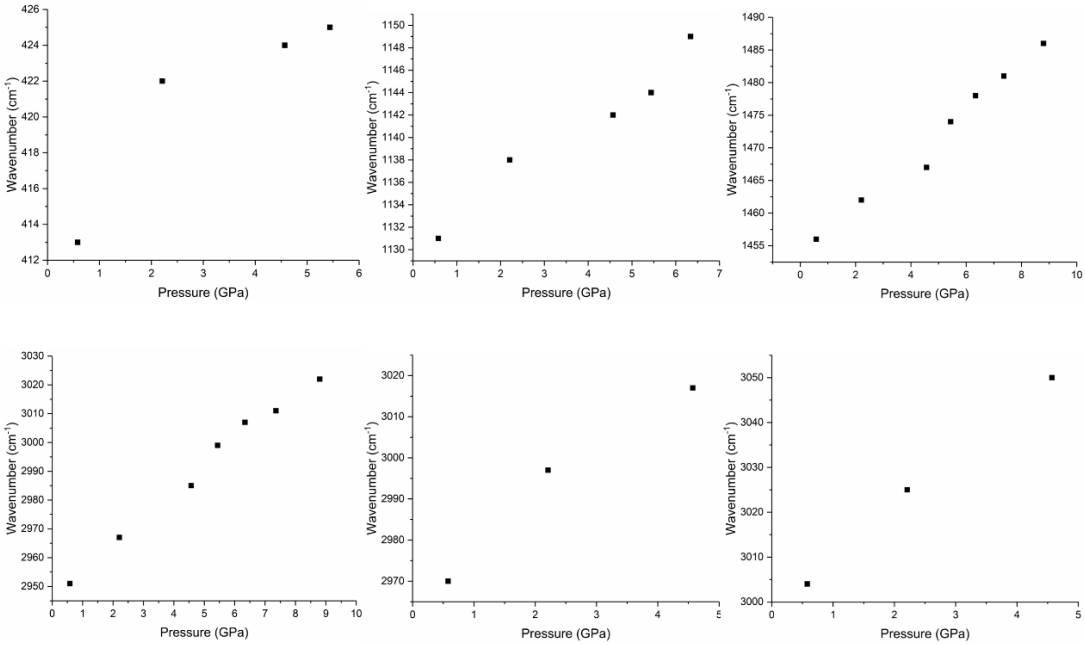

Figure 4.6 Peak positions of various Raman bands in PLA as a function of pressure. It is evident that the peak at 412 cm^{-1} presented in the top left has jumped to higher position at 2.2 GPa which indicates the phase transition (similar for peaks at 1131 cm^{-1} and 1455 cm^{-1}).

4.3.2 Poly glycolic acid (PGA)

4.3.2.1 Ambient pressure characterisation

PGA (Figure 4.1 (b)) was received from Sigma Aldrich as 2 mm long and 1 mm diameter pellets, which is not possible to be loaded into a DAC. They were difficult to grind or break down into powder. PGA pellets were ball-milled with few drops of methanol:ethanol (4:1) for 90 minutes at 30 Hz/second. The produced powder was used for high pressure studies. Another issue with PGA was fluorescence, which made it difficult to acquire Raman spectrum. Figure 4.8 shows the Raman spectrum of PGA with the fluorescence. To ensure that fluorescence is not form the material itself, but could be from by-products of the material, different techniques were explored. The sample was washed with acetone but remained fluorescent (Figure 4.7). Other

techniques including reducing the laser intensity from 100% to 50%, reducing acquisition time and changing from 532 nm to 875 nm laser, the fluorescence was still present as seen in Figure 4.8 (a) and (b) respectively.

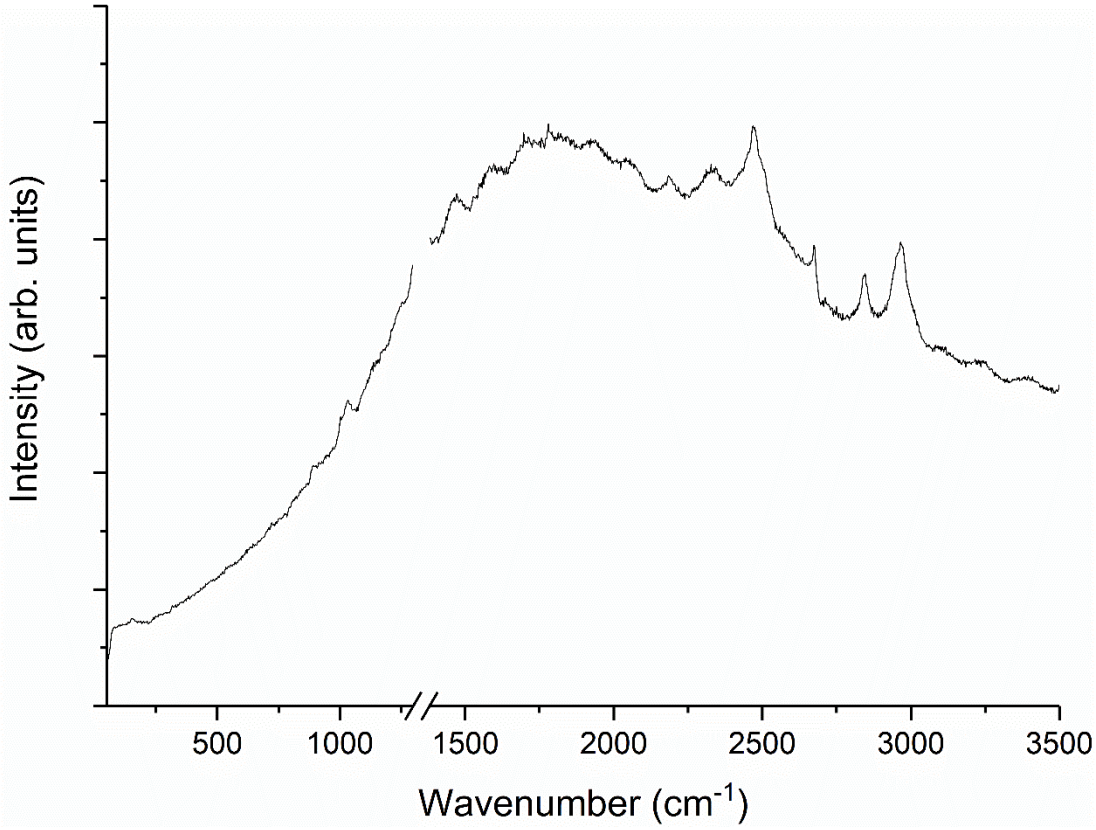

Figure 4.7 PGA ball milled, acetone washed to overcome fluorescence. This indicates that fluorescence is not from the by-products but rather from the sample.

To overcome the issue of fluorescence, surface–enhanced Raman spectroscopy (SERS) technique was adopted. Silver nanoparticles, (λ_{max} 394 nm, concentration: 0.488 nM and size of 76.8 nm), were suspended in the PTM methanol: ethanol (4:1) prior to loading in the DAC. The theory of SERS and the mechanisms involved in improving Raman signalling are fully described in Chapter 3, which describes enhancing Raman signalling under high pressure.

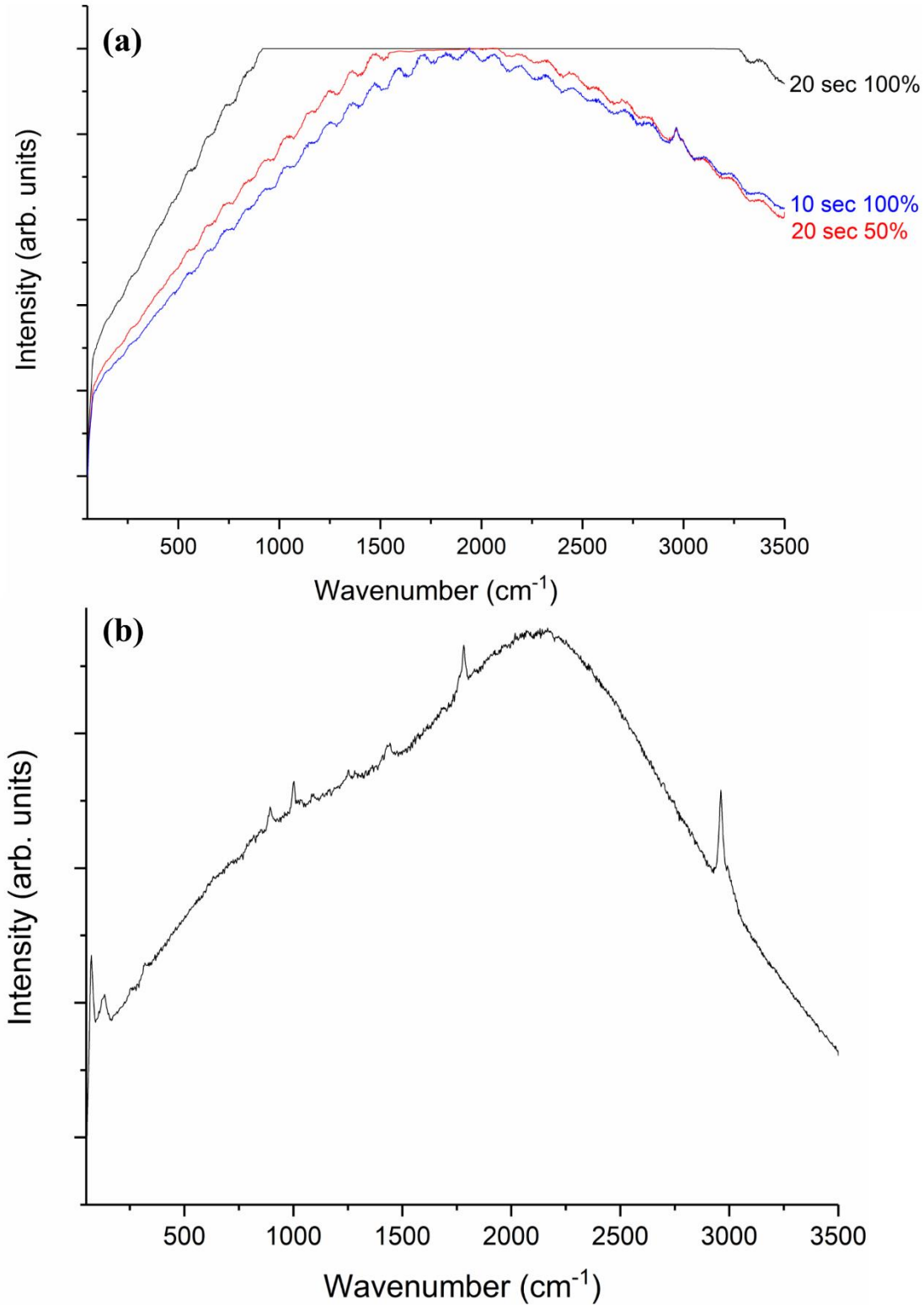

Figure 4.8 PGA at ambient pressure (a) 532 nm laser with different acquisition times and laser intensity, (b) 785 nm laser

Raman spectra of amorphous and highly crystalline PGA down to approximately 80 cm^{-1} were reported by Kister et al and those were based on their previous work on oligoglycolic acid, subtraction of PLA from PLGA and by comparison with polyglycine.[22,24,25,26] Assignments of vibrational frequencies are shown in Table 4.3.

Table 4.3 Raman peak positions of PGA and their assignments[22]

Peak Position (cm^{-1})	Assignment	Peak Position (cm^{-1})	Assignment
80	τ(CC)	884, 885	ν(C-C)+ *r*(CH_2)
92	τ(CC)	900	ν(C-C)+ *r*(CH_2)
133	τ(CO)	998, 950	ν(C-C)+ *r*(CH_2)
175	τ(CO)	1032, 1029	ν_s(COC)
213, 210	δ(COC)	1087, 1090	ν_s(COC)
250, 260	δ(COC)	1165, 1169	ν_{as}(COC)
316, 310	δ(OCC)	1248, 1244	tw(CH_2)
400	δ(OCC)	1274	tw(CH_2)
504	δ(CCO)	1403, 1400	*ω*(CH_2)
569, 560	δ(CCO)	1426, 1420	δ(CH_2)
605	γ(C=O)	1438, 1450	δ(CH_2)
624	γ(C=O)	1759	ν(C=O)
720	γ(C=O)	1776, 1760	ν(C=O)
812	γ(C=O)	2954	ν_{as}(CH_2)
850, 845	*r*(CH_2)	2988	ν_{as}(CH_2)

4.3.2.2 High pressure characterisation

Raman spectra of PGA powder, produced by ball-milling, as a function of pressure are presented in this section. They show significant improvement when compared with the ambient pressure ones presented in Figure 4.8. This sample showed to be semi-crystalline as there were few peaks in the low-energy phonon region of the spectra across all pressure points (Figure 4.9 (a)). These peaks at 70, 90 and 133 cm^{-1} represent the lattice mode of the sample and are assigned as τ(CC), τ(CC) and τ(CO) respectively. However, there was a sharp peak at 236 cm^{-1}, which existed in all pressure points. This peak has not been assigned by Kister et al.[24] but it could be

contributing from the silver nanoparticles suspended in the PTM.[27] Blanch et al.[27] have reported some Raman anomalies seen by aggregating AgNPs using different aggregating agents but the one at 236 cm^{-1} was not reported. Another study by Yamamoto et al.[28] found that Raman peaks at 125, 248 and 314 cm^{-1} found in PGA at 20 °C almost disappeared at 230 °C, which confirms that they are crystalline bands of PGA.

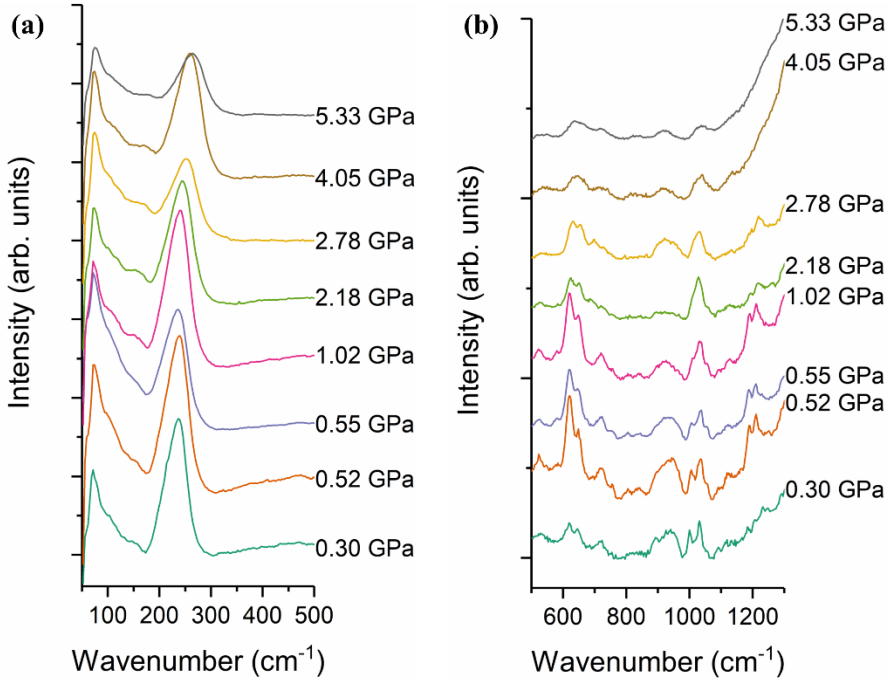

Figure 4.9 Raman spectra of PGA high-pressure compression study using AgNPs in 4:1 (meOH:etOH) as PTM. (a) 50-500 cm^{-1}, (b) 500-1300 cm^{-1} in which peak broadening is seen after 4.05 GPa. Note: Raman spectra were baseline subtracted

At the first pressure point (0.3 GPa), there was a peak at 619 cm^{-1} and a shoulder at 645 cm^{-1} with relatively low intensity (Figure 4.9 (b)). They can be assigned as γC=O stretches despite not being at their exact assigned locations. This slight shift is seen because of the AgNPs which are known to cause some shifts in the Raman bands.[29,30] They both displayed a slightly increased intensity at 0.52 GPa until 1.02 GPa. At 4.05

GPa the 619 cm^{-1} peak is broader and the peak resolution is poor (Figure 4.9 (b)). FWHM was calculated for selected peaks i.e. 619, 645 and 1032 cm^{-1}. It is clear from Figure 4.10 that peaks presented became broader apart from the shoulder at 645 cm^{-1}, which remained constant after 2 GPa. The dashed line presented in the figure gives an indication of the pressure point at which we suspect the sample undergoes a phase transition.

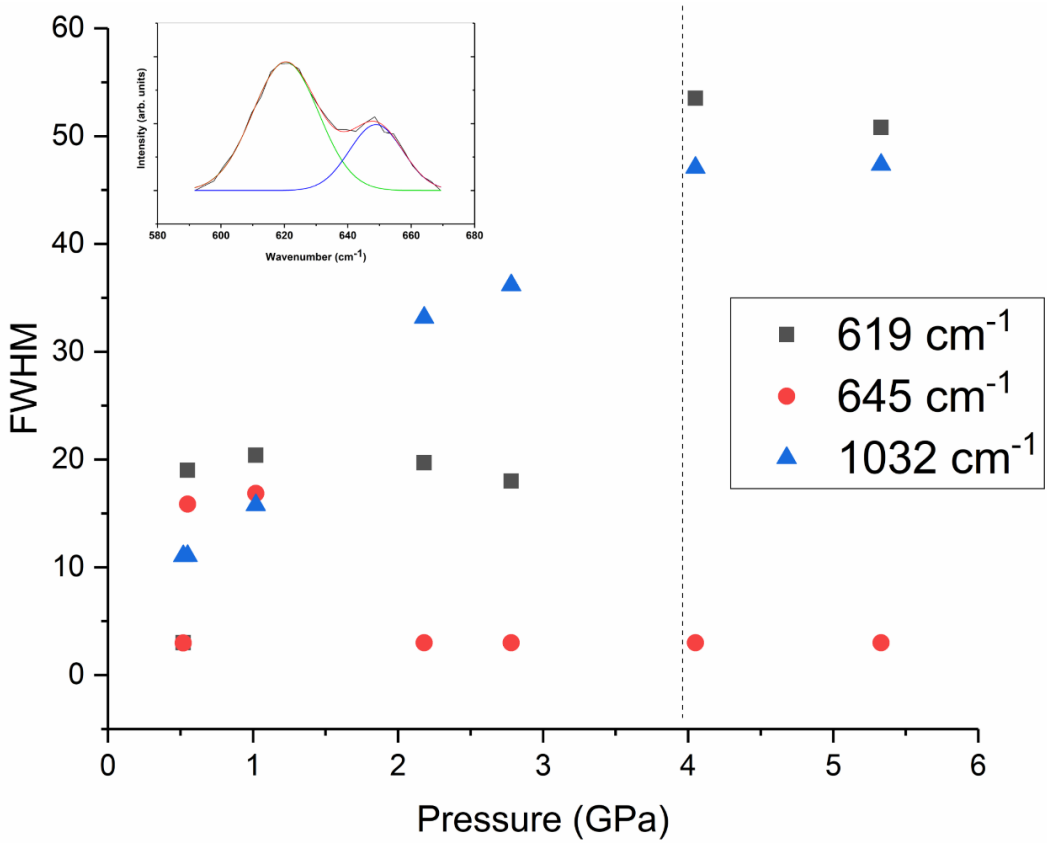

Figure 4.10 Full width half maximum for selected Raman bands of PGA with increasing pressure. Note: the dashed line indicates the possible phase transition point.

A very low intensity Raman peak at 998 cm^{-1}, as seen in Figure 4.9 (b), was observed at the lowest pressure point. The presence of this peak is crystalline-sensitive, which depicts the state of the sample i.e. semi-crystalline or amorphous.[24] This peak was assigned to highly coupled normal modes involving the skeletal ν(C-C) stretching and *r*(CH_2) rocking. Another Raman peak at 1032 cm^{-1} was also observed and assigned as

ν_s(COC). The peak at 998 cm^{-1} started to merge with the 1032 cm^{-1} at 1.02 GPa which restricts the ability to use this peak to discriminate whether the material remains semi-crystalline. At 4.05 GPa it is clear that there is an overall broadening of the spectra suggesting that the material has lost its order.

Two Raman peaks at 1422 and 1444 cm^{-1} were observed at 0.3 GPa and assigned as $\delta(CH_2)$ bending modes, as presented in Figure 4.11 (a). They started to merge together as pressure increased but did not broaden as other peaks. A shoulder at 1566 cm^{-1} and a peak at 1609 cm^{-1} were observed. They both merged and formed a broad peak at 4.05 GPa.

The Raman peak at 1776 cm^{-1} (Figure 4.11 (a)) representing νC=O has a very low intensity at the first pressure point which again confirms that the sample is either amorphous or semi-crystalline, as the same peak was seen by Kister et al.[24] to be highly intense in crystalline PGA and decrease in intensity as the crystallinity decreases. Its intensity decreased as pressure increased, which indicates the reduction in its degree of crystallinity.

In the high wavenumber spectral region i.e. CH_2 stretching region (Figure 4.11(b)) two peaks and a shoulder were observed at 2838, 2958 and 2884 cm^{-1} respectively. The shoulder started to disappear at 2.78 GPa and the peaks broadened and decreased in intensity at 5.33 GPa. A general shift of Raman peaks towards high wavenumbers was observed as pressure increased.

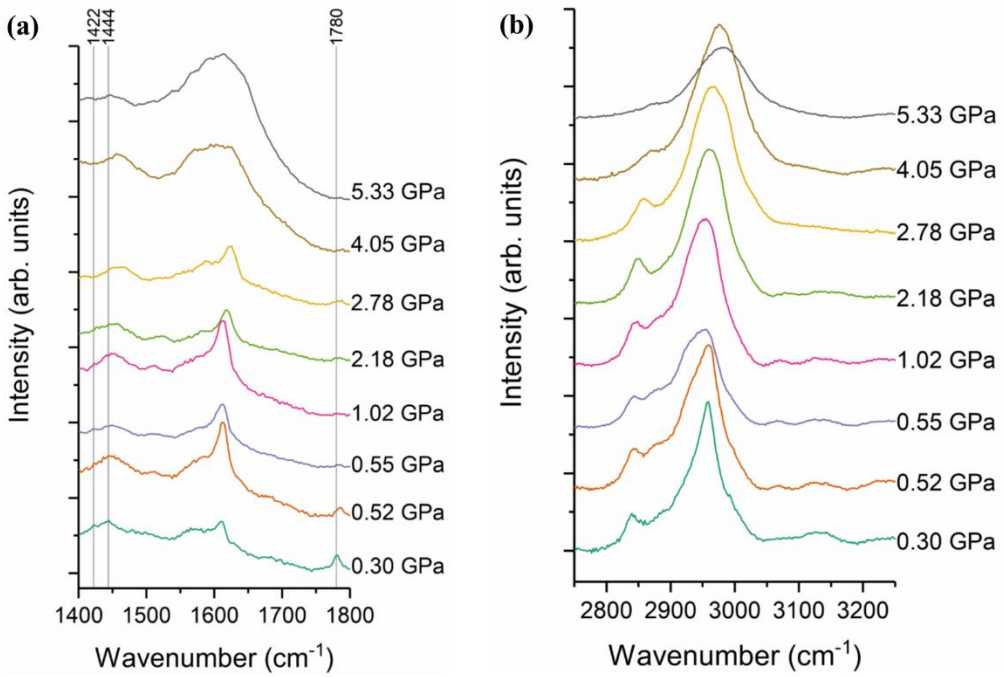

Figure 4.11 Raman spectra of PGA high-pressure compression study using AgNPs in 4:1 (meOH:etOH) as PTM. (a) 1400-1750 cm^{-1} with peak reference, (b) 2750-3250 cm^{-1}. Note: Raman spectra are baseline subtracted

4.3.3 Ethyl cellulose (EC)

Ethylcellulose is a widely used polymer in pharmaceutical industry. It is used for various purposes including taste masking, release modifying agent, stabiliser and as extrusion excipient. In this chapter, we are exploring the effect of pressure on various polymers. EC will be used as a formulation excipient in Chapter Five.

4.3.3.1 Ambient pressure characterisation

Ethyl cellulose (Figure 4.1 (c)) is one of the commonly used hydrophobic polymers in pharmaceutical formulations. An ambient pressure Raman spectrum of EC powder

was collected in the spectral range of 50-3500 cm^{-1} as shown in Figure 4.12, in which distinguishable peaks are identified.[31]

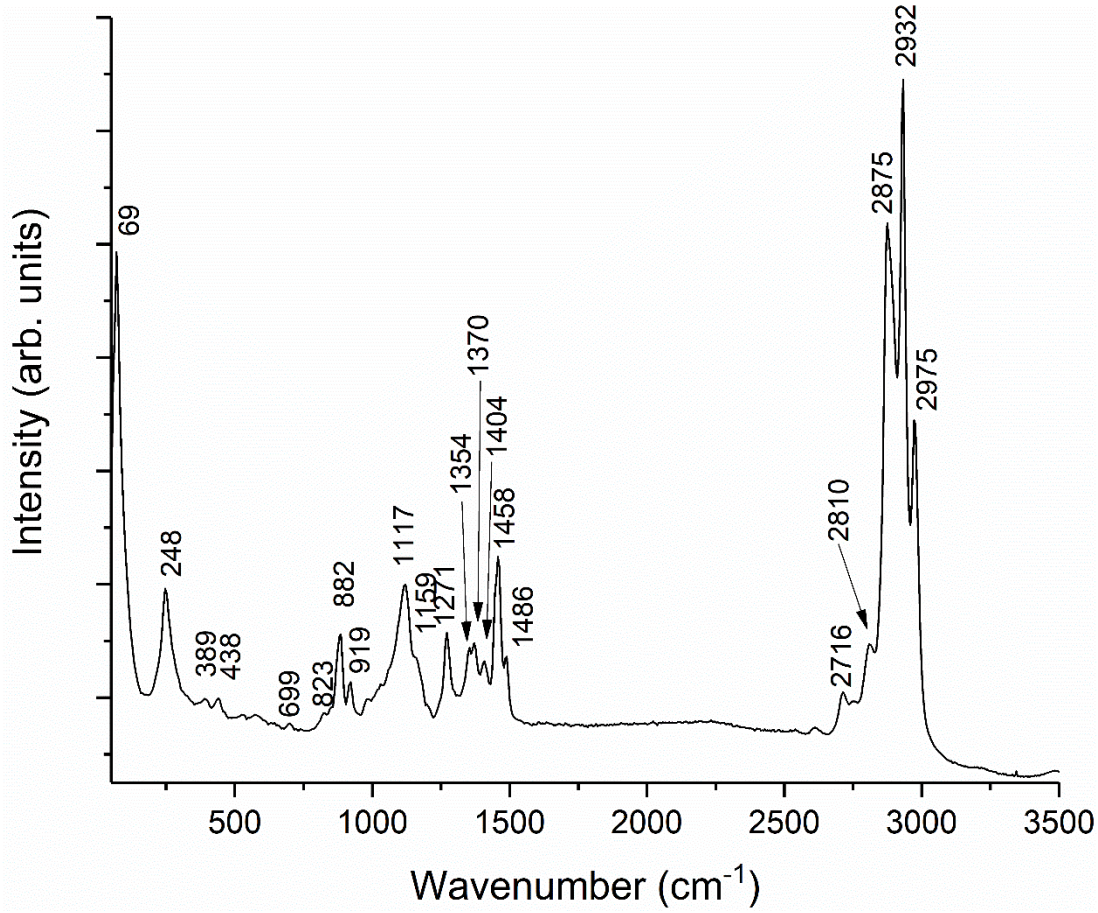

Figure 4.12 Raman spectrum of EC powder with peak numbers

The Raman spectrum of EC powder at ambient pressure is presented in Figure 4.12 with peaks numbered. The spectrum shows that the sample is semi-crystalline and peaks identified are similar to the ones found by Larken[31] and Atalla.[32] These peaks and their assignments are detailed in Table 4.4.

Table 4.4 Raman peak assignments of ethylcellulose[31, 32]

Peak Position (cm^{-1})	Assignment	Peak Position (cm^{-1})	Assignment
69	lattice	1159	HCC & HCO bending
248	lattice	1370	HCC & HCO bending
823	C-O stretch of COH-COC	1404	HCC & HCO bending
882	C-O stretch of COH-COC	1458	HCH & HOC bending
913	HCC & HCO bending at C6	2875	CH and CH_2 stretching
1271	HCC & HCO bending	2975	CH & CH_2 stretching

Atalla et al.[32] have recorded the Raman spectra of celluloses from different origins grown within their laboratory using Raman microprobe. Additionally, they recorded Raman spectra from deuterated celluloses which allowed the identification of vibrational modes involving CH and OH motions.

4.3.3.2 High pressure characterisation

The compression study of EC was performed over the pressure range 0.35 GPa to 4.7 GPa. The SERS technique was adopted in this compression study as EC was found to be a weak Raman scatterer in DAC and provided the best possible signal given the problems of fluorescence.

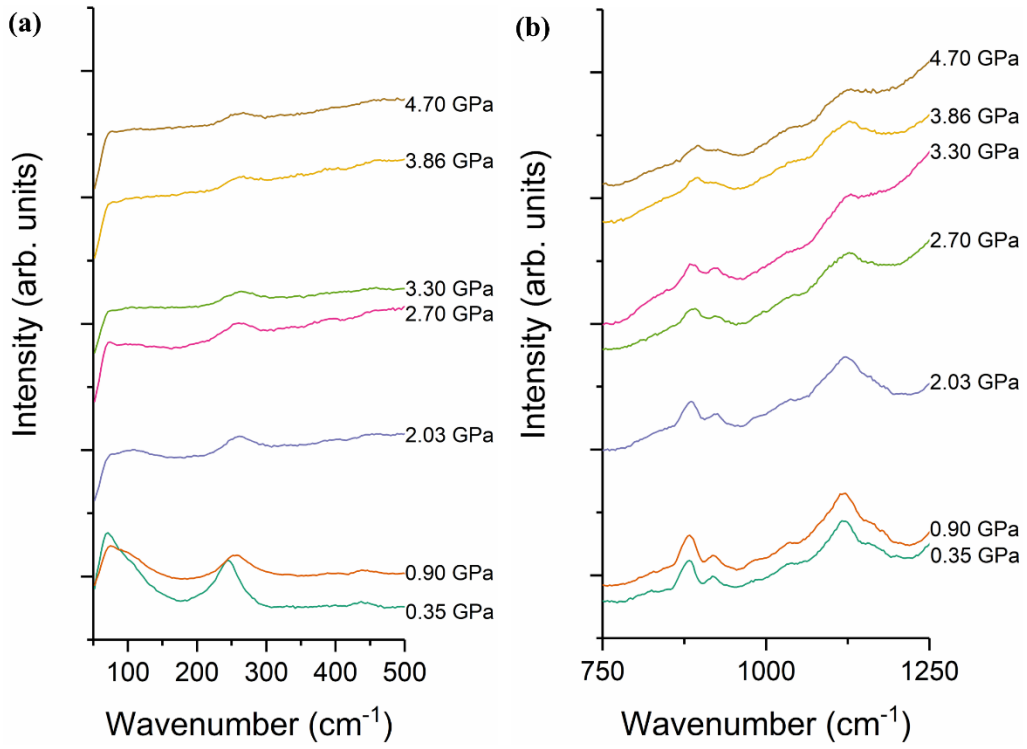

Figure 4.13 Raman spectra of EC high-pressure compression study using AgNPs in 4:1 (meOH:etOH) as PTM. (a) 50-500 cm^{-1}, (b) 750-1250 cm^{-1}Note. Peaks start to become broader at 2 GPa which indicates that the sample is becoming less ordered.

As mentioned earlier, EC sample is semi-crystalline but at the first pressure point (0.35 GPa) there are 2 Raman peaks at 70 and 245 cm^{-1} in the low-energy phonon region. They became broader as pressure was increased (Figure 4.13 (a)). This may indicate that the sample is either becoming less ordered or undergoing phase transition. A similar phenomenon was observed at Raman peaks positioned at 883 and 1122 cm^{-1} of which both assigned as C-O stretch of COH/C-O-C. They both broadened as pressure was increased (Figure 4.13 (b)).

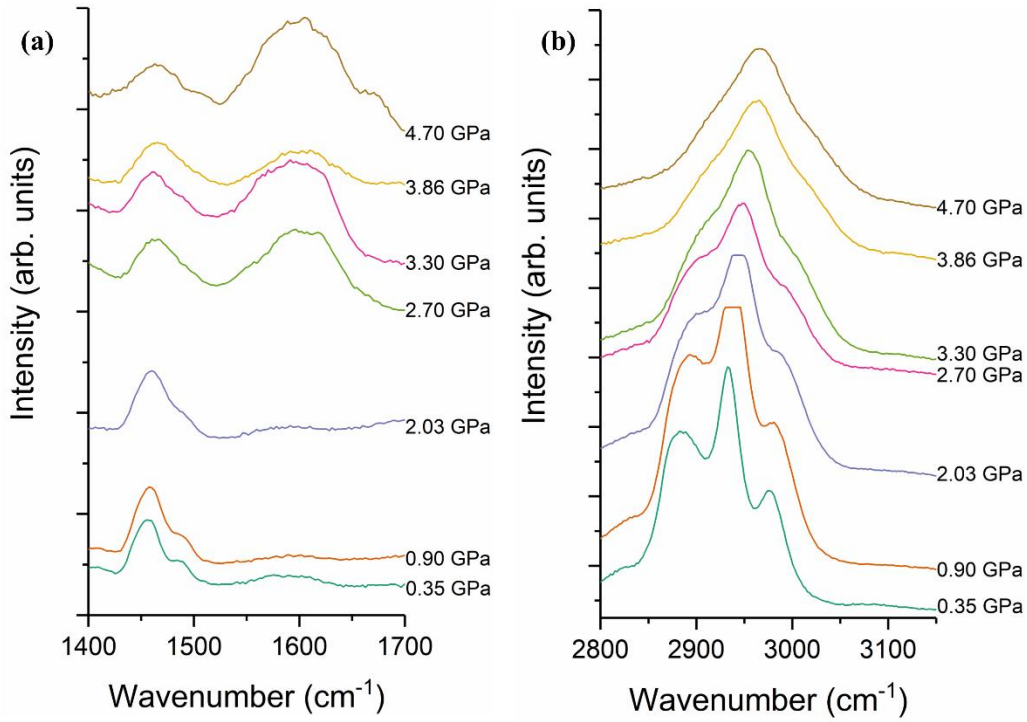

Figure 4.14 Raman spectra of EC high-pressure compression study using AgNPs in 4:1 (meOH:etOH) as PTM. (a) 1400-1700 cm^{-1}, (b) 2800-3150 cm^{-1}. Note: (b) shows spectra at 0.90 and 2.03 GPa over-exposed (saturated)

Moving to higher wavenumbers, the Raman peak at 1455 cm^{-1} which can be assigned as CH_2 deformation has decreased in intensity and started to broaden at 2.70 GPa. At the same pressure, a new peak has emerged at 1605 cm^{-1} as presented in Figure 4.14 (a). This is an intramolecular bond peak that can be assigned as C=O. Moreover, peaks at the CH stretching region shifted to higher wavenumbers as a function of pressure and at 2.70 GPa they started to become broader. These observations of peak softening and broadening point towards a change in the state of the sample i.e. becoming less ordered due to the effect of pressure.

4.3.4 Hydroxypropyl methylcellulose (HPMC)

Hydroxypropyl methylcellulose is another widely used polymer in pharmaceutical industry for different formulations including oral, nasal, ophthalmic and topical formulations. To the best of our knowledge, it has not been investigated under high pressure. It is one of the components of the formulation we explored in Chapter Five.

4.3.4.1 Ambient pressure characterisation

Hydroxypropyl methylcellulose, (Figure 4.1 (d)), is one of the commonly used hydrophilic polymers in pharmaceutical formulations of extended release systems. Raman spectrum of the received HPMC powder in spectral range of 50-3500 cm^{-1} is presented in Figure 4.15 with peaks numbers identified.[31,33]

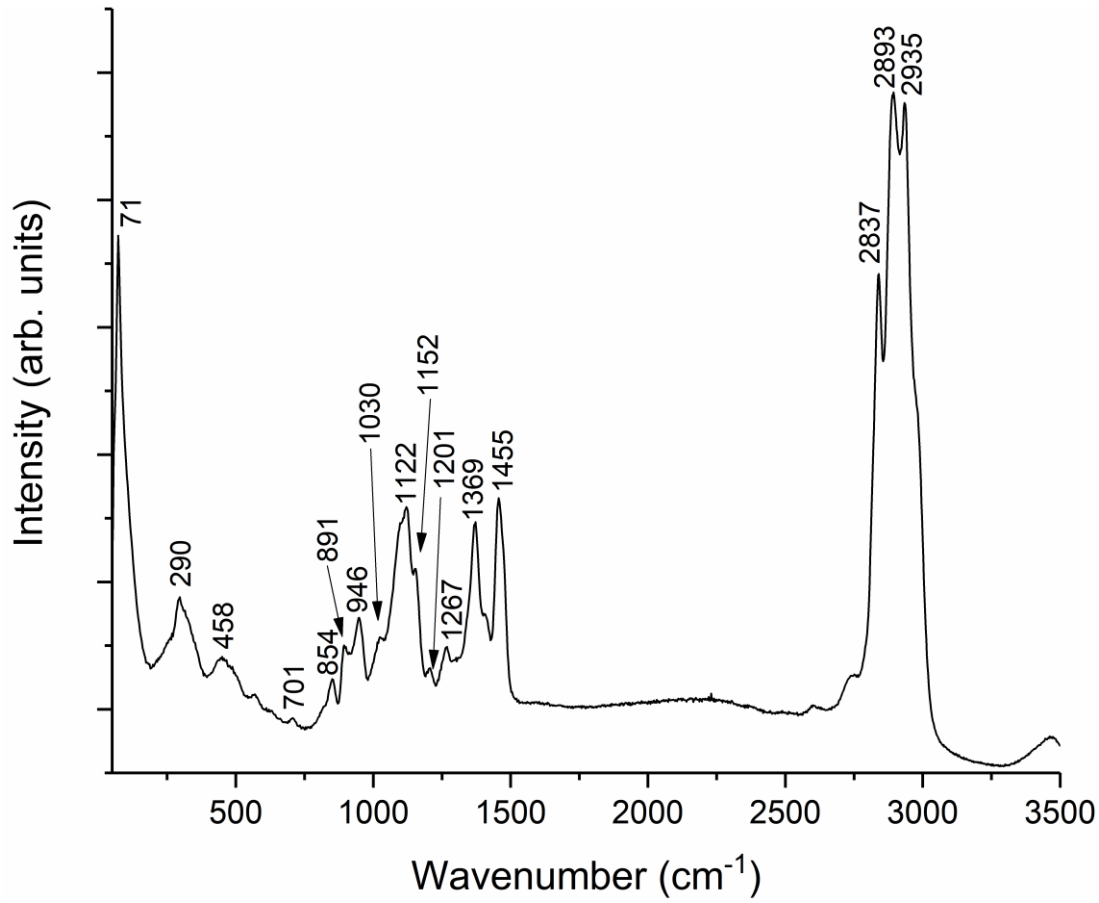

Figure 4.15 Raman spectrum of HPMC powder with peak numbers

It is evident from the Raman spectrum of HPMC that it is semi-crystalline. The received HPMC powder shows similar peaks as described by Larken[31], Adar[33] and Marleen et al.[34] as detailed in Table 4.5

Table 4.5 Raman peak assignments of HPMC[31,33,34]

Peak Position (cm^{-1})	Assignment	Peak Position (cm^{-1})	Assignment
854	ring in-phase & semi-circle stretch	1201	C-O stretch of COH/C-O-C
891			
946		1369	CH deformation
		1455	CH_2 deformation
1122	C-O stretch of COH/C-O-C	2838	Sym CH_3 stretch
1152		2934	Asym CH_2 stretch

4.3.4.2 High pressure characterisation

The compression study of HPMC was done using SERS technique to improve Raman signalling. HPMC was found to be a weak Raman scatterer especially in a DAC. For this reason, the SERS technique was adopted in order to amplify the Raman signal.[35] The study was conducted at pressures of 0.46 – 5.76 GPa. It is evident from the Raman spectra that HPMC is semi-crystalline. The high pressure spectra show two Raman peaks in the low-energy phonon regions i.e. at 71 and 290 cm^{-1}. From the 2 GPa pressure point onwards, those peaks started to become broader and lose their intensity (Figure 4.16 (a)). This indicates that the sample is going from semi-crystalline into amorphous as pressure increases. A similar observation was noted in EC at about the same pressure point.

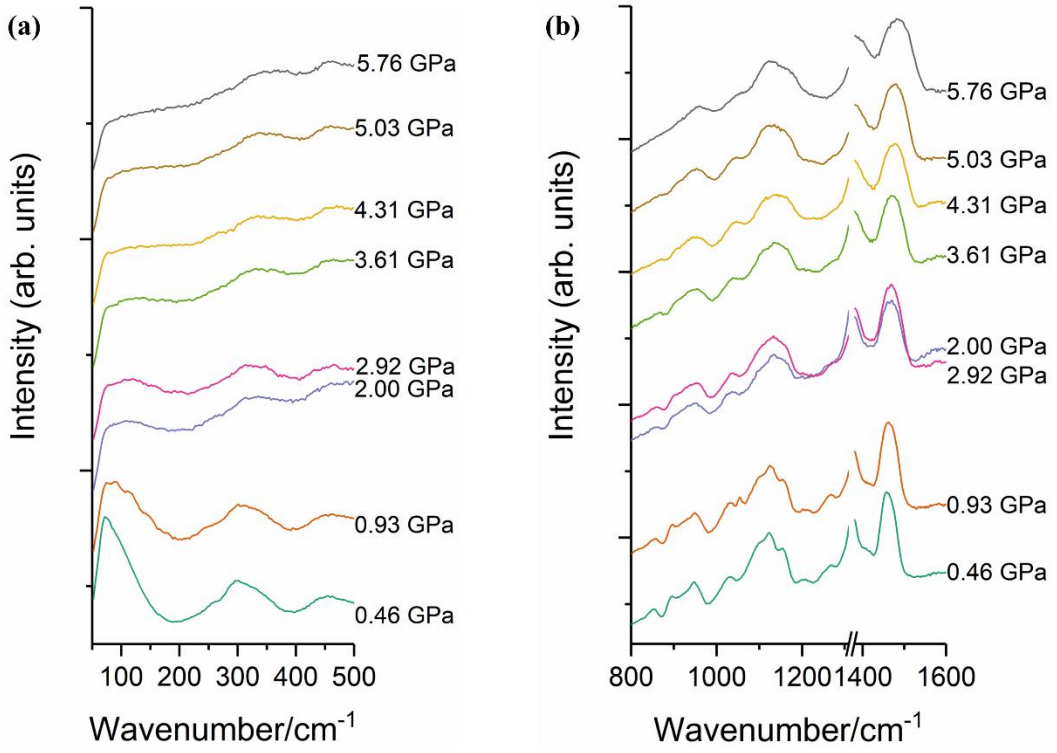

Figure 4.16 Raman spectra of HPMC high-pressure compression study using AgNPs in 4:1 (meOH:etOH) as PTM. (a) 50-500 cm^{-1}, (b) 800-1600 cm^{-1}. Note: it is notable that majority of peaks lose their sharpness and become broader at 2 GPa and above. This indicates that the sample is becoming less ordered (amorphous).

Raman peaks at 1122 and 1152 cm^{-1}, which are assigned as C-O stretch of COH/C-O-C, have lost their sharpness and broadened after 2 GPa (Figure 4.16 (b)). This effect has increased as pressure increased. This gives an indication that the sample is becoming less ordered i.e. amorphise. On the other hand, the peak at 1455 cm^{-1} assigned as CH_2 deformation did not change as pressure increased.

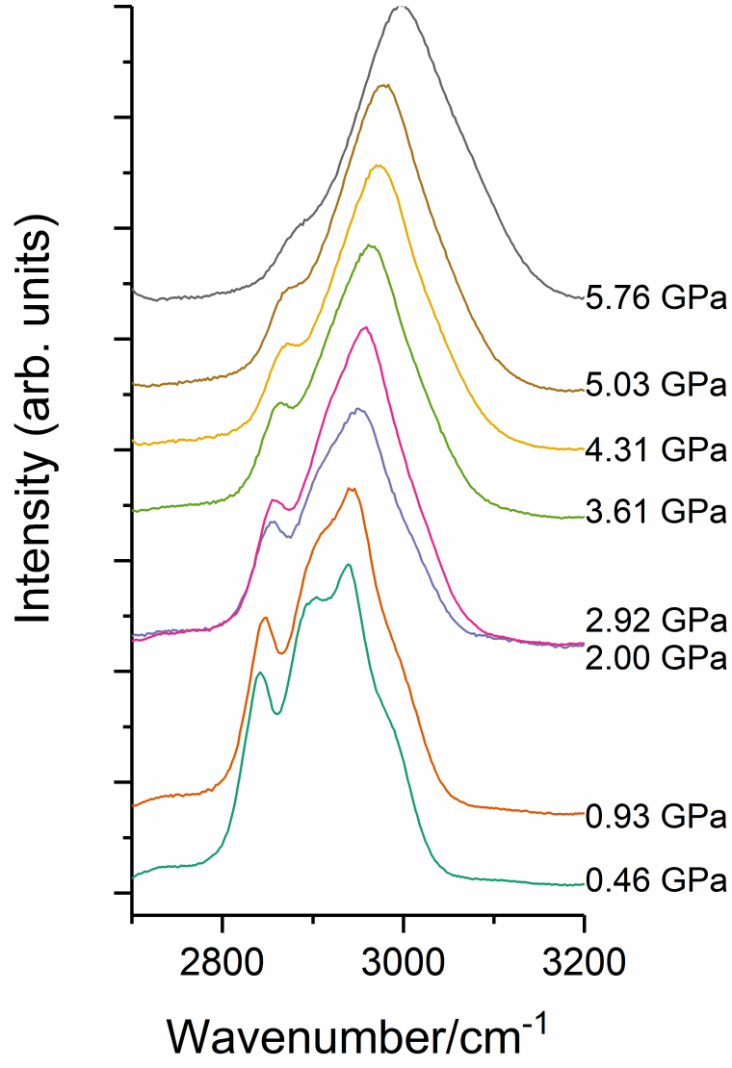

Figure 4.17 Raman spectra of HPMC high-pressure compression study using AgNPs in 4:1 (meOH:etOH) as PTM (2750-3200 cm^{-1}). Note: Peaks become broad at 2.92 GPa.

As illustrated in Figure 4.17, Raman peaks at high wavenumbers did shift to higher wavenumbers as pressure was increased. For instance, the band at 2838 cm^{-1} representing the symmetric CH_3 stretch as shifted to high wavenumbers and became broader at around 5 GPa. Other peaks at 2893 and 2945 cm^{-1} assigned as asymmetric CH_2 stretch have merged together at around 2.92 GPa and appeared as one peak.

These pressure studies were performed to investigate the effect of pressure on commonly used polymers in pharmaceutical and biomedical applications depict how they react to pressure. Two groups of these polymers were used. PLA and PGA are commonly used polyesters while EC and HPMC are commonly used cellulose derivatives. PLA was found to be crystalline as the phonon regions exhibited well defined peaks, which are indicative of crystallinity. These peaks started to become broader as pressure increased. The doublet peaks at 398 and 411 cm^{-1} corresponding to CCO deformation were clearly differentiated at pressures below 4.57 GPa but started to merge and become broader at pressures beyond this. The peak at 873 cm^{-1} corresponding to νC-COO stretching of the repeating unit of the polymeric chain has turned into a doublet at 2.2 GPa. This supports the idea of phase transition at this pressure point. Other peaks have lost their sharpness and merged with others at pressure point beyond 4.57 GPa. One of the reasons a peak may become broader and have a reduced intensity is due to the change of the environment surrounding the molecules and the decreased spatial order of molecules. In a crystalline sample the long range order is present due to the fact that the molecules are similarly orientated and the groups have a similar environment. As the molecules change orientation or environment then the molecular vibrations are no longer the same and the may have

slightly different energies hence a broader peak. The other polyester polymer PGA demonstrated a similar pattern of peaks becoming broader and having a reduced intensity at pressure points above 4.05 GPa, which is close to the pressure point at which PLA transforms into a less ordered form. It is important to note that PGA was ball-milled before being subjected to high pressure. Ball-milling is a mechanical process that grinds materials by impact and attrition. This process could also contribute in changing materials characteristics as it involves heat.

On the other hand, more complex polymeric systems like EC and HPMC demonstrated a similar behaviour in response to pressure but at lower pressures than those of PLA and PGA. Both EC and HPMC started to become less ordered at pressure points around 2.70 and 2.92 GPa respectively as Raman peaks started to become broader and less intense. Another important finding in this study was the use of SERS in high pressure studies of materials. It is evident that SERS technique worked in fluorescent and weak scattering samples in the pressure ranges required. Adopting SERS technique has improved the Raman signalling of such materials by simply suspending the silver nanoparticles in the PTM without any further chemical bonding or modification.

4.3.5 Ibuprofen (IBP)

Ibuprofen, Figure 4.1 (e), is one of the commonly used non-steroidal anti-inflammatory drugs (NSAIDs) that has both analgesic and anti-pyritic properties. IBP is a known racemic compound that contains equal of R and S ibuprofen, where the R enantiomer is capable of inhibiting cyclooxygenase enzyme leading to analgesic effect. It has been looked at under high pressure as it is used as the model API in formulations explored in Chapter 5. It is important to understand its Raman spectroscopy over pressure ranges and monitor any changes, if there are.

4.3.5.1 Ambient pressure characterisation

Raman spectrum of IBP powder in the spectral range 50-3500 cm^{-1} has been collected and is presented in Figure 4.18 with selected peaks and their corresponding assignments in Table 4.6.[36,37]

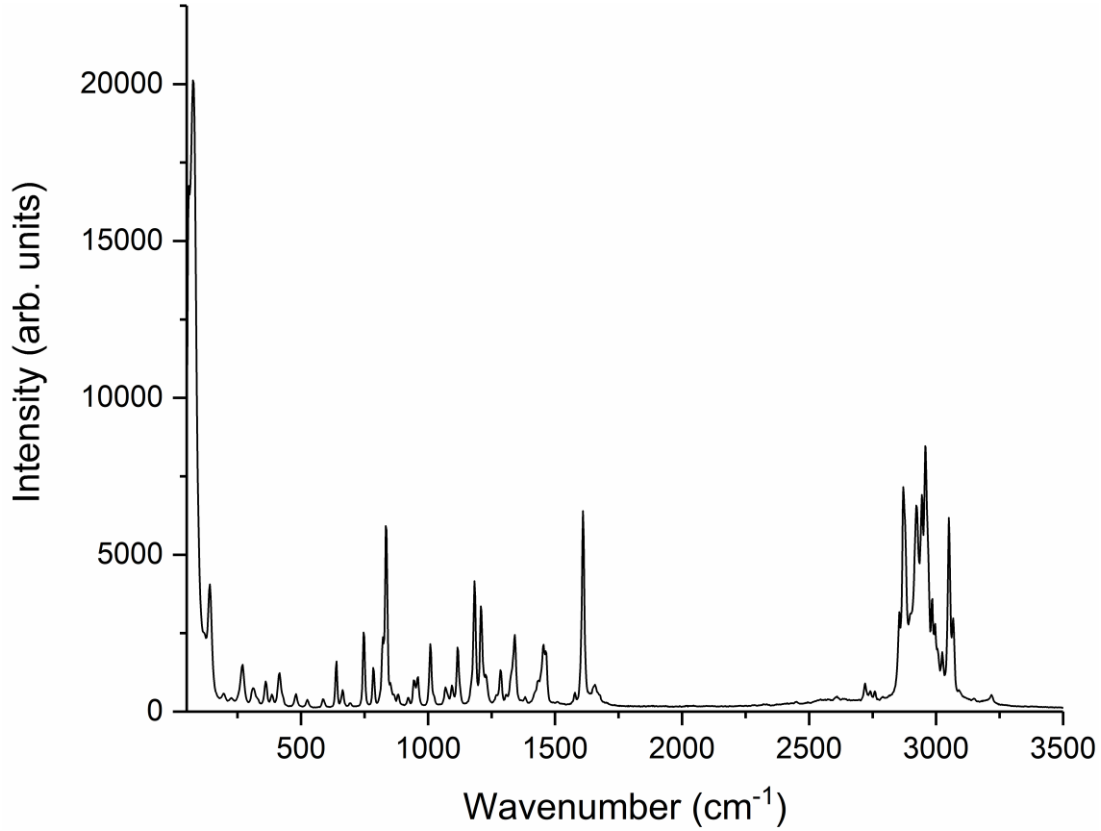

Figure 4.18 Raman spectrum of IBP powder

Table 4.6 Selected Raman peak positions of IBP and their corresponding assignments[36,37]

Peak Position (cm^{-1})	Assignment	Peak Position (cm^{-1})	Assignment
58	lattice vibration	1022	in plane CC ring def
75	lattice vibration	1452	in plane CH ring bending
141	lattice vibration	1460	CH_3 antisymmetric def
268	τCH	1609	CC stretching
414	out of plane CC def	2851	CH_2 asymmetric
819	CH ring binding	2991	CH ring stretching
835	in plane CC ring def		

As presented in Figure 4.18, it is evident that IBP is crystalline as the Raman spectrum has very sharp and intense peaks. The spectrum is full of vibrational information as the lattice vibration region contains Raman active peaks, C-C ring deformation peaks at 412, 637, 663 and 746 cm^{-1}. Another distinct peak was at 1609 and high wavenumber region was also informative of peaks corresponding CH ring stretching. In the low-energy phonon region, we have observed peaks at 58, 75 and 141 cm^{-1}, which can be assigned as phonon modes.

On the other hand, Hedoux et al. reported three different Raman peaks namely at 20, 50 and 80 cm^{-1}.[38] Although they were expecting a larger number of peaks due to system symmetry, Lazarevic et al.[39] found 4 peaks in the same region at around 21, 52, 74 and 138 cm^{-1} at room temperature, which is in agreement with our and Hedoux's findings. They performed low temperature measurements on IBP by going down to 100 K in order to decrease the linewidth of each mode and they managed to observe a larger number of peaks. A similar phenomenon is found in the compression study detailed below, as pressure decrease the linewidth as well and this is in agreement with Zallen and Slade's[40] work on the influence of pressure and temperature on phonons. A similar pattern was observed in the compression study of IBP below.

4.3.5.2 High pressure characterisation

A compression study on IBP was carried out to monitor its behaviour under high pressure in the pressure ranges of 0.3 GPa to 8.71 GPa and after removal of pressure. The high pressure study was performed on powdered ibuprofen that was finely ground and filled the hole of the gasket. Petroleum ether was used as PTM in this experiment.

Raman spectra of IBP under high pressure in the spectral range of 50-3500 cm^{-1} are presented in the following figures.

Referring to Figure 4.19 (a), it is evident that there are Raman peaks present in the low-energy phonon region at 58, 75 and141 cm^{-1}, which represent the lattice vibrations. The number of Raman bands in this region has increased as pressure increased but their intensities decreased. These bands have shifted from lower wavenumbers i.e. < 50 cm^{-1} as pressure increased. They existed through all pressure points while maintaining their peaks and shifting towards high-energy wavenumbers as a function of pressure. This is in agreement with Zallen and Slade's[40] work on the influence of pressure and temperature on phonons discussed earlier. This phenomenon has reverted back when pressure was removed at the end of the experiment.

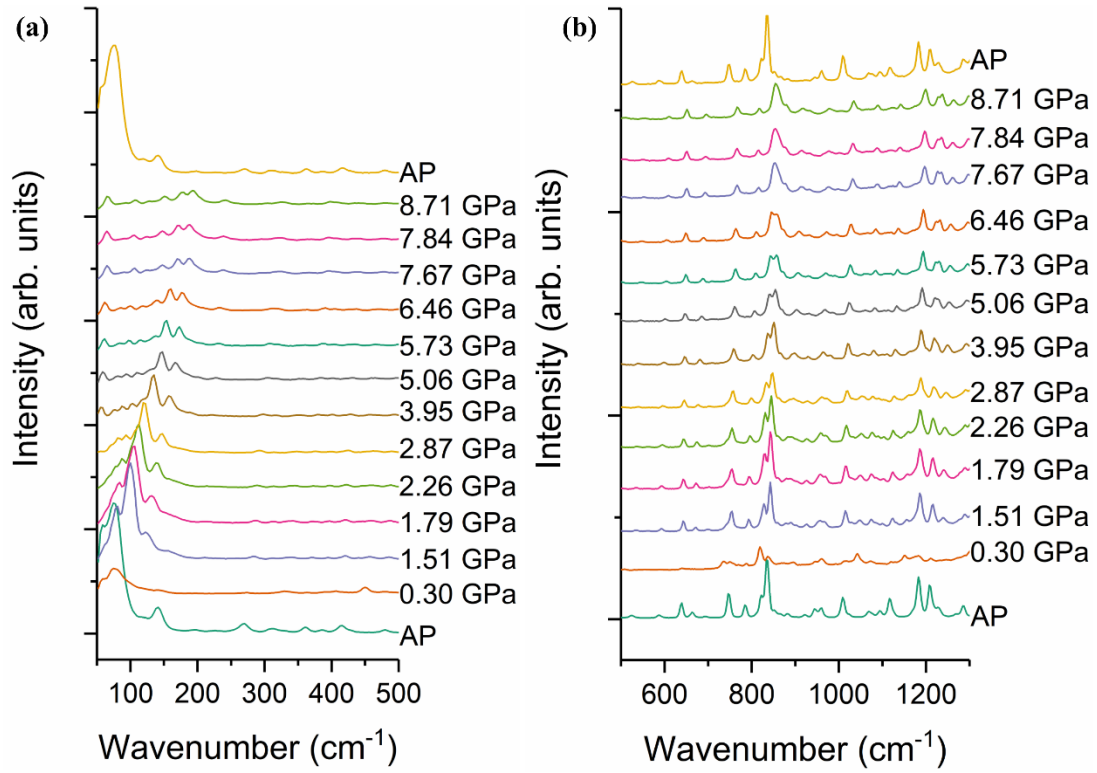

Figure 4.19 IBP compression study using petroleum ether as a PTM. (a) 50-500 cm^{-1} (b) 500-1300 cm^{-1}.

Two other peaks at 819 and 835 cm^{-1} assigned as CH ring bending and in-plane CC ring deformation respectively merged together and formed a softer peak at 7.67 GPa but reverted back once pressure was removed (Figure 4.19 (b)). Raman peaks at 1452 and 1460 cm^{-1} corresponding to CH_3 antisymmetric deformation[36] started to merge and became broader as soon as the sample was under pressure i.e. at 0.30 GPa onwards, but became sharper as soon as pressure was released (Figure 4.20 (a)). On the other hand, the Raman peak at 1609 cm^{-1} assigned as C-C stretching[36,37] remained intact across all pressure points, but shifted to higher wavenumbers (Figure 4.20 (a)).

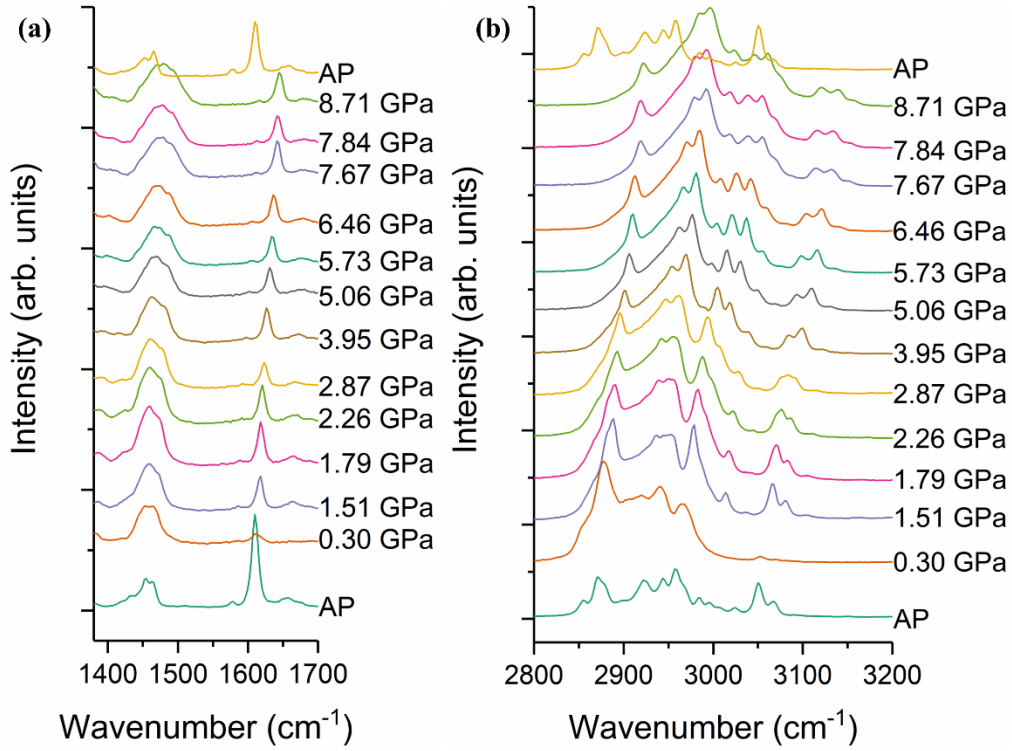

Figure 4.20 IBP compression study using petroleum ether as a PTM. (a) 1350-1700 cm^{-1} (b) 2800-3200 cm^{-1}.

The high-energy wavenumbers displayed (CH and CH ring stretching region) exhibited many peaks as shown in Figure 4.20 (b) and their corresponding assignments are presented in Table 4.6. In the compression study, these peaks shifted to higher energy wavenumbers while maintaining their integrity as pressure increased and this is presented in Figure 4.20 (b). Raman peaks across the spectrum showed a shift towards higher wavenumbers as a function of pressure. These are presented in Figure 4.21 in the pressure ranges between 0 and 1.51 GPa because the formulations containing IBP as a model API (Chapter 5) will be subjected to 0.8 GPa due to the limit of the large volume press. The data points presented give reflection of where peaks are going to shift as a function of pressure.

These findings suggest that IBP does not undergo phase transition but rather have structural transformation when subjected to high pressure and this is in line with the findings of Katrusiak et al[41] work on single crystals of IBP grown in a DAC investigated under high pressure by means of single-crystal diffraction. They found that pressure reduced the void volume of racemic IBP by 80% between 0.1 MPa and 3.5 GPA, and increased the intermolecular interactions but did not destabilise the structure up to 4 GPa.

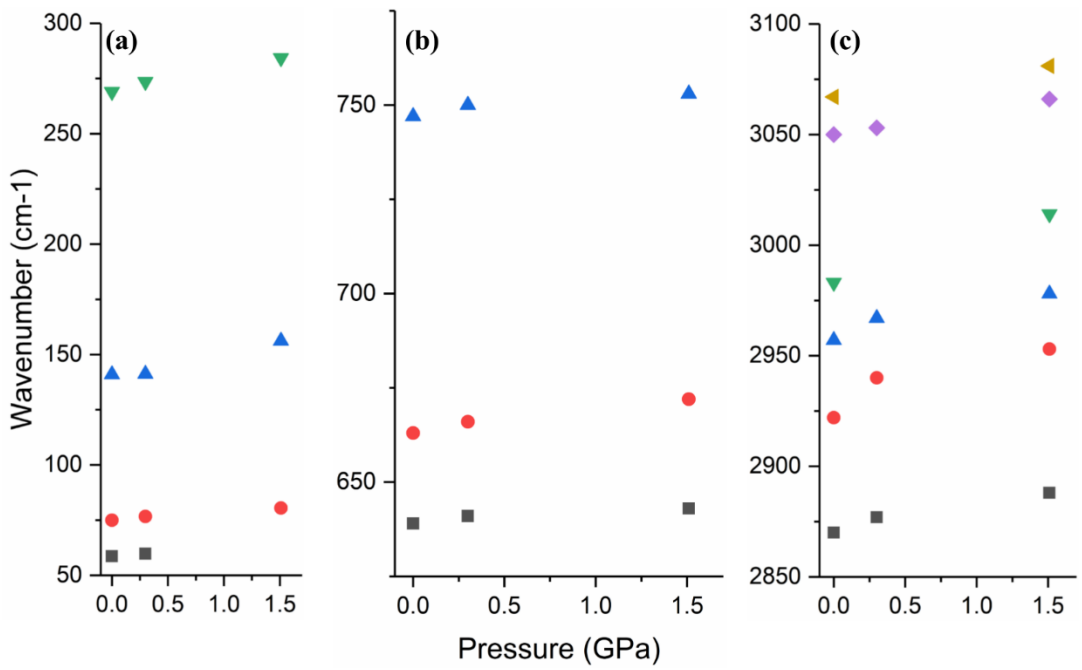

Figure 4.21 IBP (a): low-wavenumbers (50-300 cm^{-1}), (b): mid-wavenumbers (625-775 cm^{-1}) and (c): high-wavenumbers (2850-3100 cm^{-1}) bands shifting to higher wavenumbers as a function of pressure

4.4 Conclusions

In conclusion, Raman spectroscopy was used to investigate the effect of high pressure on commonly used pharmaceutical polymers and a model API (IBP). The application of high pressure on PLA shows a possible phase transition at 2.2 GPa and between 4 and 5 GPa as lattice vibration bands tend to broaden at that point as well as other bands. SERS technique was successfully adopted to overcome the fluorescence of PGA by using AgNPs in the PTM. PGA also showed phase transition at similar pressure points to PLA and this has been affirmed by FWHM of some peaks. EC and HPMC's Raman peaks tend to become broader at around 2.7 and 2.93 GPa respectively which indicates either phase transition or moving into a less ordered form i.e. from semi-crystalline to

amorphous as peaks became less defined after theses pressure points. On the other hand, the Raman spectroscopy of IBP shows that it undergoes structural transformation when subjected to high pressures but does not undergo phase transition.

4.5 References

[1] Bassett W. Diamond anvil cell, 50th birthday. High Pressure Research, 2009, Vol29(2), CP5-186.29(2).

[2] Fox D, Labes MM, Weissberger A. Physics and chemistry of the organic solid state. New York: New York: Interscience Publishers; 1963.

[3] Fabbiani FPA, Pulham CR. High- pressure studies of pharmaceutical compounds and energetic materials. Chemical Society reviews. 2006;35(10):932-42.

[4] Bauer J, Spanton S, Henry R, Quick J, Dziki W, Porter W, et al. Ritonavir: an extraordinary example of conformational polymorphism. Pharmaceutical research. 2001;18(6):859-66.

[5] Labarre DJP. Biomedical and pharmaceutical polymers. Ponchel G, Vauthier C, editors. London: London: Pharmaceutical Press; 2011.

[6] D.K. Gilding, A.M. Reed, Biodegradable polymers for use in surgery polyglycolic/poly (actic acid) homo- and copolymers: 1, *Polymer* 1979, 20, 1459-1464,

[7] Zong XH, Wang ZG, Hsiao BS, Chu B, Zhou JJ, Jamiolkowski DD, et al. Structure and morphology changes in absorbable poly(glycolide) and poly(glycolide-co-lactide) during in vitro degradation. Macromolecules. 1999;32(24):8107-14.

[8] You Y, Min BM, Lee SJ, Lee TS, Park WH. In vitro degradation behavior of electrospun polyglycolide, polylactide, and poly (lactide- co -glycolide. Journal of Applied Polymer Science. 2005;95(2):193-200.

[9] Alexander FG. Raman Spectroscopy at High Pressures. International Journal of Spectroscopy. 2012;2012(2012).

[10] Piermarini GJ, Block S, Barnett JD, Forman RA. Calibration of the pressure dependence of the R 1 ruby fluorescence line to 195 kbar. Journal of Applied Physics. 1975;46(6):2774-80.

[11] Adar F. Considerations of Grating Selection in Optimizing a Raman Spectrograph. Spectroscopy (Santa Monica). 2013;28(9)

[12] OriginLab C. OriginPro. b9.4.1.354 (Academic) ed. Northampton, MA 01060 USA2017

[13] Tsai WC, Hedenqvist MS, Laiback Å, Melin H, Ngo M, Trollsås M, et al. Physical changes and sorption/ desorption behaviour of amorphous and semi-crystalline PLLA exposed to water, methanol and ethanol. European Polymer Journal. 2016; 76:278-93.

[14] Cassanas G, Vert M, Pauvert B, Terol A. Vibrational analysis of poly (l-lactic acid). J Raman Spectrosc. 1995;26(4):307-11.

[15] Tuschel D. Raman Spectroscopy and Imaging of Low- Energy Phonons. Spectroscopy. 2015;30(9):18-31.

[16] Qin, D. and Kean, R. T. (1998) 'Crystallinity Determination of Polylactide by FT-Raman Spectrometry', Applied Spectroscopy, 52(4), 488–495.

[17] Kister G, Cassanas G, Vert M. Effects of morphology, conformation and configuration on the IR and Raman spectra of various poly (lactic acids). Polymer. 1998;39(2):267-73.

[18] Boldyreva EV, Shakhtshneider TP, Ahsbahs H, Sowa H, Uchtmann H. Effect of high pressure on the polymorphs of paracetamol. J Therm Anal Calorim. 2002; 68:437–52

[19] Hutchison IB, Delori A, Wang X, Kamenev KV, Urquhart AJ, Oswald IDH. Polymorphism of a polymer pre-cursor: metastable glycolide polymorph recovered via large scale high-pressure experiments. 2015.

[20] Roszak K, Katrusiek A, Katrusiak A. High- Pressure Preference for the Low Z′ Polymorph of a Molecular Crystal. Crystal Growth and Design. 2016;16(7):3947-53.

[21] Wasanasuk K, Tashiro K, Hanesaka M, Ohhara T, Kurihara K, Kuroki R, et al. Crystal structure analysis of poly (l- lactic acid) α form on the basis of the 2-dimensional wide-angle synchrotron X-ray and neutron diffraction measurements. Macromolecules. 2011;44(16):6441-52.

[22] G. Cassanas, G. Kister, E. Fabrègue, M. Morssli, L. Bardet, Raman spectra of glycolic acid, l-lactic acid and d,l-lactic acid oligomers, Spectrochimica Acta Part A: Molecular Spectroscopy, Volume 49, Issue 2, 1993, 271-279.

[23] Huang F. High pressure Raman scattering and X-ray diffraction studies of MgNb 2 O 6. RSC Advances. 2013;3(32):13210.

[24] Kister G, Cassanas G, Vert M. Morphology of poly (glycolic acid) by IR and Raman spectroscopies. Spectrochimica Acta - Part A: Molecular and Biomolecular Spectroscopy. 1997;53(9):1399-403.

[25] Abe Y. Normal vibrations of crystalline polyglycine I. Biopolymers: Peptide Science. 1972;11(9):1817.

[26] Wh M. Vibrational analysis of peptides, polypeptides, and proteins. I. Polyglycine I. Biopolymers: Peptide Science. 1976;15(12):2439.

[27] Yaffe NR, Blanch EW. Effects and anomalies that can occur in SERS spectra of biological molecules when using a wide range of aggregating agents for

hydroxylamine- reduced and citrate- reduced silver colloids. Vibrational Spectroscopy. 2008;48(2):196-201.

[28] Yamamoto S, Miyada M, Sato H, Hoshina H, Ozaki Y. Low-Frequency Vibrational Modes of Poly (glycolic acid) and Thermal Expansion of Crystal Lattice Assigned On the Basis of DFT-Spectral Simulation Aided with a Fragment Method. Journal of Physical Chemistry B. 2017;121(5):1128-38.

[29] Brown KE, Dlott DD. High- pressure raman spectroscopy of molecular monolayers adsorbed on a metal surface. Journal of Physical Chemistry C. 2009;113(14):5751-7.

[30] Joo S-W, Kim Y-S. Surface- enhanced Raman scattering study of benzyl mercaptide and benzyl isocyanide on gold and silver nanocolloid surfaces. Colloids and Surfaces A: Physicochemical and Engineering Aspects. 2004;234(1):117-22.

[31] Larkin P. Infrared and raman spectroscopy [internet resource] principles and spectral interpretation. Elsevier, Dawsonera, editors. Amsterdam; Boston Oxford: Amsterdam; Boston: Elsevier; 2011.

[32] Wiley JH, Atalla RH. Band assignments in the Raman spectra of celluloses. Carbohydrate Research. 1987 Feb 15; 160:113-29.

[33] Adar F. Characterizing modified celluloses using Raman spectroscopy. (Molecular Spectroscopy Workbench). Spectroscopy. 2016;31(11):22.

[34] De Veij M, Vandenabeele P, De Beer T, Remon JP, Moens L. Reference database of Raman spectra of pharmaceutical excipients. Journal of Raman Spectroscopy. 2009;40(3):297-307.

[35] Meyer N1, Nestler K, Engisch L, Marx G, Füting M, Kiesow A, Heilmann A, Wartewig S, Kleinebudde P. Raman spectroscopic surface characterization of cellulose derivatives. Fresenius J Anal Chem. 2001 Jul;370(6):789-91.

[36] Vueba ML, Pina ME, Batista De Carvalho LAE. Conformational stability of ibuprofen: Assessed by DFT calculations and optical vibrational spectroscopy. Journal of Pharmaceutical Sciences. 2008;97(2):845-59.

[37] Jubert A, Legarto ML, Massa NE, Tévez LL, Okulik NB. Vibrational and theoretical studies of non-steroidal anti-inflammatory drugs Ibuprofen [2-(4-isobutylphenyl) propionic acid]; Naproxen [6-methoxy-α-methyl-2-naphthalene acetic acid] and Tolmetin acids [1-methyl-5-(4-methylbenzoyl)-1H-pyrrole-2-acetic acid]. Journal of Molecular Structure. 2006;783(1):34-51.

[38] Hédoux A, Guinet Y, Derollez P, Dudognon E, Correia NT. Raman spectroscopy of racemic ibuprofen: Evidence of molecular disorder in phase II. International Journal of Pharmaceutics. 2011;421(1):45-52.

[39] Lazarević JJ, Uskoković-Marković S, Jelikić-Stankov M, Radonjić M, Tanasković D, Lazarević N, et al. Intermolecular and low- frequency intramolecular Raman scattering study of racemic ibuprofen. Spectrochimica Acta Part A: Molecular and Biomolecular Spectroscopy. 2014; 126:301-5.

[40] Zallen R, Slade ML. Influence of pressure and temperature on phonons in molecular chalcogenides: Crystalline As4S4 and S4N4. Physical Review B. 1978;18(10):5775-98

[41] Ostrowska K, Kropidowska M, Katrusiak A. High- pressure crystallization and structural transformations in compressed R, S -ibuprofen. Crystal Growth and Design. 2015;15(3):1512-7.

Chapter Five: The Impact of High Pressure on the Release Patterns of Ibuprofen from Polymeric Formulations

5.1 Introduction

Oral drug delivery systems are the most common and convenient dosage platform for the majority of patients mainly due to their ease of administration, accurate dosing, patient acceptability and longer shelf life.[1] However, one disadvantage of immediate release oral drug delivery systems is that the pharmacological effect of the drug may be transient, particularly if the drug has a short half-life, necessitating frequent (multiple) dosing to maintain a clinical effect. Scientists are therefore working to improve oral delivery systems that either afford controlled delivery of drugs, with enhanced bioavailability, decreased toxicity and reduced dosing frequency that all lead to improved clinical efficacy and patient compliance.

Modified release (MR) formulation development is a major area of drug delivery research. Such formulations are designed to deliver the drug at a pre-determined rate that is often linked to the daily onset of certain diseases and conditions. There are many clinical advantages for such formulations like enhanced patient compliance by reducing the frequency of administration, reduced usage compared with conventional immediate release formulations, reduced systemic toxicity, better controlled medical conditions due to sustained API levels and improved bioavailability.[2,3] The first controlled release formulation was marketed in 1952 by Smith, Kline & French (SKF). The Spansule® system, was used for the delivery of dextroamphetamine sulfate (Dexedrine®). This capsule technology incorporated multiple small drug-loaded beads coated with variable layers of natural waxes. As the layers dissolved within the gastrointestinal tract, controlled drug release was realised with more rapid release from

the beads with thinner coats. The administration of different beads resulted in sustained drug release over 10-12 hours.[4]

A few years later, SKF launched a formulation variant as a cold remedy (Contact®), in which each hard gelatin capsule contained several hundred beads. This formulation was intended for a 12-hour symptomatic relief of cold symptoms. The beads were divided into four groups according to the coat thickness and intended time for drug release.[5,6]

Extended release (ER) dosage forms are considered as a class of the MR formulations and defined as one that allows at least a 2-fold reduction in dosing frequency when compared with conventional dosage forms. Other terms like sustained release, controlled release, long acting, retard and slow release are used synonymously with ER, which falls under either of the following two technologies (Figure 5.1):[2]

1. Hydrophilic, hydrophobic or inert matrix system

2. Reservoir coated system

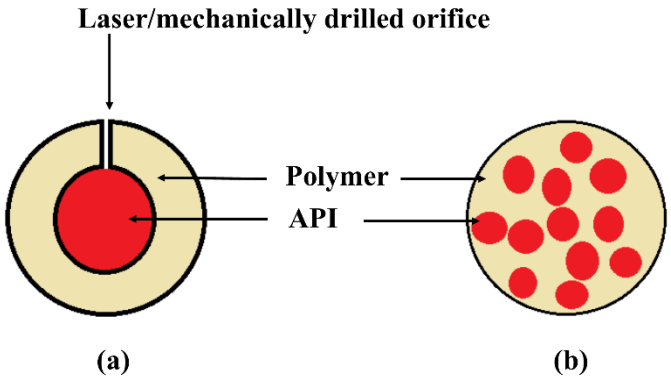

Figure 5.1 Schematic diagrams of ER systems (a) reservoir coated system, (b) monolithic matrix system

The matrix system is the simplest and most cost-effective oral delivery system to formulate. It accounts for the majority of commercially available formulations. The API is dissolved or dispersed in a rate controlling matrix. There are many factors that govern the release of API from MR formulations. These factors include the API:polymer ratio, molecular weight of polymers, the amount of hydrophilic polymers and partition coefficient of the API.

The reservoir coated system has the API-containing core enclosed and surrounded typically by a polymer coating. Such systems act by simple diffusion or by osmosis. In simple diffusion, the API either diffuses through the coating or after the erosion of the polymer that could be either hydrophilic, hydrophobic or a mixture of both. The nature of the polymer determines the API release, which is governed by Fick's law of diffusion. In osmotic systems, the API is contained within a semi-permeable membrane with a laser/mechanical drilled orifice which controls drug delivery. The API is released by the osmotic pressure generated within the core of the formulation.[7]

The process of manufacturing ER formulations is not different from the process of manufacturing conventional formulations as it includes similar steps such as granulation, blending, compression and in some cases film coating. The major difference is that the ER systems often contain polymers that retard the release of the API. These polymers can be either hydrophilic, hydrophobic or have amphiphilic characteristics (through use of co-polymers). Examples of both types of polymers are given in Table 5.1.[2,8]

Table 5.1 Examples of polymers commonly used in ER formulations[2,8]

Hydrophilic polymers	Hydrophobic polymers
Cellulose derivatives	Ethylcellulose
Methylcellulose	Cellulose acetate
Hydroxypropyl methylcellulose	Methacrylic acid
Hydroxypropylcellulose	Poly vinyl acetate
Hydroxyethylcellulose	**Fatty acids / waxes**
Sodium carboxymethylcellulose	Bees wax
Gums / polysaccharides	Paraffin wax
Xanthan gum	Hydrogenated palm oil
Chitosan	Hydrogenated castor oil
Pectin	Hydrogenated soybean oil
Sodium alginate	
Others	
Polyethylene oxide	
Acrylic acid	

Hydroxypropyl methylcellulose (HPMC) and ethylcellulose (EC) are commonly used polymers in modified release oral formulations. HPMC is widely used in pharmaceutical preparations, especially oral platforms as a release controlling agent. It is also used as a coating agent, tablet binder, thickening agent and film forming agent, etc. Different uses are governed by the concentration used in each formulation and the molecular weight of the polymer. For example, concentrations of 2-5% (w/w) of lower molecular weight HPMC may be used as binders whereas concentrations between 10-80% (w/w) of high viscosity HPMC grades may be used to retard the release of APIs from controlled release formulations.[8] EC is a hydrophobic polymer that is used in pharmaceutical formulations as a coating agent, tablet binder, viscosity enhancer and release modifier. The combination of HPMC and EC polymers has been

extensively explored in pharmaceutical formulations.[9,10,11] EC was found to sustain the release of IBP for longer time than HPMC alone when it was combined in equal quantities with HPMC. That is mainly attributed to its different behaviour with water as it tends to form a gel layer that holds the API for longer.[11]

In an attempt to identify an analgesic that replaces aspirin and might be suitable for long term use for rheumatoid arthritis, and after screening more than 600 compounds, Stewart Adams and John Nicolson filed a patent for 2-(4-isobutylphenyl) propionic acid that was granted in the early 1960s. This became a very successful drug and is currently known as ibuprofen (IBP).[12] IBP is known to have less gastric side effects than aspirin, rendering it a potentially safer option for long-term use in patients with inflammatory conditions. In the late 1960s, IBP was launched in the UK as a prescription medicine for the treatment of rheumatic diseases but several decades later it became deregulated and can be purchased as an over the counter medicine. Arguably, it is the most commonly used anti-inflammatory worldwide.

IBP is a commonly used non-steroidal anti-inflammatory drug (NSAID) that is used both as an analgesic and antipyretic agent. It is typically administered three or four times a day. It is commonly prescribed for rheumatoid arthritis, osteoarthritis, mild to moderate pain and other musculoskeletal disorders. It is a non-selective cyclooxygenase-1 and cyclooxygenase-2 enzyme inhibitor, which both catalyse the production of prostaglandin and thromboxane that are both responsible for pain and inflammation.

There are different techniques to prepare MR formulations that contain polymers including hot melt extrusion (HME), which has an advantage of good mixing and content uniformity. HME is a continuous pharmaceutical process that includes stress, strain and heat to efficiently blend materials together. It is used for mixing polymers and APIs by moving them through a rotating screw that applies pressure at temperatures above their glass transition to achieve molecular levels of mixing. It can be used to improve the dissolution of poorly water soluble drugs. A study by Brabander et al.,[13] in which they developed sustained release mini-matrices of IBP and EC and other excipients by means of HME found that the release of IBP from a 60:40 w/w of IBP:EC was very low, with only 20% drug was released in 24 hours. Addition of hydrophilic excipients such as HPMC and xanthan gum enhanced release rate. By adding 10% of HMPC to the formulation (IBP 60%: EC 30), the release of IBP from the extrudates reached about 50 % in 24 hours. Increasing the content of HPMC to 20% and reducing EC to 20% while API was constant (60%) has improved the release of IBP to 90% in 24 hours. HPMC was substituted for xanthan gum making the formulation consisting of 60% IBP, 20% EC and 20% xanthan gum. The release rate was better controlled by xanthan gum than HPMC but 90% of IBP was release in 24hours in both cases. These results were obtained by in vitro dissolution (paddle method) and analysed using UV-vis spectrophotometry. Release form matrices manufactured by HME was swelling/diffusion controlled.

Another study by Brabander et.al.[14] has tested the bioavailability of IBP produced using hot-melt extruded mini-matrices of EC/HPMC (3 mm diameter, 2 mm long). The formulation was compared with a formulation containing xanthan gum instead of HPMC and a commercially available formulation (Ibu-slow® 600). They found that

the hot-melt extruded formulations containing EC and HPMC or xanthan gum sustained the release of IBP longer than (Ibu-slow® 600). Similar to their previous study[13], xanthan gum had a better control on the release but all the formulation released 90-100% of IBP in 24 hours.

The aim of the present research was to develop sustained release formulations i.e. tablets and capsules, by subjecting API and excipients to high pressure (0.8 GPa) before using them to formulating oral delivery systems. The application of pressure is known to induce polymorphism, which may in turn change the physicochemical properties of materials leading to changes in their stability and/or in vitro in vivo performances.[15,16] A study by Moggach et al[17] found that the application of pressure (0.78 GPa) resulted in solvent being pushed into the pores of metal-organic framework materials and making them resistant to compression. In this study, we explore the effect of pressure on pushing the API into the polymers, hence sustain its release. A fixed amount of IBP (100 mg) mixed with different ratios of EC and HPMC using varied processing parameters to explore their relative impact upon subsequent drug release patterns. Resultant drug-polymer blends were mixed using a novel technique called resonant acoustic mixing (RAM) as an alternative to ball-milling in order to create the formulations before applying pressure.

5.2 Materials and Methods

5.2.1 Materials

Ibuprofen powder (IBP, purity ≥98% GC), sodium chloride (ACS reagent, Ph. Eur ≥99.8%), sodium phosphate monobasic monohydrate (ACS reagent, ≥99.0%) were purchased from Sigma-Aldrich UK. Hydroxypropyl methylcellulose (HPMC) E50 (Methocel™) with apparent viscosity, 2% in water, of 40-60 mPa.s and ethyl cellulose (EC) (ethoxyl content: 48–49.5% (w/w); viscosity: 9–11 mPa.s were kindly donated by Colorcon®, Kent, UK. Petroleum ether 35/60 ACS grade and sodium hydroxide 98% were purchased from Alfa Aesar, UK.

5.2.2 Methods

5.2.2.1 Raman spectroscopy

Raman spectra were acquired using Raman XplorA Microscope by Horiba Scientific John Yvon Technology with an excitation wavelength of 532 nm. Spectra were summed using 2 accumulations and a grating of 1200-gr/mm, which was found to be the best suitable to yield good resolution. Raman data analysis and graph production was done using OriginPro® 2017 software (OriginLab, Northampton, MA).[18]

5.2.2.2 Preparation of dosage forms

As per the information provided in Table 5.2, all formulations contained a fixed quantity of IBP (100mg). Three different formulations namely F1, F2, and F3 containing IBP:EC:HPMC at a weight ratio of either (30:35:35%), (60:20:20%) and (80:10:10%) respectively were prepared. These ratios were selected in order to investigate the effects of high and low polymer to API ratio and the effect on the release patterns. Individual formulation components were weighed and transferred into

glass vials for mixing using RAM technology at 40 G for 30 minutes as per the RAM mixing guidelines, tested and validated at the University of Edinburgh, and standard configurations (Table 5.3). This mixing technique was adopted to prevent or minimise the introduction of any kind of mechanical energy, to the formulation blends, which may introduce thermal or mechanical energy that can damage the particles, alter their crystallinity or amorphise them.[19,20] Pulham et al.[20] observed that co-crystallisation can be achieved in the absence of milling bodies using the RAM. They obtained *in situ* co-crystals of nicotinamide and carbamazepine and monitored that using synchrotron X-ray powder diffraction. Another important advantage of using the RAM is the speed of mixing as well as yielding a homogenous mixture.

Table 5.2 F1-F3 formulations composition

Component	**Formulation**		
	F1 (w/w%)	**F2 (w/w%)**	**F3 (w/w%)**
IBP	100.0 mg (30%)	100.0 mg (60%)	100.0 mg (80%)
HPMC E50	116.7 mg (35%)	33.3 mg (20%)	12.5 mg (10%)
EC 10	116.7 mg (35%)	33.3 mg (20%)	12.5 mg (10%)
Total weight	333.4 mg	166.6 mg	125.0 mg

Table 5.3 RAM mixing guidelines tested and validated at the University of Edinburgh - Standard configuration

Procedure	Recommended vessel	Recommended parameters
Mixing unreactive powders (similar particle size)	Glass or plastic. As little head space as possible	10-30 G 5-15 minutes
Mixing unreactive powders (disparate particle sizes)	Glass or plastic. As little head space as possible	20-40 G 10-30 minutes

Formulations F1, F2 and F3 were similarly treated under three different process conditions:

1. Powder blend (powders were used as received)
2. Powder blend left in petroleum ether 35/60 for 24 hours at ambient pressure (AP) as a control
3. Powder blend in petroleum ether 35/60 under high pressure (0.8 GPa), in the large volume press, for 24 hours (HP). NB. 0.8 GPa is the maximum pressure of the press.

The ambient pressure (AP) and high pressure (HP) formulations were dried to ensure the removal of petroleum ether by using vacuum desiccator until samples were completely dried. Petroleum ether was used as a pressure transmitting medium (PTM) to surround the formulation when subjected to pressure in order to ensure hydrostasticity. The choice of PTM is driven by different factors including ease of removal, stability and chemical inertness. The drying process was monitored by weighing the samples before and after treatment. The retrieved samples were then formulated into the relevant dosage forms. All formulations were treated in the same manner.

5.2.2.3 Tablet direct compression

All the formulations (F1-F3) were tableted by direct compression of the blend using an 8 mm diameter tablet die punch mould pressed by a manual load cell connected to a digital compression sensor as shown in Figure 5.2. The formulation powder was carefully transferred into the die and subjected to a load of 80 kg for one minute then the load topped up to 80 kg for another two minutes as the load decreased over the first minute. The tablets were then labelled and stored in airtight vials at ambient room temperature (23°C) before any further investigations.

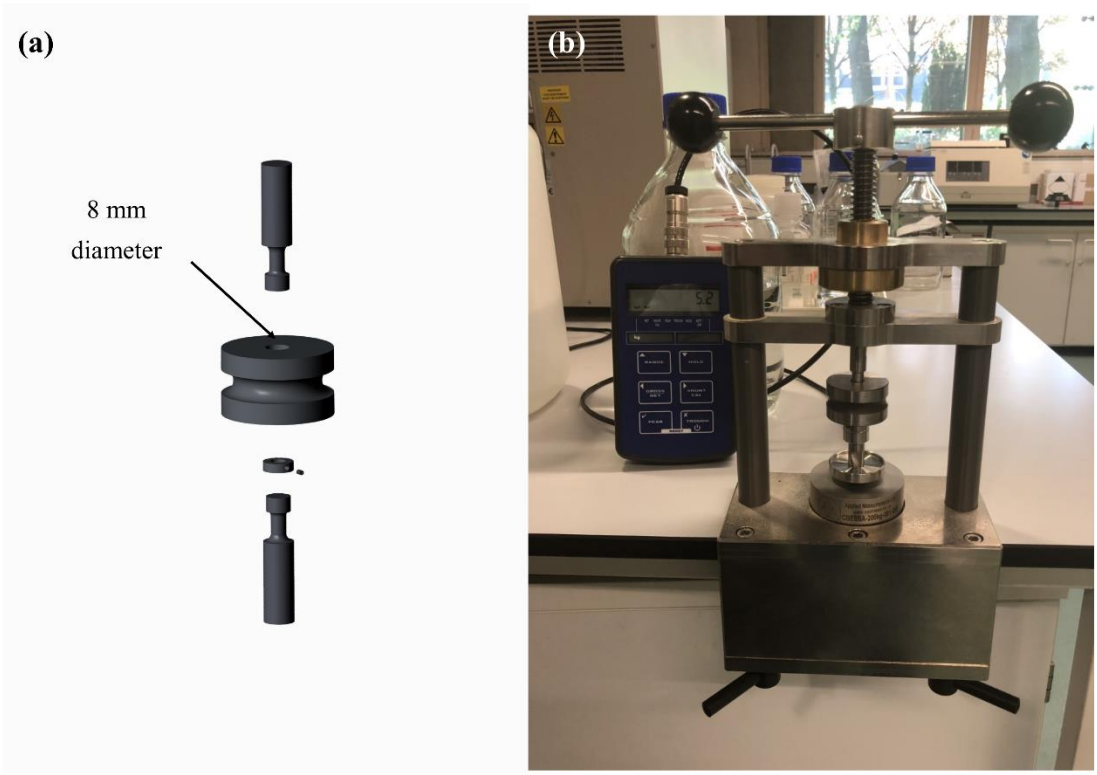

Figure 5.2 (a) schematic of tablet die (b) compression device used to compress tablets connected to a digital compression sensor to measure weight applied

5.2.2.4 Capsules

A second batch of formulations was prepared and added to hard gelatin capsules of size 0, labelled and stored in airtight vials at ambient room temperature (23°C) before any further investigations.

5.2.2.5 Dissolution media preparation

Biorelevant media was chosen because it gives a better simulation of the gastro-intestinal tract, hence better *in vivo* correlation as they are more predictive of *in vivo* dissolution.[21,22,23]

In this experiment, this media was used as dissolution media and prepared using the following components in (g/l):

0.420 g of Sodium hydroxide pellets (NaOH)
3.954 g of Monobasic sodium phosphate monohydrate (NaH2PO4· H2O)
6.186 g of Sodium chloride (NaCl)
Deionised water filled up to 1L

After dissolving the constituents of the dissolution media in deionised water, pH was measured and adjusted to 6.8 using (0.1 M) HCl or (0.1 M) NaOH dropwise. All dissolution media were freshly prepared before the dissolution test.

5.2.2.6 Preparation of standard solutions

100 mg of IBP was weighed and transferred into a 100 mL volumetric flask and 30 mL of the dissolution media was added. The flask was shaken and sonicated to dissolve the contents of the flask. Additional media was added up gradually until the complete volume was made up and sonicated to ensure complete solubilisation of IBP to a concentration of 1mg/mL. Further dilutions were prepared from the stock solution with

concentrations of 100 µg/mL, 50 µg/mL, 25 µg/mL, 12.5 µg/mL, 6.25 µg/mL, 3.125 µg/mL, 1.5625 µg/mL. From each of these concentrations, 1 mL was taken and further diluted in 4 mL of the dissolution media (total 5 mL). Solutions were prepared for analysis in triplicate.

5.2.2.7 Dissolution studies

The in vitro release of IBP from the polymeric tablets and capsules was measured using the United States Pharmacopoeia (USP) method II (paddle method). A Copley tablet dissolution tester DIS 6000 (Nottingham, UK) was used for this process. 900 ml of biorelevant dissolution media (pH 6.8) was stirred at 100 rpm at a constantly maintained temperature of 37.0 ± 0.5 °C. The temperature of the dissolution media was allowed to equilibrate with dissolution bath temperature and checked before the start of the experiment. Each vessel was coded and the corresponding sample results were assigned the same code. Individual dosage units were coupled with helix sinkers to prevent floating in the dissolution bath. The experiment was initiated as soon as formulations sunk to the bottom of the vessel. At specific time intervals of 0, 5, 10, 20, 40, 60, 90 minutes, 2, 4, 6, 8, 12, 16, 20, 24, 36 and 48 hours, 5 mL aliquots of samples were collected and immediately replaced with an equivalent volume of dissolution media stored at the same temperature. 1 mL was taken from each aliquot and diluted with 4 mL of dissolution media to give a total of 5 mL before being analysed in triplicates using UV-Visible spectrophotometry (Helios α Thermo Electron Corporation, Cambridge, UK). Samples were added to a 1 cm quartz cuvette and measured at a fixed wavelength (λ_{max} of 222 nm). This value of λ_{max} was obtained by scanning different concentrations of IBP in UV range (190-600 nm) against

biorelevant media as a blank. The absorbance value was used to determine concentration against a calibration curve and converted into % drug release.

The mean release of three tablets or three capsules of each formulation was calculated and a plot of drug release against time was used to determine the drug release profile.

5.2.2.8 Scanning electron microscope imaging (SEM)

Individual formulation components and the resultant powder blends were evaluated for shape morphology by an FEI Quanta 250 FEG-ESEM (Oregon, USA). Samples were fixed with conductive double-sided carbon adhesive tape on stubs without being coated. Images were captured at multiple magnifications (x2,000 and x10,000).

5.2.2.9 Tablet hardness test

The hardness of 10 tablets from individual formulations was assessed using a Copley Tablet Hardness Tester TBF 1000 (Copley Scientific, Nottingham, United Kingdom). The mean, minimum and maximum hardness values were determined.

5.3 Results and Discussion

5.3.1 Raman Spectroscopy

Raman spectra for individual components of the formulations with different treatments i.e. (P, AP, HP) was collected in the spectral region of 50-3500 cm^{-1} (Figure 5.3). This was done to investigate if different treatments will have any changes in the spectrum.

It is evident that AP and HP samples Raman spectra are exactly like the powder Raman for all the 3 formulation constituents. This indicates that the PTM and application of pressure (0.8 GPa) did not have any conformational changes to the samples. Full compression studies of the individual components were explored in Chapter 4.

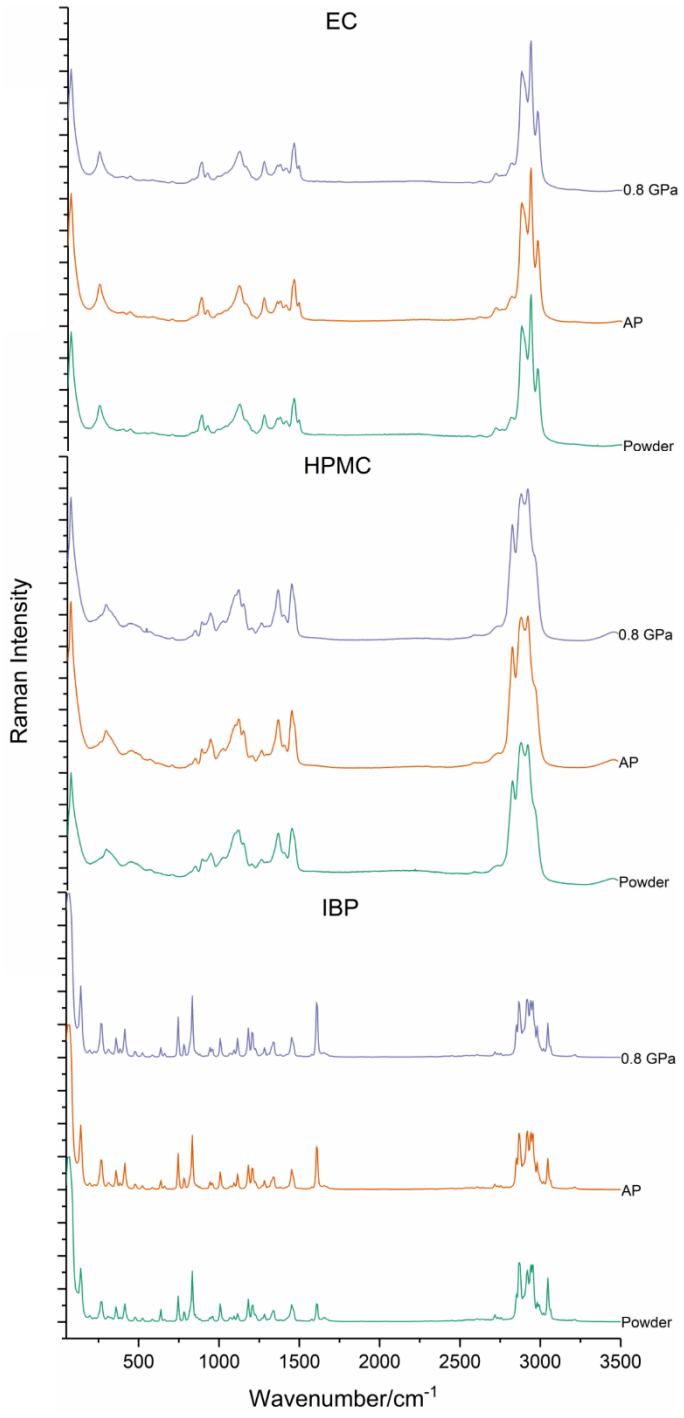

Figure 5.3 Raman spectra of ethylcellulose (EC), hydroxypropyl methylcellulose (HPMC) and ibuprofen (IBP) under different conditions (P: powder), (AP: powder treated by PTM at ambient pressure) and (HP: powder treated by PTM under high pressure (0.8 GPa))

5.3.2 Preparation of dosage forms

Tablets of F1, F2 and F3 were manufactured by direct compression of the powder blend using an 8 mm diameter tablet die punch mould pressed by a manual load cell connected to a digital compression sensor as shown in Figure 5.2. Examples of tablets produced are shown in Figure 5.4, which shows that different formulations have different heights due to different weights (fixed amount of IBP per tablet).

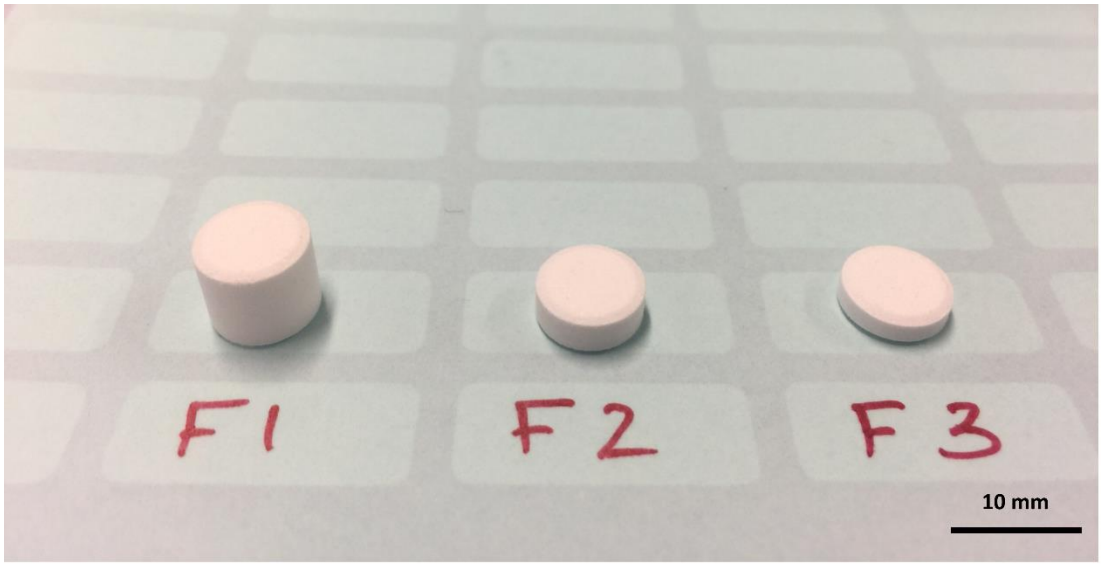

Figure 5.4 Examples of F1, F2 and F3 tablets prepared for dissolution studies

Tablet height was measured for all formulations variants. Average height is reported in Table 5.4. It is evident that all tablets were similar in height with difference due to slight weight variation.

Table 5.4 Average tablet thickness for formulations F1-F3 and standard deviation (n=3)

Formulation	F1			F2			F3		
	P	AP	HP	P	AP	HP	P	AP	HP
Av. tablet thickness (mm)	7.63 (±0.03)	7.59 (±0.09)	7.60 (±0.08)	3.76 (±0.04)	3.72 (±0.07)	3.73 (±0.05)	2.80 (±0.02)	2.82 (±0.09)	2.80 (±0.06)

5.3.3 Tablet hardness testing

Tablet hardness is defined as the force required to break a tablet in a diametric compression test. Such a test is used to investigate if the tablet can withstand post manufacturing transportation and handling. The testing apparatus consists of two jaws facing each other, of which one moves towards the other. The flat surfaces of both jaws are perpendicular to the direction of movement.[24] In this experiment, the hardness of 10 tablets of each formulation for F1-F3 P and AP tablets was tested as a further investigation of the delayed release of AP compared to P formulations.

Table 5.6 Hardness values in (kp) of P and AP tablets of F-F3 formulations (n=10)

Formulation	F1		F2		F3	
	P	AP	P	AP	P	AP
mean	3.87	7.45	1.345	1.821	0.83	1.25
minimum	3.47	6.00	1.22	1.38	0.72	0.95
maximum	4.27	9.68	1.50	2.75	1.04	1.49
SD	0.23	1.17	0.09	0.40	0.09	0.18

It is evident from Table 5.6 that the tablet hardness values are higher in AP formulations than the P despite being compressed using the same force for the same time. The higher tablet hardness value means that it will take the tablet longer to disintegrate, hence sustain the release of the impeded drug for a longer time. This was not as noticeable in F2 and F3 formulations. This could be attributed to effect of tablet compression-induced mechanical interlocking, which is caused by the PTM. As explained earlier, the PTM has weakened the structure of EC and formed halls which could serve potential site for particle interlocking. Additional to that, the tablet compression forces will assist particle interlocking.

5.3.4 Standard solutions and calibration curve

Different concentrations of standard solutions were prepared in triplicates and the absorbance was measured. The average absorbance is shown in Table 5.5 and used to plot the calibration curve. The calibration curve for ibuprofen was created using different concentrations to permit the analysis of the release of ibuprofen from the formulations.

Table 5.5 Concentration versus average absorbance of IBP dissolved in biorelevant media measured at λ_{max} 222 nm (n=3)

Concentration (µg/mL)	Average Absorbance
100.000	0.903
50.000	0.452
25.000	0.229
12.500	0.116
6.250	0.060
3.125	0.031
1.562	0.012

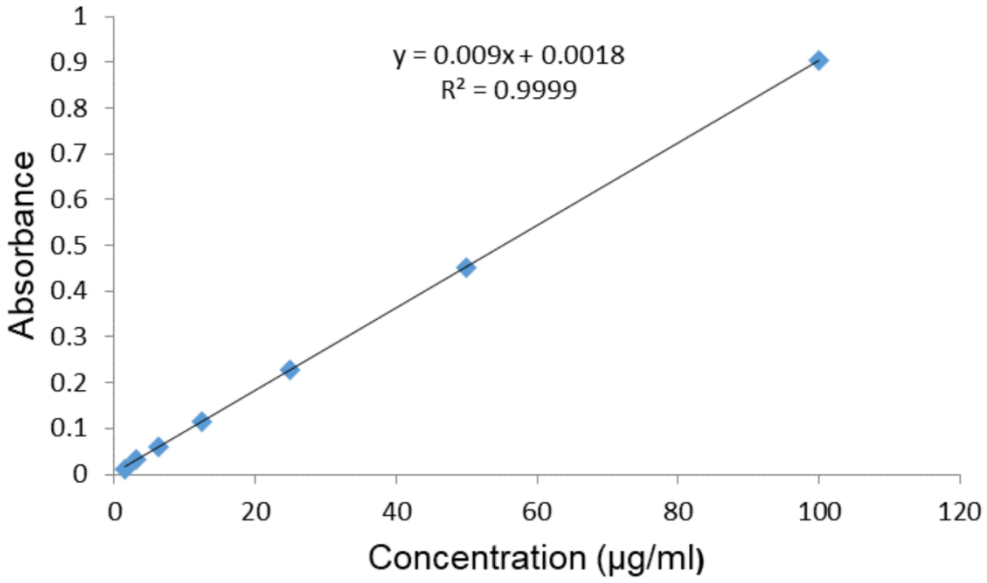

Figure 5.5 Calibration curve of standard solutions of IBP dissolved in biorelevant dissolution media

A linear calibration curve of IBP was obtained by plotting the average absorbance of IBP throughout the concentration ranges tested (Figure 5.5), with R^2= 0.9999 and y=0.009x + 0.0018. The amount of IBP released was calculated using Beer's law ($A=\varepsilon bc$), where A is the absorbance, ε is the extinction coefficient, b is the path length that light has travelled (1 cm) and c is concentration.

5.3.5 Dissolution studies

The United States Pharmacopoeia (USP) defines the modified release (MR) dosage forms as "the one for which the drug release characteristics of time course and/or location are chosen to accomplish therapeutic or convenience objectives not offered by conventional dosage forms such as solutions, ointments, or promptly dissolving dosage forms".[25]

The cumulative percentage of IBP released at the defined time intervals was obtained by calculating the mean release of three tablets or three capsules (n=3) of each formulation and a plot of drug release against time was used to determine the drug release profile. This was calculated using the linear regression equation for IBP $y=0.009x + 0.0018$, $R^2= 0.999$ as shown in Figure 5.5.

Dosage form dissolution testing is regarded as an important and mandatory tool for quality control of pharmaceutical products. Despite the real barrier and complexity of understanding drug absorption in the gastrointestinal tract, dissolution studies are considered the best for in vitro/in vivo correlations for pharmaceutical dosage forms in development. Although it cannot be completely relied upon, it is used as a qualitative tool to evaluate the availability of the drug within the body and to ensure batch to batch consistency.[26]

5.3.4.1 Tablet release patterns

5.3.5.1.1 Tablets prepared from powder formulations

One of the aims of this experiment is to investigate the release properties of IBP from different (polymer:API) ratios. The release pattern of F1-F3 IBP tablets is presented in Figure 5.6, where it is apparent that F1 tablet formulation showed a slower release profile compared to F2 and F3. This effect is mainly attributed to the higher polymeric composition of the tablet which impedes drug release. A visually apparent gel layer formed upon addition of the tablet into dissolution media. This was thought to be due to the hydration of HPMC formulation component. This phenomenon is known as polymer swelling and it is dominant in hydrophilic polymers like HPMC in this case.[27]

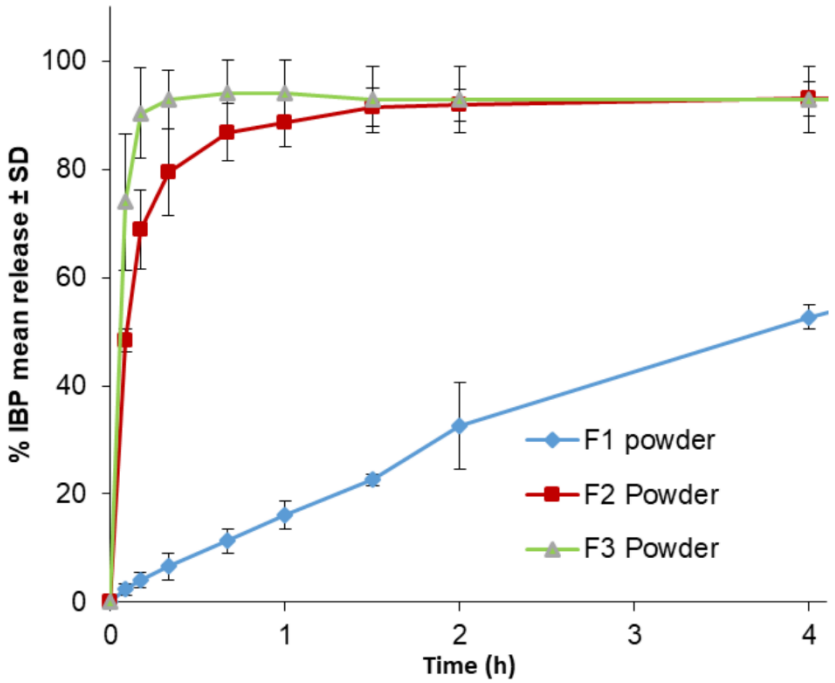

Figure 5.6 Cumulative IBP release from F1-F3 tablets of powder formulations versus time (n=3), where F1 released about 50% at 4 hours while F2 released 100% at 1.5 hour and F3 at 15 minutes.

As the formulation contacts the dissolution medium, the medium ingresses within the tablet formulation. This leads to breakage of hydrogen bonds formed during tablet compression and the formation of new ones that can accommodate water within their network. As water content increases, a gel layer is formed. The gel layer retards further water uptake by the rest of the tablet, hence slows the release of tablet contents.[28] In a comparative study evaluating plastic, hydrophilic and hydrophobic polymers as matrices for controlled release drug delivery by Reza et al.,[29] it has been reported that regardless of the physicochemical properties of polymers, the release profile was largely affected by the polymer content in the matrix and this is in line with the findings of this experiment.

Another study by Ebube et al.[30] also supports this proposed mechanism as they also observed that the release of acetaminophen was influenced by the polymer loading promoting greater physical cross linking between polymers, slower water ingress and slower diffusion of API.[31] It has also been confirmed in studies by Jain et al.[32] and Ghori et al.[33] that the use of higher polymer content in a tablet matrix slows down the matrix erosion rate, hence slowing down the release of API.

In comparison with Brabander et al.[14] work on the bioavailability of IBP from hot-melt extruded mini-matrices, the F1 formulation is the equivalent to their mini-matrices in terms of (polymer:API) ratio which is 35%:35%:30% w/w of (EC:HPMC:IBP). At 2-hour time point, the IBP cumulative release was observed to be similar to our F1 tablet formulation release i.e. around 30%. On the other hand, at the 4-hour time point, the formulation in our experiment has released about 50% of IBP compared to about 35% of IBP from the mini-matrices. This may be attributed to the way that mini-matrices were processed as hot-melt extrusion is known to give higher tensile strength to the constituents of the formulation which in turn will lead to slower release as reported by Avgerinos et al.[34] The same phenomenon was evident on the 24-hour release pattern where the IBP release in F1 tablet peaked at 12 hours (Figure 5.7) while in the mini-matrices peaked at 16 hours.

The commercial product used by Brabander et al.[14] (Ibu-slow® 600, half a tablet) released 50% at 4 hours whereas the mini matrices released 50% at about 6 hours. This study shows that the F1 used in this experiment has a similar dissolution profile to the commercially available Ibu-slow®. It is evident from Figure 5.6 that F1 tablet has released 50% of the IBP content at 4 hours, whereas F2 and F3 formulations released the same amount at 5 minutes and ~ 2 minutes respectively. Both F2 and F3 tablet

powder formulations peaked at 2 hours and 15 minutes respectively. On the other hand, F1 reached its peak at 20 hours. This can be explained by the phenomenon of polymer swelling as formulation with high polymer content will show a slower release due to the fact that the API will be entrapped in the matrix for longer, whereas, in F2 and F3 less polymer will be surrounding the API, hence the release is faster as the gel layer formed may not be sufficient to hinder the API diffusion from the matrix.

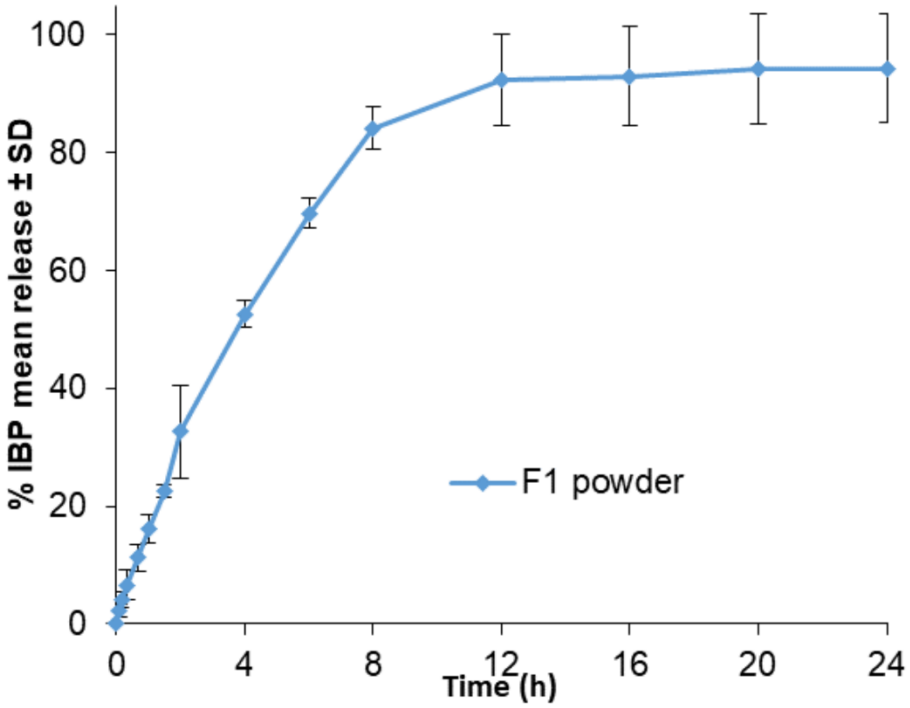

Figure 5.7 F1 Cumulative release of IBP vs time from F1 P tablets (n=3)

5.3.5.1.2 Comparative release pattern of IBP from powder, ambient pressure and high-pressure tablet formulations

Each of the formulations was investigated under different conditions such as the received powder blend (P), powder blend in the PTM, petroleum ether, for 24 hours (AP) and the powder blend in the PTM under 0.8 GPa for 24 hours (HP). As mentioned

earlier in Table 5.2, F1 formulations contain 35% EC, 35% HPMC and 30% IBP. The IBP content was fixed at 100 mg/tablet. The AP and HP formulations explored the role of pressure. Referring to Figure 5.8, the F1 P, AP and HP tablet formulations exhibited different release patterns. The IBP release pattern from the AP and HP formulations was significantly slower (*p-value* < 0.05, statistically evaluated by two-way ANOVA) than the P formulation but the difference between AP & HP was insignificant. The release of IBP from the powder formulation peaked and plateaued at 20 hours whereas the AP and HP were still releasing at 48 hours and the tablets did not fully disintegrate. This may be due to the effect of PTM rather than the pressure. The PTM may have helped the API to disperse and entrap within the polymers more efficiently.

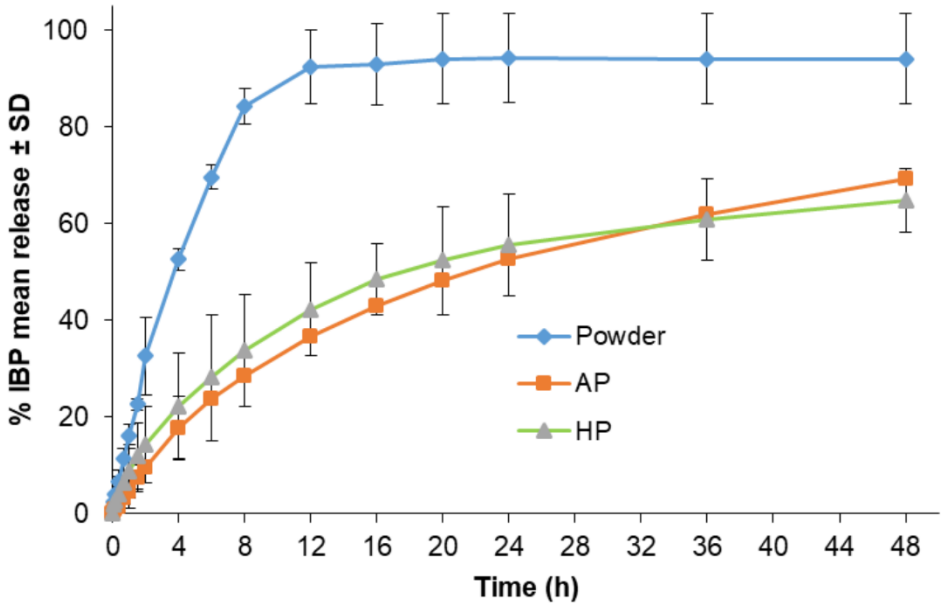

Figure 5.8 F1 P, AP and HP tablet formulations release patterns versus time (n=3). F1 P tablet peaked at about 20 hours while AP and HP tablets were still releasing until the experiment was stopped at 48 hours.

A similar phenomenon was observed in F2 tablet formulations. The AP and HP formulations released IBP from the tablets at a slower rate than the P formulation, which was statistically significant (*p-value* <0.05). The P formulation plateaued as early as 4 hours while the AP and HP ones plateaued at 20 and 16 hours respectively (Figure 5.9). A similar effect of PTM is evident in this formulation as it aided the API entrapment within the polymers.

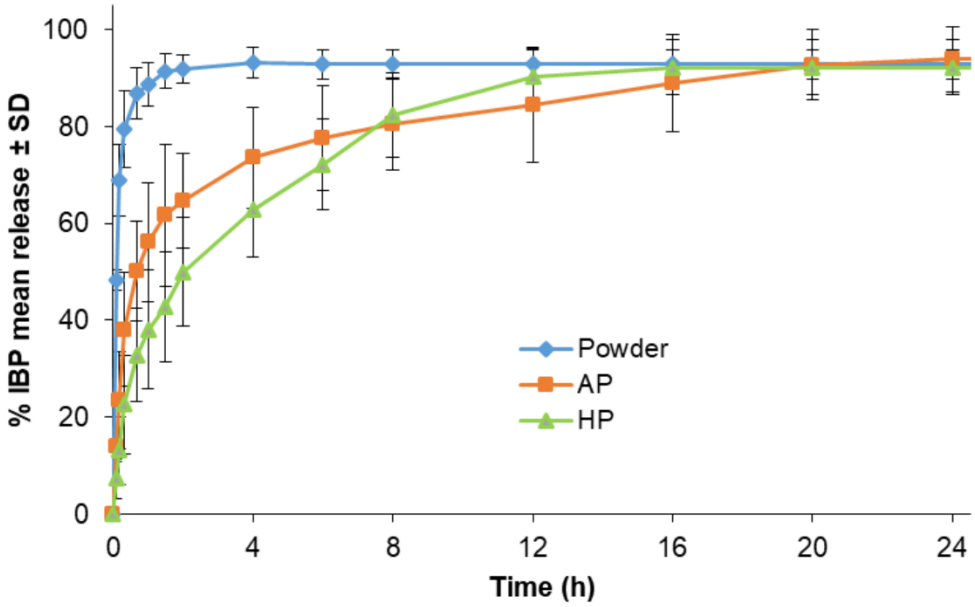

Figure 5.9 F2 P, AP and HP tablet formulations release patterns versus time (n=3). F2 P tablet peaked at 4 hours while AP and HP release IBP in a slower manner until they peaked at 20 and 16 hours respectively.

The F3 tablet formulations released the API in a quicker manner compared to F1 and F2,mainly due to their lower polymeric content i.e. (80:10:10%) (IBP:HPMC:EC).[28] Similar to F1 and F2 tablets, the powder formulation in F3 showed a quicker release compared to AP and HP formulations as shown in Figure 5.10. The release of IBP

from the powder formulation plateaued at 20 minutes whereas in AP and HP formulation, the plateau was observed at 4 and 2 hours respectively. The low polymer concentration makes the disintegration of the tablet quicker as polymers have a binding role in tablets.

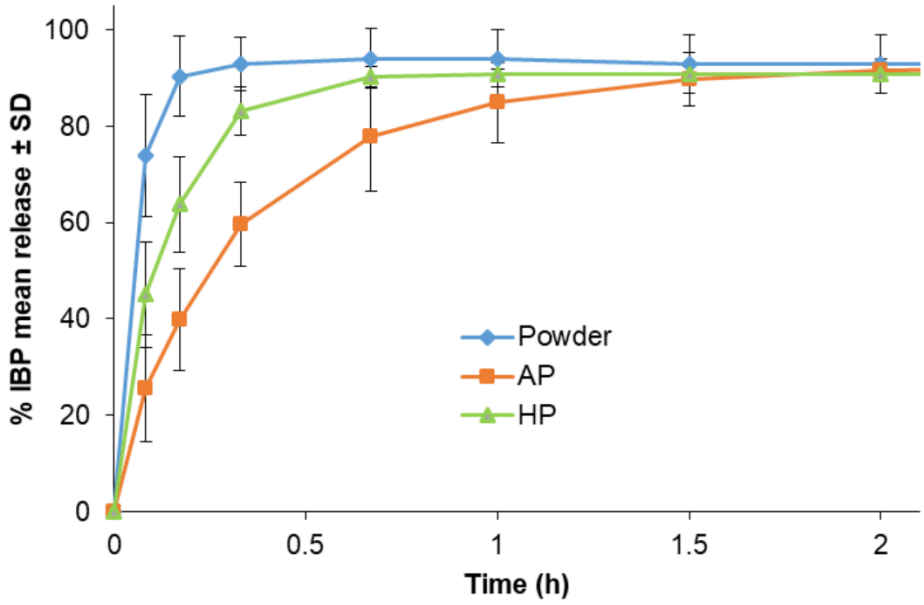

Figure 5.10 F3 P, AP and HP tablet formulations release patterns versus time (n=3). The F3 P tablet peaked at 20 minutes whereas in AP and HP formulation, the peak was observed at 4 and 2 hours respectively.

5.3.4.2 Capsules release pattern

5.3.5.2.1 Capsules prepared from powder formulations

Similar formulations of F1-F3 were prepared into capsule dosage form using hard gelatin capsules (size 0). Capsule dosage form was used to rule out the impact of compression on the polymers during the tabletting process on the release pattern of IBP from the formulations. As shown in Figure 5.11, the powder capsule formulations

F1-F3 showed a release pattern that is similar to the powder tablet formulations in terms of sustaining the release of IBP. F1 showed a slower release pattern than F2 and F3. The F1 capsule powder formulation released 50% of IBP at about 1 hour and peaked at 8 hours (Figure 5.11), whereas in the powder tablet formulation 50% of IBP was released at 4 hours (Figure 5.6). This phenomenon was expected as tablet dosage forms have to undergo disintegration, which is the mechanical break-up of the dosage form into smaller particles, before releasing the API.[35] This is not the case in capsules as the constituents are not compacted together and have a larger surface area in contact with the dissolution media as soon as the capsule erodes. This observation was supported by the polymeric content ratio and its effect on the release pattern of APIs.[28]

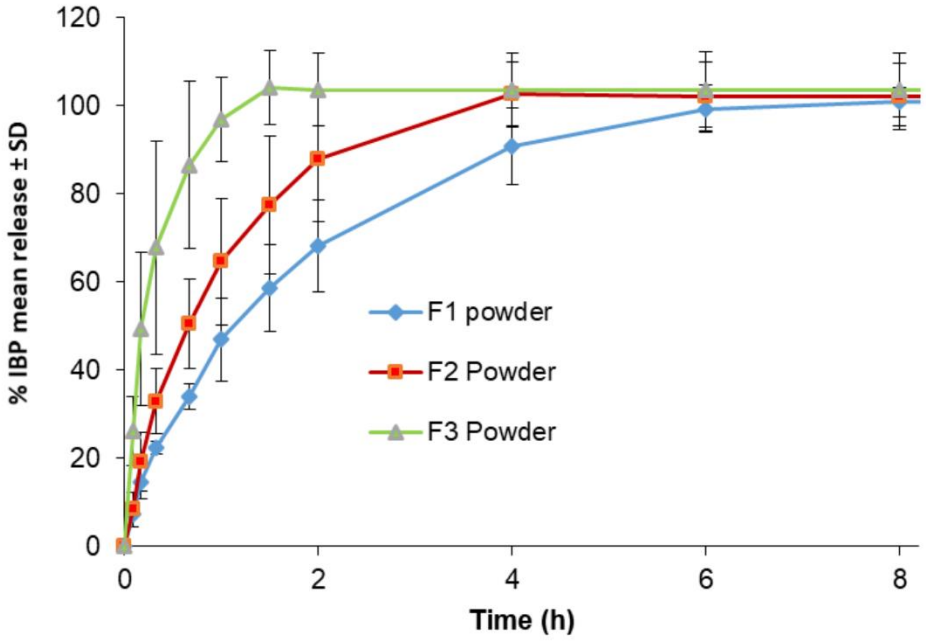

Figure 5.11 Cumulative IBP release from F1-F3 capsules of powder formulations versus time (n=3). The F1 showed a slower release of IBP compared to F2 and F3 and this is because it contains a higher polymer concentration.

5.3.5.2.2 Comparative release pattern of IBP from powder, ambient pressure and high-pressure capsule formulations

Each of the formulations was investigated using the same conditions as used in tablets namely P, AP and HP. In comparison to F1 tablets release pattern, F1 powder capsules followed F1 tablets in the release of IBP but in a different time scale. The release from the P capsule was at a faster rate than AP and HP capsules. The release of IBP from F1 P capsules peaked at 8 hours while the AP and HP of the same formulation peaked at 20 hours (Figure 5.12). This was attributed to effect of PTM aiding the entanglement of the API to the polymers. Nevertheless, the difference in release was statistically insignificant.

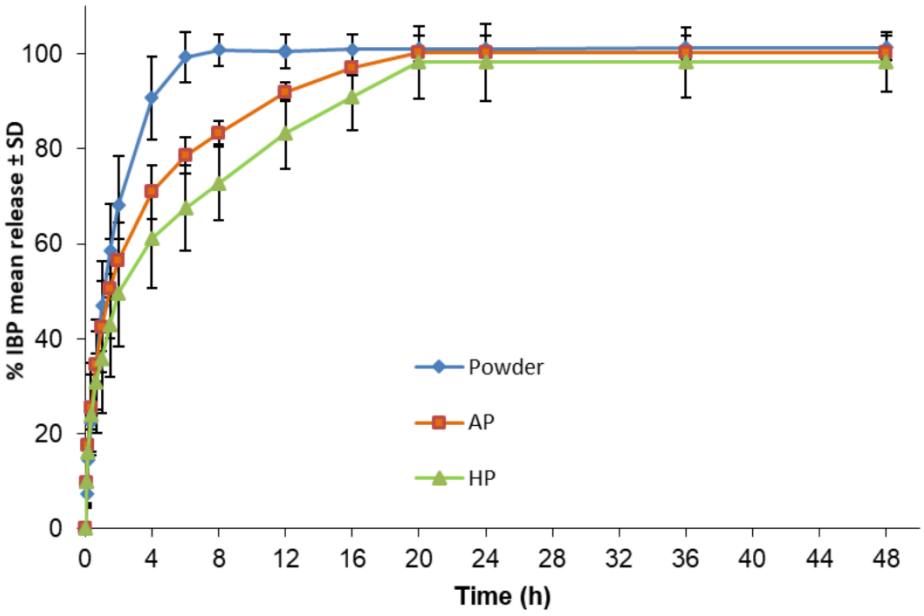

Figure 5.12 F1 P, AP and HP capsule formulations release patterns versus time (n=3). The P capsules peaked at 8 hours while both AP and HP which released in a lower manner peaked at 20 hours.

The release pattern of IBP from F2 and F3 capsules formulations presented in Figure 5.13 and Figure 5.14 respectively show little difference in release of IBP as a function of treatment within each formulation. The time of releasing 100% of IBP in F2 capsules was 4 hours for the P formulation and 6 hours for the AP and HP formulations, while for the F3 formulations was about 1.5 hours. F3 capsules formulations did not follow the trend of F3 tablet formulation. The release from F3 capsules was indistinguishable and did not differ depending on the prior treatment of the formulation. The reason behind this is that 80% of the formulation was the API and only 20% for the polymers.

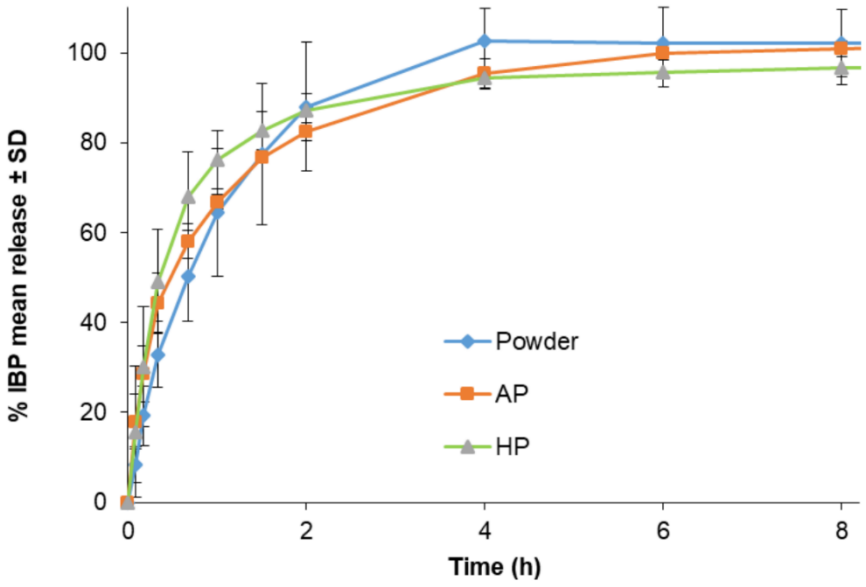

Figure 5.13 F2 P, AP and HP capsule formulations release patterns versus time (n=3). The release of IBP from P and HP formulation peaked at 4 hours while the AP peaked at 6 hours.

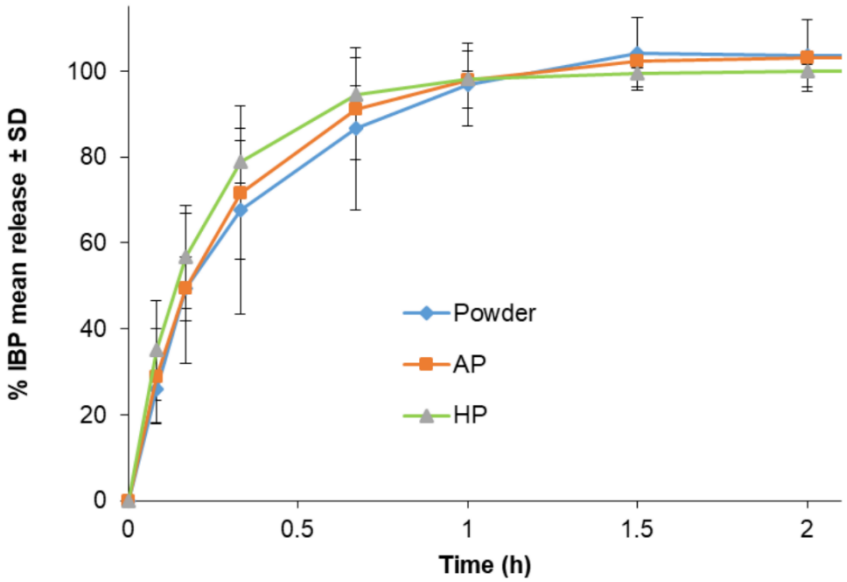

Figure 5.14 F3 P, AP and HP capsule formulations release patterns versus time (n=3).

5.3.6 Scanning electron microscopy

The morphology of individual formulation components and the formulation blends was investigated using SEM. The aim of SEM imaging was to explore if the PTM has caused any morphological changes in the samples. The SEM images of EC (Figure 5.15) have shown that the AP sample, which has been in contact with PTM for 24 hours, (c&d) has changed in morphology when compared with the P form (a&b). The PTM created pockets of holes within the particles. These holes could serve as pockets for other components including IBP to become entrapped. This could serve as an explanation for the delayed release of IBP from AP formulations compared to P formulations, especially in F1 and F2 formulations. These holes could be potentially hosting the IBP by mechanical interlocking mechanism especially in the tablet formulations, facilitated by compression forces.[34] On the other hand, in capsules

formulations, solid bridges may form between the particles of AP and HP capsule formulations. These bridges may help to bind particles together. The solid bridges are defined as the contact at an atomic level between adjacent surfaces of particles.[34]

SEM images of P and AP HPMC (Figure 5.16) show no difference in morphology after being treated with the PTM. IBP samples also show no difference in morphology between the P and AP formulations (Figure 5.17).

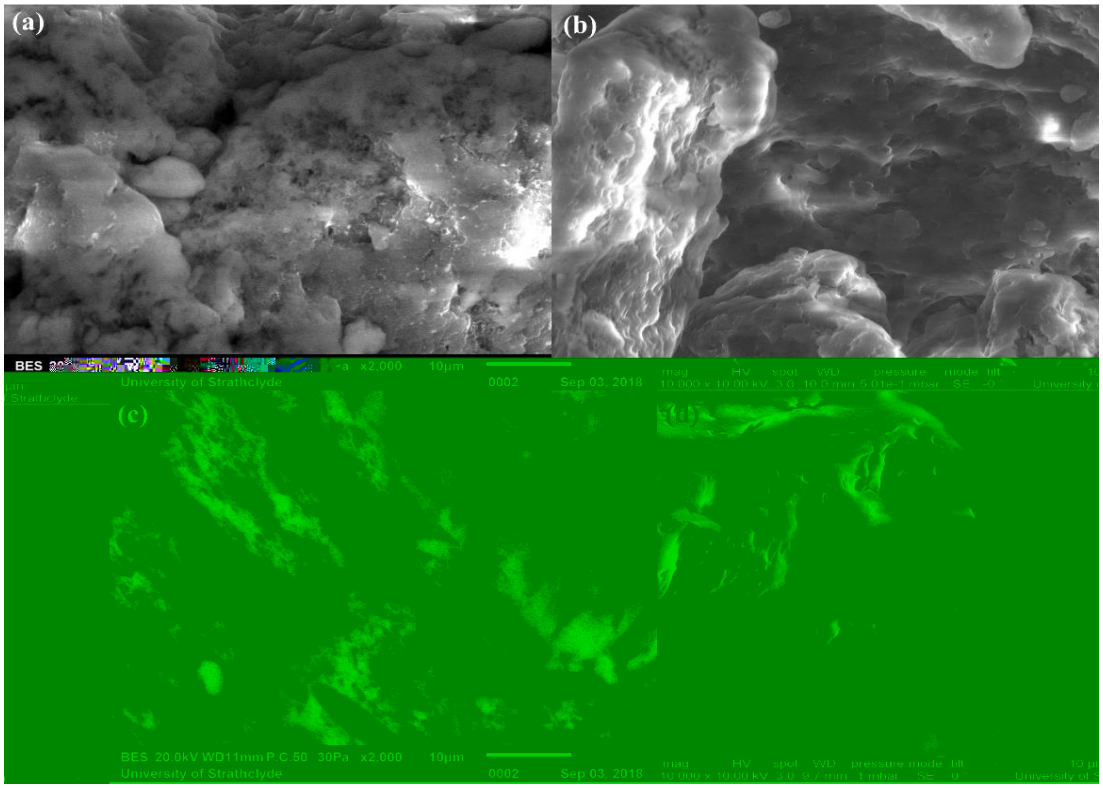

Figure 5.15 SEM images with different magnifications of ethylcellulose (a:x2,000 &b:x10,000) powder (c:x2,000 & d:x10,000) AP. The holes are seen in the AP (c&d)

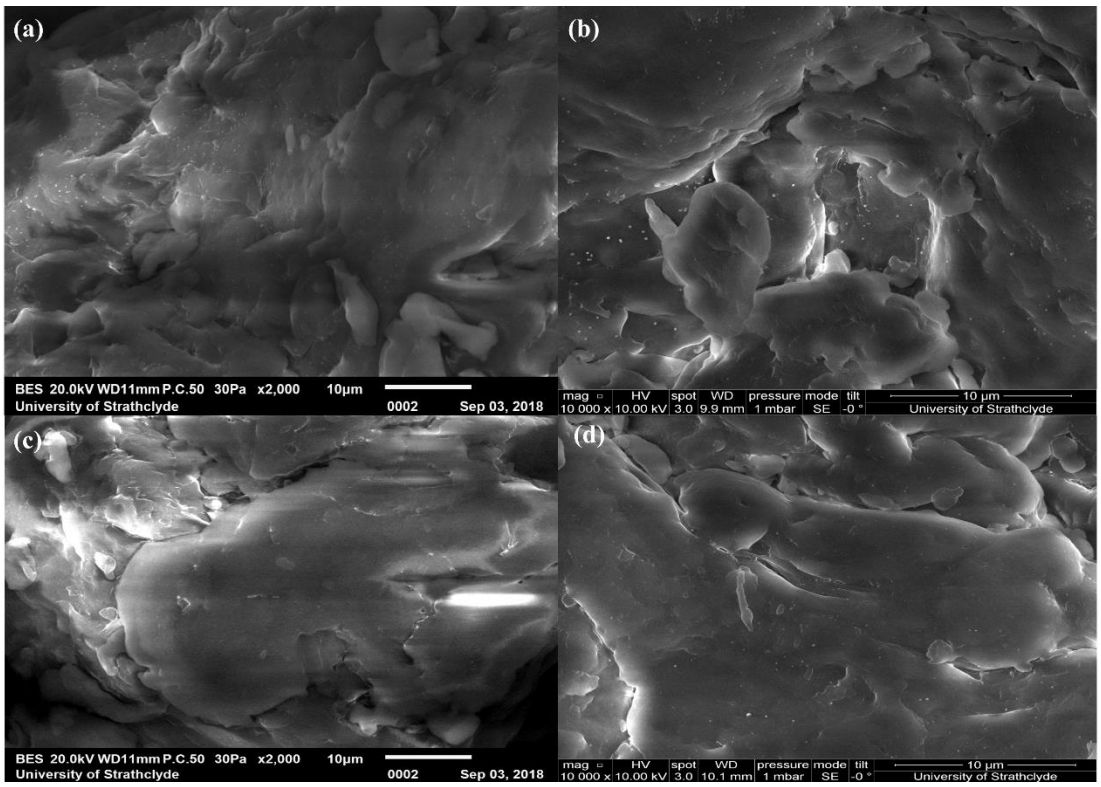

Figure 5.16 SEM images with different magnifications of hydroxypropyl methylcellulose (a: x2,000 & b: x10,000) powder (c: 2,000 & d: x10,000) AP

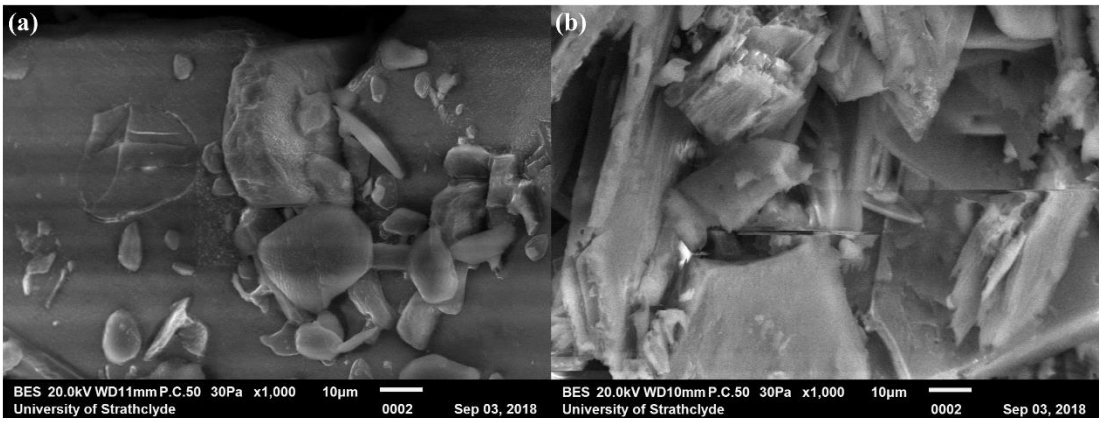

Figure 5.17 SEM images of ibuprofen (a: x1,000) powder (b: x1,000) AP

SEM images of F1-F3 of P and AP formulations are presented in Figure 5.18. It is evident that particles are clumped together in AP formulations as an effect of the PTM,

which may have resulted in formation of solid bridges and mechanical interlocking between the particles. This is more evident in Figure 5.18 (b) and (d), of F1 AP and F2 AP respectively, as they contain higher polymer content than F3.

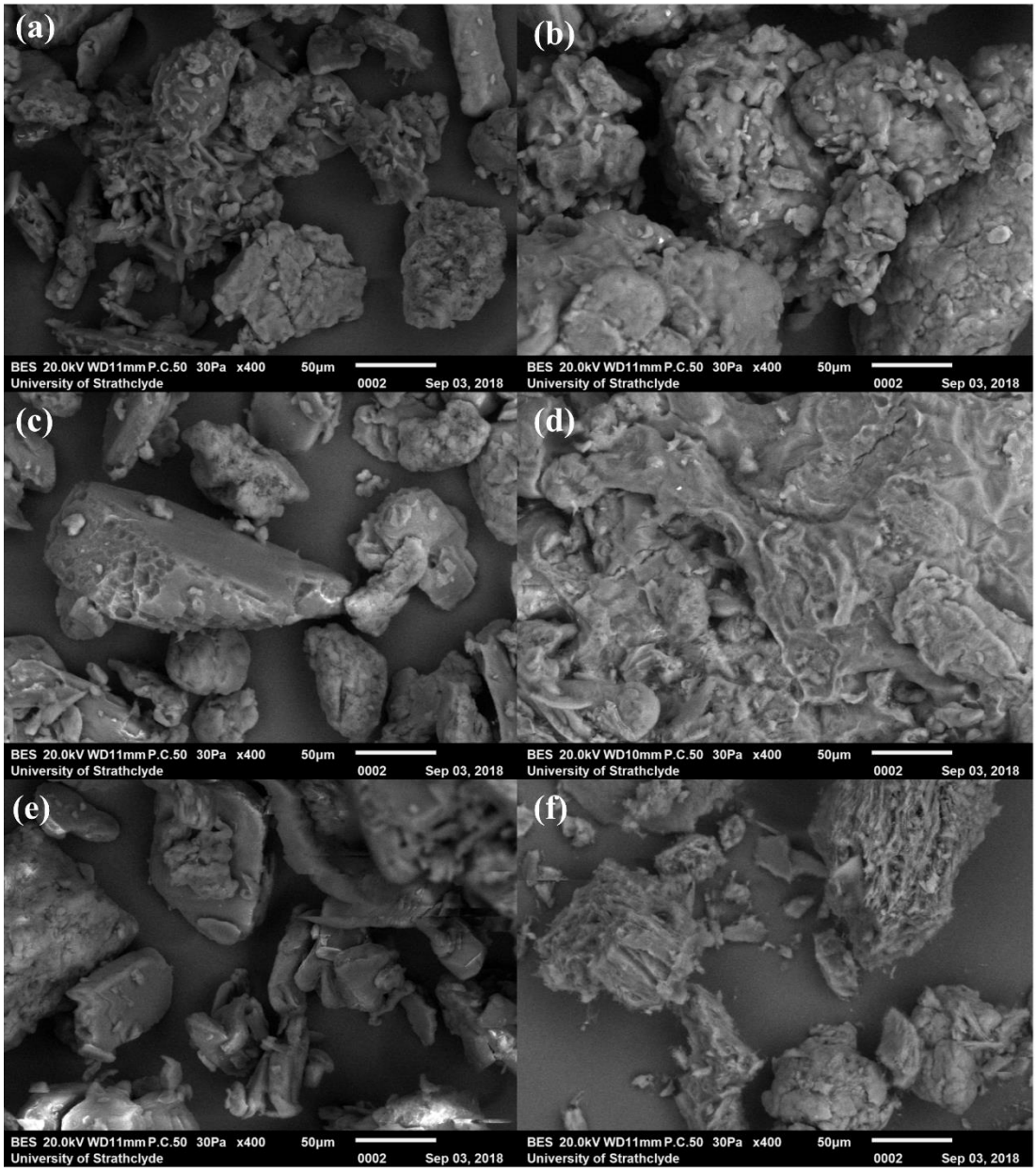

Figure 5.18 SEM images of F1-F3 P and AP. (a: x400)F1 P, (b: x400) F1 AP, (c: x400) F2 P, (d: x400) F2 AP, (e: x400) F3 P, (f: x400) F3 AP

5.4 Observations on the effect of the PTM vs high pressure (0.8 GPa) on the formulations

The results of this study show that the sustained release of the drug was mainly caused by effects exerted by petroleum ether, which was used as a pressure transmitting medium, rather than the application of pressure (0.8 GPa). The PTM has introduced some morphological changes in EC seen by SEM. Such changes were not seen in HPMC SEM images. This could be due to imaging technique i.e. the spot imaged did not give a true reflection of the whole sample and show changes if there are any. The sustained release of IBP was more apparent in the tablet dosage forms than the capsule dosage form. This is mainly due to compression forces involved in tabletting. These forces facilitated the particle mechanical interlocking initiated by the PTM. This finding was reaffirmed by the results of tablet hardness test. The hardness of AP tablet formulations was higher than the ones of powder formulations. Moreover, the release of IBP was slower in AP tablet formulations as the tablets were stronger and required higher forces to break as per the tablet hardness results.

On the other hand, capsule dosage forms of F1 showed a similar phenomenon of delayed release where the IBP release from the HP formulation was slower than the AP formulation. In F2 and F3 capsule formulations, the IBP release did not show a similar pattern as in tablet formulations. This is mainly due to the absence of compression forces.

Another finding of this study suggest that polymeric content of the formulations has greatly influenced the release of the model drug (IBP). Formulations with higher polymer content sustained the release of IBP for longer time in both dosage forms i.e.

tablets and capsules. This is mainly due to gelling and swelling effect of HPMC when in contact with dissolution media while EC is known to impede water ingress hence, slows the release.

5.5 Conclusions

The findings of this study suggest that the application of pressure did not show significant difference in the release of IBP from tablet and capsule dosage forms. Tablets prepared by direct compression exhibited a slower release pattern than capsules due to the particle interlocking mechanism facilitated by compression forces, thus they require longer time to disintegrate. The IBP release was slower in tablets and capsules treated by PTM petroleum ether potentially due to the pockets formed in EC, seen by SEM, that aided the entrapment of IBP within polymers. The preparation of formulations F1 and F2 has proved a potential to control the release of IBP from the polymeric formulations. The results of this study demonstrate that the IBP release rate was significantly affected by the (polymer:API) ratio. Formulations with higher polymer content showed a slower release than formulations with less polymer content. This effect is due to polymer swelling and the formation of gel layer upon the contact of the polymers with the dissolution media. F1 and F2 capsules formulations also exhibited a sustained release pattern but different in time scale compared to tablets and that is attributed to the absence of compaction forces. Finally, tablet hardness testing reaffirmed the mechanical strength of AP tablets compared to P tablets.

5.6 References

[1] L. Zhu, L. Lu, S. Wang, J. Wu, J. Shi, T. Yan, C. Xie, Q. Li, M. Hu, Z. Liu, Chapter 11 - Oral Absorption Basics: Pathways and Physicochemical and Biological Factors Affecting Absorption, Editor(s): Yihong Qiu, Yisheng Chen, Geoff G.Z. Zhang, Lawrence Yu, Rao V. Mantri, Developing Solid Oral Dosage Forms (Second Edition), Academic Press, 2017, 297-329.

[2] Jain KK. Drug Delivery Systems [electronic resource]. Jain KK, editor: Totowa, NJ: Humana Press; 2008.

[3] Lee PI, Li J-X. Evolution of oral controlled release dosage forms. In: Wen H, Park K, editors. Oral Controlled Release Formulation Design and Drug Delivery. John Wiley & Sons, Inc.; Hoboken, NJ: 2010. 21–31.

[4] Chapter 2 - Modification of drug release, Editor(s): Marcos Luciano Bruschi, Strategies to Modify the Drug Release from Pharmaceutical Systems, Woodhead Publishing, 2015, 15-28.

[5] Helfand WH, Cowen DL. Evolution of pharmaceutical oral dosage forms. Pharmacy in history. 1983 Jan 1;25(1):3-18.

[6] Blythe RH, inventor; GlaxoSmithKline LLC, assignee. Sympathomimetic preparation. United States patent US 2,738,303. 1956 Mar 13.

[7] Perrie Y. Pharmaceutics: drug delivery and targeting. 2nd ed. ed. Rades T, Dawsonera, Proquest Ebook C, editors. London: London: Pharmaceutical Press; 2012.

[8] Sheskey PJ, Cook WG, Cable CG. Handbook of pharmaceutical excipients. Eighth edition. ed: London: Alpha/Pharmaceutical Press; 2017.

[9] Dabbagh MA, Ford JL, Rubinstein MH, Hogan JE. Effects of polymer particle size, compaction pressure and hydrophilic polymers on drug release from matrices containing ethylcellulose. International Journal of Pharmaceutics. 1996;140(1):85-95.

[10] Quinten T, Beer TD, Vervaet C, Remon JP. Evaluation of injection moulding as a pharmaceutical technology to produce matrix tablets. European Journal of Pharmaceutics and Biopharmaceutics. 2009;71(1):145-54.

[11] Lopes CM, Manuel Sousa Lobo J, Costa P, Pinto JF. Directly compressed mini matrix tablets containing ibuprofen: preparation and evaluation of sustained release. Drug development and industrial pharmacy. 2006 Jan 1;32(1):95-106.

[12] Connelly D. A brief history of ibuprofen. The Pharmaceutical Journal, PJ July 2017 online, online | DOI: 10.1211/PJ.2017.20203273

[13] De Brabander C, Vervaet C, Remon JP. Development and evaluation of sustained release mini- matrices prepared via hot melt extrusion. Journal of Controlled Release. 2003;89(2):235-47.

[14] De Brabander C, Vervaet C, Van Bortel L, Remon JP. Bioavailability of ibuprofen from hot- melt extruded mini- matrices. International Journal of Pharmaceutics. 2004;271(1-2):77-84.

[15] Fabbiani FPA, Pulham CR. High- pressure studies of pharmaceutical compounds and energetic materials. Chemical Society reviews. 2006;35(10):932-42.

[16] Snider DA, Addicks W, Owens W. Polymorphism in generic drug product development. Advanced Drug Delivery Reviews. 2004;56(3):391-5.

[17] Graham AJ, Allan DR, Muszkiewicz A, Morrison CA, Moggach SA. The Effect of High Pressure on MOF- 5: Guest- Induced Modification of Pore Size and Content at High Pressure. Angewandte Chemie International Edition. 2011;50(47):11138-41.

[18] OriginLab C. OriginPro. b9.4.1.354 (Academic) ed. Northampton, MA 01060 USA2017

[19] Descamps M, Willart JF. Perspectives on the amorphisation/ milling relationship in pharmaceutical materials. Advanced Drug Delivery Reviews. 2016; 100:51-66.

[20] Michalchuk AAL, Hope KS, Kennedy SR, Blanco MV, Boldyreva EV, Pulham CR. Ball- free mechanochemistry: In situ real- time monitoring of pharmaceutical co-crystal formation by resonant acoustic mixing. Chemical Communications. 2018;54(32):4033-6.

[21] Friedel HD, Brown CK, Barker AR, Buhse LF, Keitel S, Kraemer J, et al. FIP Guidelines for Dissolution Testing of Solid Oral Products. Journal of Pharmaceutical Sciences. 2018;107(12):2995-3002.

[22] Reppas C, Friedel H-D, Barker AR, Buhse LF, Cecil TL, Keitel S, et al. Biorelevant in Vitro Performance Testing of Orally Administered Dosage Forms--Workshop Report. (Report). Pharmaceutical Research. 2014;31(7):1867.

[23] E. Jantratid and M. Vertzoni. Dissolution Testing to Forecast in Vivo Performance of Immediate-Release Formulations. Dressman JB, Reppas C. (eds) In Oral Drug Absorption: Prediction and Assessment, Informa Healthcare, New York, 2010 pp. 224-243.

[24] British Pharmacopoeia C. British Pharmacopoeia 2014. London: London: Stationery Office; 2013.

[25] 2016 U.S. Pharmacopoeia-National Formulary [USP 39 NF 34]. Volume 1. Rockville, Md: United States Pharmacopeial Convention, Inc; 2015. Accessed online http://www.uspnf.com/uspnf/login.

[26] Felton LA. Remington: essentials of pharmaceutics. Philadelphia: Philadelphia College of Pharmacy; London: Philadelphia: Philadelphia College of Pharmacy; London: Pharmaceutical Press; 2013.

[27] Chaibva FA, Khamanga SMM, Walker RB. Swelling, erosion and drug release characteristics of salbutamol sulfate from hydroxypropyl methylcellulose- based matrix tablets. Drug Development and Industrial Pharmacy. 2010;36(12):1497-510.

[28] 12. Li CL, Martini LG, Ford JL, Roberts M. The use of hypromellose in oral drug delivery. Oxford, UK2005. 533-46.

[29] Reza, M. S., Quadir, M. A. & Haider, S. S. 2003. Comparative evaluation of plastic, hydrophobic and hydrophilic polymers as matrices for controlled-release drug delivery. Journal of Pharmacy and Pharmaceutical Sciences, 6**,** 282-291.

[30] Ebube NK, Jones AB. Sustained release of acetaminophen from a heterogeneous mixture of two hydrophilic non- ionic cellulose ether polymers. International Journal of Pharmaceutics. 2004;272(1):19-27.

[31] Mitchell K, Ford JL, Armstrong DJ, Elliott PNC, Rostron C, Hogan JE. The influence of concentration on the release of drugs from gels and matrices containing Methocel ®. International Journal of Pharmaceutics. 1993;100(1):155-63.

[32] The influence of hydroxypropyl methylcellulose (HPMC) molecular weight, concentration and effect of food on in vivo erosion behavior of HPMC matrix tablets

[33] Ghori MU, Ginting G, Smith AM, Conway BR. Simultaneous quantification of drug release and erosion from hypromellose hydrophilic matrices. International Journal of Pharmaceutics. 2014;465(1-2):405-12.

[34] Avgerinos T, Kantiranis N, Panagopoulou A, Malamataris S, Kachrimanis K, Nikolakakis I. Mechanical properties and drug release of venlafaxine HCl solid mini

matrices prepared by hot-melt extrusion and hot or ambient compression. Drug development and industrial pharmacy. 2018 Feb 1;44(2):338-48.

[35] Markl D, Zeitler JA. A Review of Disintegration Mechanisms and Measurement Techniques. Pharmaceutical research. 2017;34(5):890-917.

Chapter Six: The Impact of High Pressure on Powder Flowability

6.1 Introduction

Particle technology is an important branch of science that deals with individual solid particles behaviour on their own and their collective behaviour when in bulk as well as when mixed with other different particles. This part of science is very important when dealing with particles for designing pharmaceutical formulations. Particles are mainly found together rather than individually, thus forming what is called "particulate solid" or bulk solid that may be surrounded by a gas, e.g. air, or a fluid which has the potential to allow them to be in contact with each other.[1] There is a constant increase in the area of particle engineering that is mainly due to the increased demand in its applications including food technologies, e.g. instant dried soups, pharmaceuticals, personal and household cleaning products *etc*.[2,3] In the development of such products, a particular attention is required in their design and manufacturing from microstructures to the end product. The microstructure design is important and its effect is visible in the use of end product, for example, the release of flavour from food or the release of API in a timely manner from modified release pharmaceuticals.

In the production of the majority of end products, chemistry, formulation engineering and process engineering are combined to provide efficient process. Formulation engineering is central to product production and improvements in this area can lead to efficiencies in cost as well as improvements in the production process. It is used to overcome many challenges through enhanced understanding of the properties and behaviours of molecules and single particles which is particularly important for the scaled production in industrial processes. An in-depth knowledge of the formation of particles helps in the design of new routes of making smaller or larger particles.

Moreover, the area of formulation or particle engineering helps in developing new measurement techniques for monitoring particle behaviours at all scales including during production stages.[4]

According to the British Standards,[5] bulk solids are classified into two categories that is based on the size of the constituent particles. They are granular materials and powders. In granular materials, particle size is > 1 mm whereas in powders it is < 1 mm. Pharmaceutical solid formulations are considered as powders and they are made into bulk solids like tablets and capsules.

Powder flowability is an important feature in every powder industry. This feature informs design engineers how the bulk material flows during processing i.e. from a silo or a hopper. The flowability parameters are important in designing processing compartments and depends mainly on factors like size, density, shape, surface area as well as the process itself. To define flowability, important indices are proposed including angle of repose, flow function and critical fill speed.[1] The angle of repose, (Figure 6.1), is known as the slope angle of free surface of bulk solid settled under gravity that could be either poured angle of repose, drained angle of repose or dynamic angle of repose depending on the way that the free surface is created.

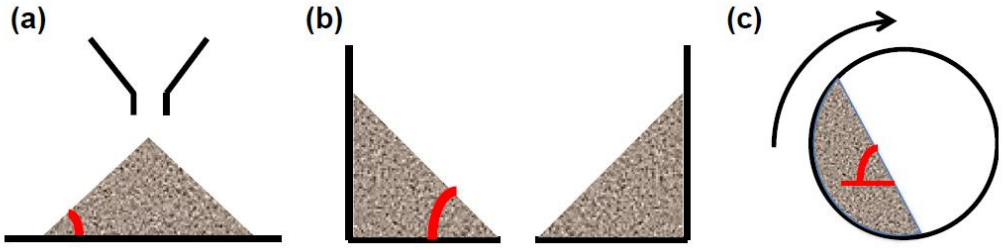

Figure 6.1 (a) poured angle of repose, (b) drained angle of repose, (c) dynamic angle of repose[1]

The poured angle of repose is defined as the slope of an angle of a heap of the bulk material poured from a specific height; this helps in storage design. In contrast, the drained angle of repose is identified by measuring the slope of the free surface once the bulk surface is discharged from a silo which helps in the design of hoppers, such as the angles, so they promote mass flow. Finally, the dynamic angle of repose is defined as the maximum angle of a stable free surface of the bulk material and helps in designing rotating drums and kilns.[6]

In the pharmaceutical industry, formulations are prepared by mixing powders of active ingredients with other excipients and processed through different steps i.e. granulation, drying, milling and compaction until the final product is produced.[7,8] These processes should be clearly understood and closely monitored as their failure impacts the quality of the end product.[9] Pharmaceutical industry studies flow properties of materials rigorously before starting their processing.

The Jenike flow index (ff_c) is used as a marker to determine the flowability of solid materials as shown in Table 6.1, where a higher value indicates better flowability. Classically, the shear cell test is used to obtain the flowability.[10]

Table 6.1 The classification of powder flowability by flow index[10]

ff_c Value	Flowability
$ff_c < 1$	Hardened (not flowing)
$1 \leq ff_c < 2$	Very cohesive
$2 \leq ff_c < 4$	Cohesive
$4 \leq ff_c < 10$	Easy flowing
$ff_c > 10$	Free flowing

The shear test is performed by applying shear stress to a powder sample until the powder reaches a failure point and starts to flow. The stress is applied by the shear head to induce vertical and rotational stresses. This is done as the head moves down into the powder until the required normal stress is established. After that, a slow rotation of the head begins to induce shear stress. As the sample resists the rotation of the shear head, the stress increases until the powder bed fails or shears. The shear test can be done using the FT4 powder rheometer and this rheometer has been employed in this study (Freeman Technology Inc., Worcestershire, UK). One of the main advantages of using this device that it has the test protocols built in and cannot be altered by the user providing a robust and reproducible test of materials. The rheometer also generates a considerable amount of data from the mathematical equations embedded within its software. They are produced within the data analysis package and the user can select which parameters to choose (Table 6.2).

Table 6.2 Powder flow parameters obtained from FT4 powder rheometer

Parameter	Symbol	Unit
Cohesion	C	Pa
Unconfined Yield Strength	σ_c (UYS)	Pa
Major Principal Stress	σ_1 (MPS)	Pa
Flow Function	ff_c	-
Angle of Internal Friction	δ (AIF)	degree
Effective Angle of Internal Friction	δ_e (AIF)(E)	degree
Angle of Internal Friction at Steady State	δ_{ss} (AIF) (SS)	degree

The aim of this chapter is to explore the effect of high pressure on the flowability characteristics of ethylcellulose (EC) and hydroxypropyl methylcellulose (HPMC) which are commonly used pharmaceutical polymers as well as the model active pharmaceutical ingredient (API) ibuprofen (IBP). Additionally, mixtures of these components in different API:polymer ratios (used for drug release studies in chapter

five) are also tested. The application of high pressure required the use of a pressure-transmitting medium (PTM) to allow for hydrostatic compression therefore control experiments of these polymers in the PTM were also investigated.

6.2 Materials and Methods

6.2.1 Materials

Ibuprofen powder (IBP), purity ≥98% GC was purchased from Sigma-Aldrich UK. Hydroxypropyl methylcellulose (HPMC) E50 (Methocel™) with apparent viscosity, 2% in water, of 40-60 mPa.s and ethyl cellulose (EC) (ethoxyl content: 48–49.5% (w/w); viscosity: 9–11 mPa.s were kindly donated by Colorcon®, Kent, UK. Petroleum ether 35/60 ACS grade was purchased from Alfa Aesar, UK.

6.2.2 Methods

6.2.2.1 Sample preparation

Each sample was studied separately under three different conditions i.e. powder, powder in PTM at ambient pressure for 24 hours (AP) and powder in PTM at high pressure, using the large volume press, (0.8 GPa) for 24 hours. Petroleum ether 35/60 was used as the PTM in this experiment.

IBP, EC and HPMC were used as received from the suppliers in the powder form preparations. In the ambient pressure (AP) preparations, 500 mg of each sample was left in 3 mL petroleum ether at room temperature (23°C) for 24 hours. The high pressure (HP) form of samples was subjected to high pressure of 0.8 GPa using petroleum ether as the pressure transmitting medium in the large volume press for 24

hours and at room temperature (23°C). The AP and HP formulations were dried to ensure the removal of petroleum ether by using vacuum desiccator until samples were completely dried. This was monitored by weighing the samples before and after treatment.

6.2.2.2 Formulation preparation

Formulations F1, F2 and F3 used in Chapter 5 were also studied to evaluate their flowability under 2 different conditions i.e. formulation blend in powder form and formulations in powder form left in PTM at ambient pressure (AP) for 24 hours.

These formulations contained IBP:EC:HPMC (30:35:35%), (60:20:20%) and (80:10:10%) respectively. Formulations 1-3 were weighed and mixed in glass vials using RAM technology at 40 G for 30 minutes as per the RAM mixing guidelines, tested and validated at the University of Edinburgh, and standard configurations (Table 6.3). RAM technology uses low frequency and high intensity acoustic energy to induce mixing even in small scale blends.[11,12]

Table 6.3 RAM mixing guidelines tested and validated at the University of Edinburgh - Standard configuration

Procedure	Recommended vessel	Recommended parameters
Mixing unreactive powders (similar particle size)	Glass or plastic. As little head space as possible	10-30 G 5-15 minutes
Mixing unreactive powders (disparate particle sizes)	Glass or plastic. As little head space as possible	20-40 G 10-30 minutes

6.2.2.3 Shear cell

To determine the flow function coefficient and cohesion of the examined samples, a Freeman powder rheometer (FT4) system (Freeman Technology, Worcestershire, UK) with 1 ml shear test module was used. As detailed in Chapter 2, the samples being tested were loaded into the 1 ml shear cell module.

The flow properties of all samples and formulation blends were characterised using a 1 mL shear cell module on the FT4 Powder Rheometer (Freeman Technology Inc., Worcestershire, UK) (Figure 6.2 (a)). This device was used because it allows the measurement of shear properties using a limited quantity of materials. This is very useful in our case as we can subject limited quantity of the sample to high pressure (typically 1-3 grams). Another advantage of using the 1 mL shear cell is that it can be used in very expensive pharmaceutical materials in the early stage of their development.

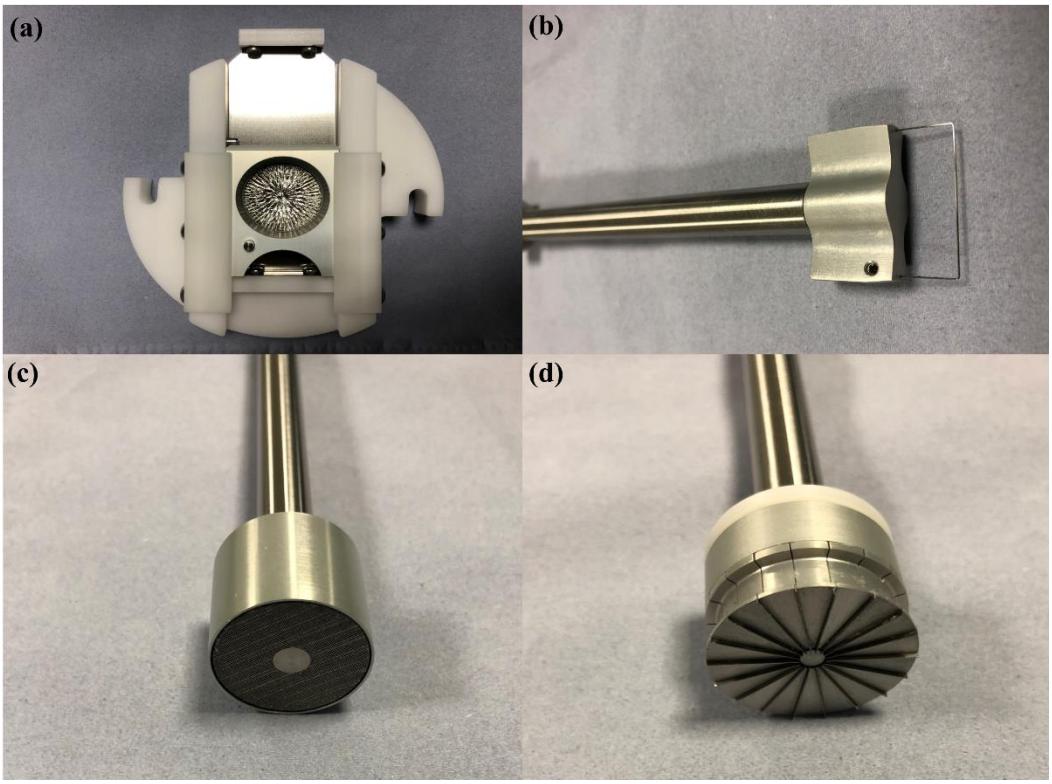

Figure 6.2 (a) 1ml shear cell module assembled, (b) conditioning wire used to condition the sample before the test, (c) 24 mm vented piston used for pre-consolidation, (d) 24 mm shear cell used to shear the sample

As normal practice with rotational shear cells, four steps were followed after loading the sample in the 1 ml shear cell module. The sample was initially conditioned using a conditioning wire shown in Figure 6.2 (b). The wire is moved upwards and downwards the powder bed and rotated with gentle shaking. This is done to ensure uniformity of packing of the sample. This step is important before any test as it helps in establishing a uniform stress in the sample bed and eradicates air pockets and possible agglomerations which could occur due to handling or during previous storage or when the powder is placed into the vessel. It helps in constructing a homogenously packed powder bed. Samples were then pre-consolidated using a 24 mm vented piston

(Figure 6.2 (c)) at a normal stress of 9 kPa. After that, the excess of the sample was removed by the splitting shim and a flat powder is left to be tested. Finally, the vented piston was replaced with a 24 mm shear cell (Figure 6.2 (d)) by which shear tests were carried at normal stresses of 3, 4, 5, 6, and 7 kPa. The shear stress was recorded at each normal stress and yield loci were derived from shear stresses. In each test, one pre-shear point and five yield points were generated.[13] The shear stress was plotted against the normal stress by the embedded software using Mohr's circles to generate linear yield locus. Cohesion τ_1 is found at the intercept of yield locus on the shear stress axis and it is defined as the shear stress required to deform the powder when no normal stress is applied. The slope of the linear yield locus line is tan φ, where φ is the angle of internal friction (Figure 6.3). The angle of internal friction can be used to measure the ease of particle movement past each other.[14] Other parameters including unconfined yield strength (UYS) (σ_c) and major principal stress (MPS) (σ_1) are derived by plotting Mohr's circles. The first circle passes through the origin such that the yield locus is the tangent to this semi-circle. The intercept of the circle with the normal stress axis generates the UYS. The principal stress (σ_1) is derived from plotting a second Mohr's circle such that the yield locus is a tangent to the circle but additionally the circle passes through the preshear point; the intercept with the normal stress axis is denoted as the MPS. The flow function coefficient (ff_c) is the ratio between MPS and UYS and calculated as:[10]

$$(ff_c) = \sigma_1 / \sigma_c$$

The bulk cohesion forces of each sample were calculated by extrapolating the yield loci to intercept the y-axis (shear stress) using the following equation:

$$\tau = C + \sigma \tan \eta$$

where τ is the shear stress, σ is the normal stress, η is the angle of friction and C is the cohesion force (intercept of shear stress).[15] The yield locus, Mohr circles and other parameters related to flow properties were derived using the data analysis software associated with the FT4 Powder Rheometer.

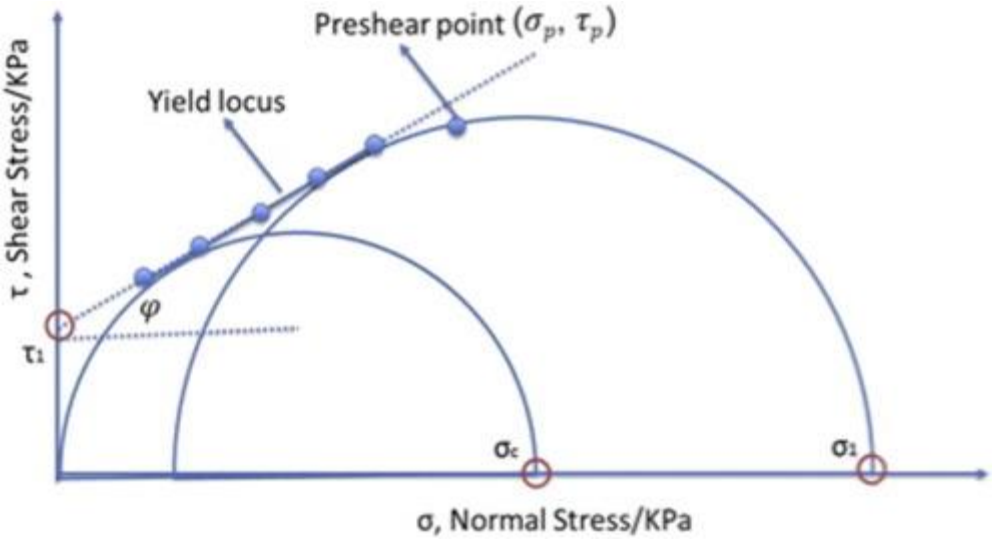

Figure 6.3 Schematic of yield locus and pre-shear point. Mohr circle analysis was used to derive cohesion (τ), unconfined yield strength (σ_c) and major principal stress (σ_1) (Figure reproduced from reference 15 Wang et al.)

6.3 Results and Discussion

Before the introduction of automated and computer controlled shear cell, like the FT4 powder rheometer, the measurements were complicated and to some extent unreliable as the variability of the results were considerable. In FT4 powder rheometer, the normal force applied to the sample is motorised and recorded and this is very important in understanding how the yield point is developed. In addition to that, it ensures the

validity of test points and guarantees that consolidation has been reached during the test.

Nonetheless, to obtain reliable results, it is recommended to obtain the average of at least three tests for each sample. This is justified by the theory that some materials may degrade, especially friable ones, when being under shear stress. Another advantage of the FT4 rheometer is that it has a built-in balance that weighs the sample before and after splitting and this avoids spillage and user interference with the sample. This is a very important aspect especially in the case where sample quantity is of concern.

6.3.1 Ethylcellulose

Ethyl cellulose is a commonly used polymer in pharmaceutical formulations. The flow function of EC in powder form was 7.58 (± 1.87) which is considered as an easy flowing powder (Figure 6.4). The flow function has increased to 10.75 (± 3.39) in EC in the PTM at ambient pressure moving the flowability to a higher stage and considering it as a freely flowing powder. Additionally, the high pressure sample has an increased value of flow function of 12.28 (± 1.52) rendering it as a freely flowing powder as well. In contrast, the cohesion of EC powder was found to be 0.67 kPa (± 0.26) and declined to 0.3 (± 0.15) and 0.38 (± 0.05) kPa in the ambient pressure and high pressure samples. The angle of internal friction of EC was 24.69° (± 2.07) in the powder sample, and reduced slightly to 24.54° (± 0.68) and 22.15° (±1.75) in the ambient pressure and high pressure samples respectively, which indicates that particles move next to each other freely.

These changes are mainly attributed to the PTM, petroleum ether, which has changed the characteristics responsible for the flow of EC. SEM images of EC in P and AP

conditions (Figure 6.5) show some morphological changes in the AP form. These changes are the formation of holes in EC These holes could be as a result of possible degradation of EC by the PTM. These hole may have created void spaces in the particles and weakened their structure making them lighter and free flowing.

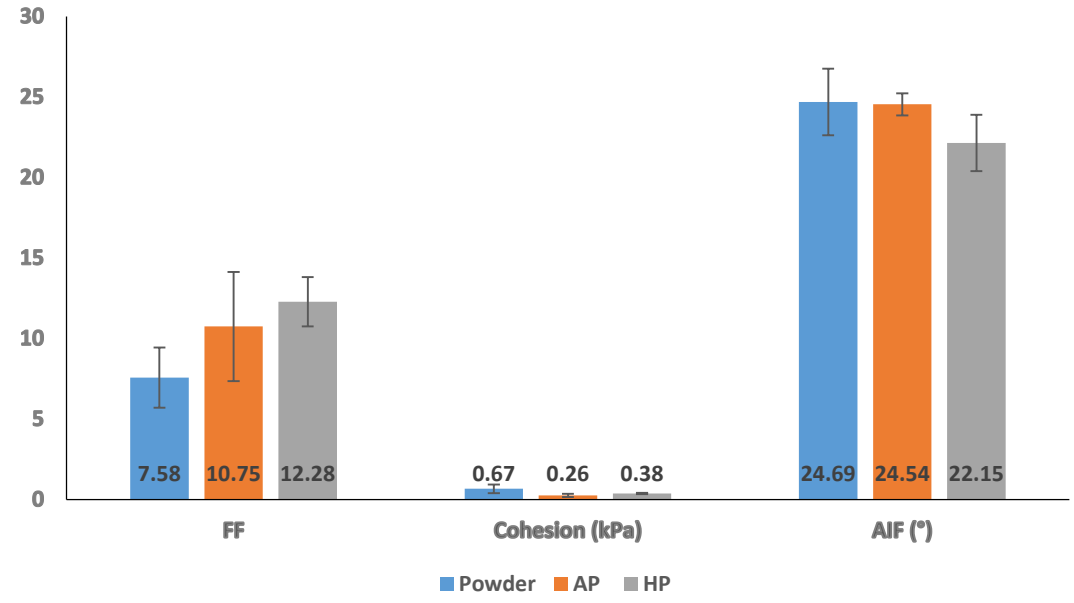

Figure 6.4 Ethylcellulose average flow parameters (ff: flow function, cohesion, AIF: angle of internal friction) under different conditions powder, ambient pressure and high pressure (n=3). The flow function has increased by the effect of PTM and high pressure treatment

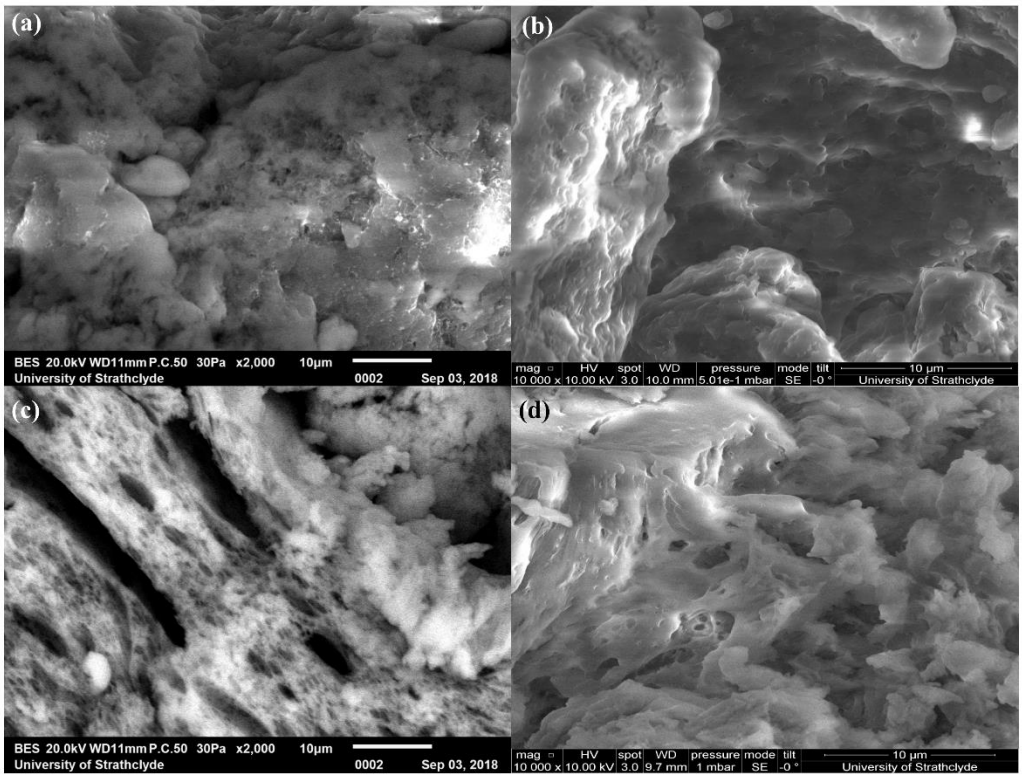

Figure 6.5 SEM images of ethylcellulose in powder from (a) x2,000 (b) x10,000. Ambient pressure form mixed with PTM at ambient pressure for 24 hours (c) x2,000 (d) x10,000

6.3.2 Hydroxypropyl methylcellulose

In HPMC, (Figure 6.6) the average flow function in the powder sample was 9.54 (± 1.47) which is considered as an easy flowing powder. This has increased to 12.63 (± 1.36) in the ambient pressure sample and moved it to a higher category of flowability making HPMC as a free flowing powder. In the high pressure sample, flow function was found to be 13.69 (± 1.54), which is slightly higher than the AP sample and in the similar category of flowability. The average cohesion value has decreased from 0.5 kPa (± 0.09) in the powder sample to 0.37 kPa (± 0.15) in the ambient pressure sample and subsequently to 0.34 kPa (± 0.04) in the high pressure sample. This decrease in cohesion explains the increased flow function of HPMC. A slight decrease was also

noticed in the angle of internal friction from 23.73° (± 0.39) in the powder sample to 22.36° (± 0.68) in the ambient pressure sample. Moreover, in the pressure sample, the angle of internal friction has increased slightly to 22.98° (± 2.57) when compared to the ambient pressure sample. SEM images of HPMC P and AP forms did not show any morphological changes in the sample (Figure 6.7).

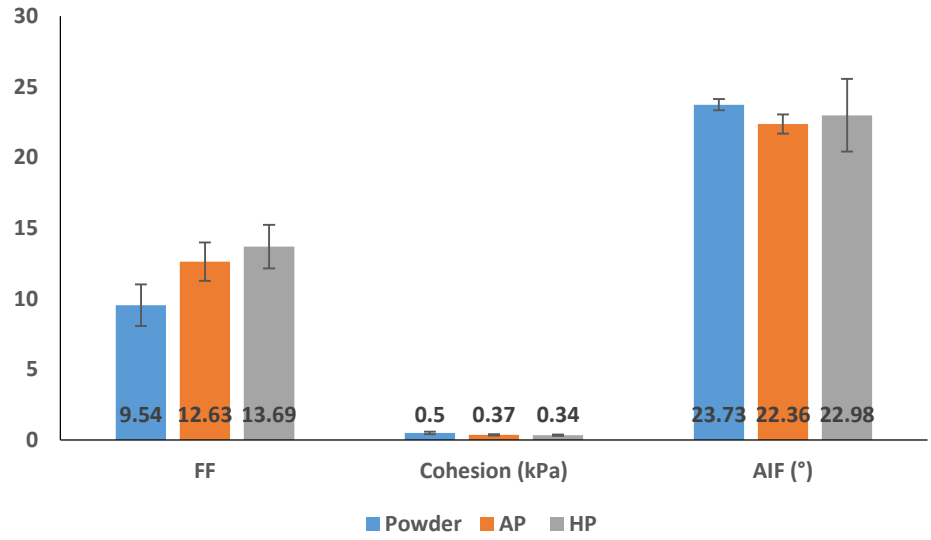

Figure 6.6 Hydroxypropyl methylcellulose average flow parameters(ff: flow function, cohesion, AIF: angle of internal friction) under different conditions powder, ambient pressure and high pressure (n=3). The flow function has increased by the effect of PTM and high pressure treatment

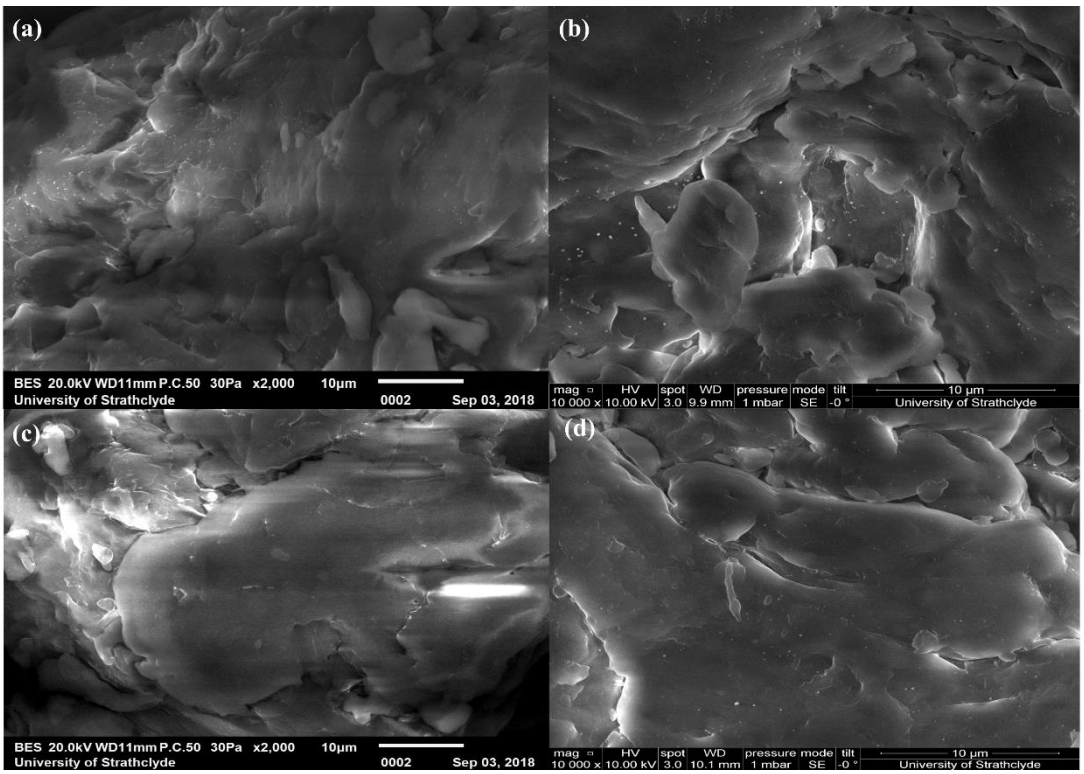

Figure 6.7 SEM images of hydroxypropyl methylcellulose in powder from (a) x2,000 (b) x10,000. Ambient pressure form (c) x2,000 (d) x10,000

Both polymers studied in this experiment (EC & HPMC) exhibited an increase in flow function in different treatments. They both moved from easy-flowing category ($4 \leq ffc < 10$) to free-flowing category ($ff_c > 10$). The flow of EC function has increased from 7.58 to 10.75 to 12.28 in P, AP and HP samples respectively. A similar increase in the flow function pattern of HPMC was seen in different treatments but with less error values compared to EC. This finding reaffirms the difference in EC particles response to shear stress, especially the AP and HP samples. Although HPMC SEM images not showing any sample degradation of deformation, the change in flow function is evident and almost similar to EC. This is attributed to limitations of microscopy in general and SEM in particular, as moving imaging location may show differences.

6.3.3 Ibuprofen

The flow parameters of ibuprofen were also tested in three different conditions namely powder (P), powder in PTM at ambient pressure (AP) and powder in PTM at high pressure (0.8 GPa) for 24 hours (HP). These parameters are depicted in Figure 6.8. Ibuprofen is classified as an easy flowing powder as its flow function is between 4 and 10. Neither treatment had an impact on the ibuprofen sample as the flow function was 6.02 (± 0.63) in the powder sample and slightly reduced to 5.79 (± 0.97) in the ambient pressure sample. The high pressure sample's flow function was 6.08 (± 0.38). It is clearly evident that the AP and HP treatments did not change the flow function of ibuprofen. This was also the case in the cohesion of ibuprofen, which changed very slightly between different treatments. On the other hand, the angle of internal friction has slightly increased from 17.74° (± 0.85) in the powder form of ibuprofen to 19.16° (± 0.69) in the ambient pressure sample. In the high pressure sample, it has decreased to 16.03° (± 0.89) while the cohesion values remained consistent in the three different forms. The angle of internal friction is no longer a measure of flow function as there was no correlation between them as found by Yang et al.[16]

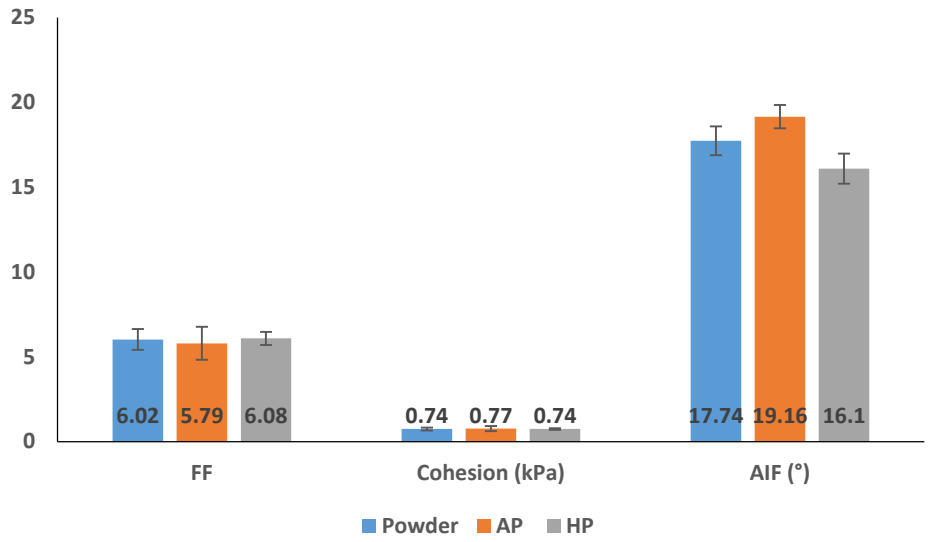

Figure 6.8 Ibuprofen average flow parameters (ff: flow function, cohesion, AIF: angle of internal friction) under different conditions powder, ambient pressure and high pressure (n=3). The flow function and cohesion have not changed by the effect of PTM or high pressure treatment

6.3.4 Formulation blends

As the differences were mainly confined to the addition of PTM or not, only these two conditions were tested. The formulations F1, F2 and F3 were tested in triplicates under two different conditions namely powder formulations (P) and powder formulations in PTM at ambient pressure (AP). The correlation between the flow function coefficient and the cohesion at the same consolidation stress is shown in Figure 6.9. The correlation (R^2 is 0.9607) is found to be inversed i.e. less cohesion leads to a higher flow function. This is in line with a previous study by Wang et al.[15] that looked at the classification of flow properties of a mixture during formulation development consisting of a model API and three excipients. It also found that cohesion was in a linear relationship with UYS, which is also the same in our experiment.

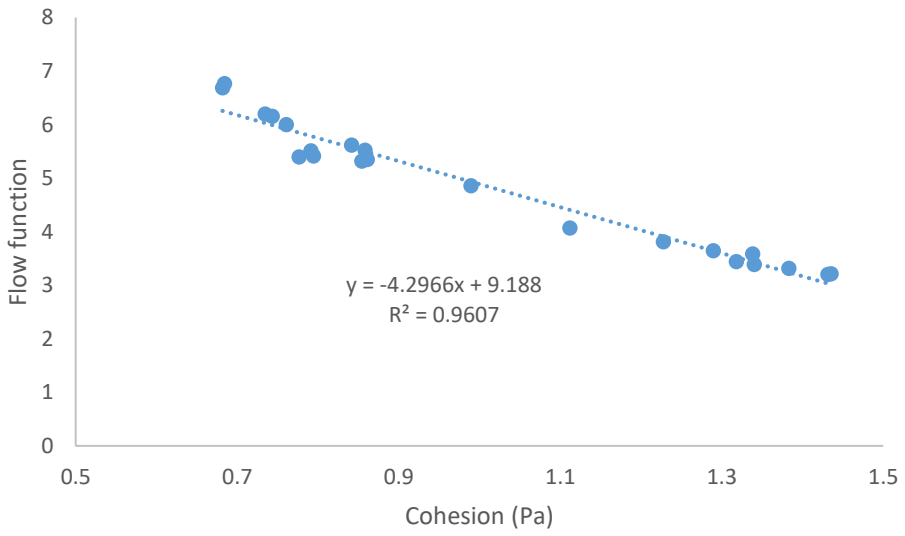

Figure 6.9 Correlation between flow function and cohesion in F1-F3(powder and AP) (n=3)

Table 6.4 Comparison of flow parameters between powder and ambient pressure formulations of F1-F3 (n=3). The cohesion forces increased in the formulation blends when subjected to PTM (AP) compared with powder blends (P)

Sample		Cohesion (kPa)	UYS (kPa)	FF	AIF (°)
F1	Powder	0.80 (± 0.10)	2.578	5.87 (± 0.79)	26.110
	AP	1.00 (± 0.22)	3.077	4.70 (± 0.81)	26.695
F2	Powder	0.78 (± 0.05)	2.247	5.93 (± 0.28)	20.332
	AP	1.33 (± 0.01)	4.029	3.47 (± 0.10)	23.275
F3	Powder	0.76 (± 0.09)	2.102	6.08 (± 0.68)	18.350
	AP	1.31 (± 0.18)	4.221	3.45 (± 0.46)	25.229

The SEM images of the AP formulations show that particles are seen in closer proximity and cluster together than the P formulations (Figure 6.10). Although flowability is measured to help in designing hoppers and orifices of feeding systems, the increased cohesion of AP formulations can justify the delay in the release of API from those formulations at ambient pressure when compared to the powder formulations which is detailed in chapter 5. This effect was more pronounced in F1 and F2 than F3 and this is because of higher polymer content in the former ones. The

phenomenon of particle clustering observed in the AP formulation could be due to the solid bridge formation between particles and mechanical interlocking.

The findings of this study are in line with the findings of Leung et al.[16] in which they analysed 1130 pharmaceutical powder flow measurement data and found a near perfect correlation between the flow function and cohesion and no correlation between flow function and angles of internal friction.

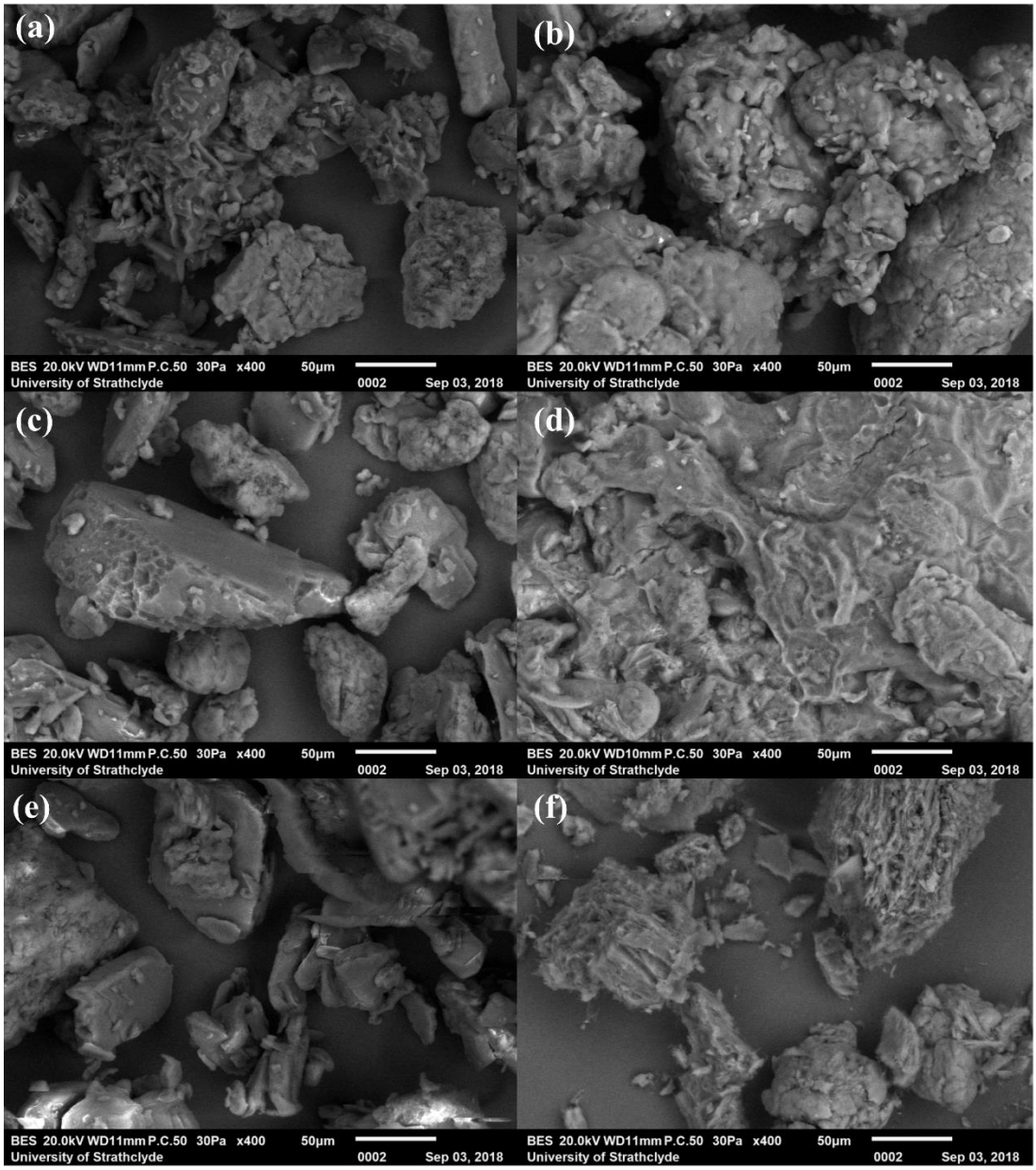

Figure 6.10 SEM images of formulation blends (F1-F3) in powder and AP forms. (a) F1 powder, (b) F1 in PTM at ambient pressure, (c) F2 powder, (d) F2 powder in PTM at ambient pressure, (e) F3 powder and (f) F3 powder in PTM at ambient pressure. It is evident that AP formulations (b, d & f) are sticking together.

It is clearly seen that the PTM has changed the flow function of EC and HPMC but not of IBP. This was clearly observed in the EC sample as it changed the morphology by forming holes or pockets in the sample. HPMC flow parameters have also changed but no changes were observed in the morphology by SEM.

The formulation blends treated by petroleum ether for 24 hours have shown an increase in cohesion values when compared to the powder blends. This effect is attributed to PTM as it may have possibly caused the particles to roughen and stick together. Another explanation for this phenomenon is particle interlocking. Particle interlocking is more potential when particle surface is rough than when it is smooth as these particles can form interparticulate attraction bonds when they are in close proximity to each other. These bonds can be intermolecular bonds, bridges formed by particles and mechanical interlocking.[17] This increase in cohesion forces could be considered as an advantage especially in large scale processes like tabletting, as free flowing powder blends which have low cohesion tend to segregate if they differ in particle size.[9]

It is evident that in formulation blends the flowability characteristics are changing in the opposite direction when compared to the individual polymer components of the formulations. The flow function has decreased in all formulations when treated with the PTM and cohesion has increased (Table 6.4), which is contrary to the findings in individual polymers. This could be due to change in particle properties caused by the RAM as the individual polymers were not subjected to the RAM but rather used as received. As the RAM mixes the formulation components, there will be shear and strain generated as particles collide. This could lead to attrition and de-agglomeration into smaller particles and change in the attractive forces between them.[18] Another important factor to consider in this case is the difference in particle size and shape distribution, particle roughness and inter-particle forces in the blends.

The cohesion has considerably increased in F2 and F3 (AP) formulations in comparison to the (P) formulations. The change in cohesion was marginal between F1 P and F2 AP blends. This difference could be attributed to the API:polymer ratio as

F2 and F3 have higher API ratio than F1 and this may reduce polymers degradation by the PTM. As seen in the SEM images (Figure 6.10), the AP formulations cluster together and become sticky. This will increase their roughness, hence aid the mechanical interlocking.

6.4 Conclusions

The results showed that the pressure transmitting media affected the flow function coefficient and cohesion of the polymers EC and HPMC when tested on their own. The medium caused an increase in their flow function and a reduced cohesion. Additionally, high pressure treatment has also further increased the flow function values. These values did not change in ibuprofen under all conditions. In F1-F3 formulation blends, the flow function has decreased and cohesion increased when treated by the PTM. This is opposite to the pure compounds by themselves which can be explained by the increased mechanical interlocking or change in particle characteristics caused by the RAM. Overall, the shear cell methodology is a convenient way in measuring flowability of individual components as well as formulation blends especially when sample quantity is of a concern. This method can be successfully used for screening formulations in early stages to avoid cohesive and problematic formulations. The findings of these tests also help in designing hoppers and orifices which blends are dispensed from.

6.5 References

[1] Seville JPK. Particle technology and engineering: an engineer's guide to particles and powders: fundamentals and computational approaches / [internet resource]. Wu C-Y, Elsevier, editors: Kidlington, Oxford, UK: Butterworth-Heinemann is an imprint of Elsevier; 2016.

[2] Fan LT, Chen Y-M, Lai FS. Recent developments in solids mixing. Powder Technology. 1990;61(3):255-87.

[3] Poux M, Fayolle P, Bertrand J, Bridoux D, Bousquet J. Powder mixing: Some practical rules applied to agitated systems. Powder Technology. 1991;68(3):213-34.

[4] Wesselingh JA. Structuring of products and education of product engineers. Powder Technology. 2001;119(1):2-8.

[5] British Standard BS2955, 1993. Glossary of Terms Related to Particle Technology. British Standards I. British Standards Online

[6] Prescott, J.K., Barnum, R.A. On powder flowability. Pharmaceutical Technology. 2000; 24 (10), 60-84.

[7] Pingali KC, Mendez R. Physicochemical behavior of pharmaceutical particles and distribution of additives in tablets due to process shear and lubricant composition. Powder Technology. 2014; 268:1-8.

[8] Mullarney MP, Beach LE, Dave RN, Langdon BA, Polizzi M, Blackwood DO. Applying dry powder coatings to pharmaceutical powders using a comil for improving powder flow and bulk density. Powder Technology. 2011;212(3):397.

[9] Muzzio FJ, Shinbrot T, Glasser BJ. Powder technology in the pharmaceutical industry: the need to catch up fast. Powder Technology. 2002;124(1):1-7.

[10] Schulze D. Powders and bulk solids [internet resource]: behavior, characterization, storage and flow. Springerlink, editor. Berlin; New York: Berlin; New York: Springer; 2007.

[11] Descamps M, Willart JF. Perspectives on the amorphisation/ milling relationship in pharmaceutical materials. Advanced Drug Delivery Reviews. 2016; 100:51-66.

[12] Michalchuk AAL, Hope KS, Kennedy SR, Blanco MV, Boldyreva EV, Pulham CR. Ball- free mechanochemistry: In situ real- time monitoring of pharmaceutical co-crystal formation by resonant acoustic mixing. Chemical Communications. 2018;54(32):4033-6.

[13] Carson JW, Wilms H. Development of an international standard for shear testing. Powder Technology. 2006;167(1):1-9.

[14] Falticeanu LC, Chang ITH, Falticeanu CT, Ciortan S. New methods for assessing the frictional properties in a mass of consolidated powders. Tribology in Industry. 2005;27(1-2):17-21.

[15] Wang Y, Snee RD, Meng W, Muzzio FJ. Predicting flow behaviour of pharmaceutical blends using shear cell methodology: A quality by design approach. Powder Technology. 2016; 294:22-9.

[16] Leung LY, Mao C, Srivastava I, Du P, Yang C-Y. Flow Function of Pharmaceutical Powders Is Predominantly Governed by Cohesion, Not by Friction Coefficients. Journal of Pharmaceutical Sciences. 2017;106(7):1865-73.

[17] Markl D, Zeitler JA. A Review of Disintegration Mechanisms and Measurement Techniques. Pharmaceutical research. 2017;34(5):890-917.

[18] Osorio JG, Sowrirajan K, Muzzio FJ. Effect of resonant acoustic mixing on pharmaceutical powder blends and tablets. Advanced Powder Technology. 2016;27(4):1141-8.

Chapter Seven: Concluding Remarks and Future Directions

7.1 General conclusions

The high pressure research area is gaining popularity among scientific disciplines and that is due to its effect on materials. This study set out to determine the effect of application of high pressure on commonly used polymers in biomedical and pharmaceutical applications using Raman spectroscopy. These polymers were poly lactic acid (PLA), poly glycolic acid (PGA), ethylcellulose (EC) and hydroxypropyl methylcellulose (HPMC). Additionally, ibuprofen was also investigated as a model drug with a view to incorporate it into a pharmaceutical dosage form.

Raman spectroscopy is an important technique in studying materials but is sometimes hindered by the phenomenon of fluorescence, which may be caused by impurities, or sample degradation by laser light. Chapter 3 has explored adopting surface enhanced Raman spectroscopy technique to enhance *in-situ* Raman signalling from fluorescent polymers and weakly scattering amino acids. Silver nanoparticles were suspended in the pressure transmitting medium (PTM) and Raman spectra were acquired at *ca* 1 GPa. This was achieved successfully without the need of chemical binding between the substrate and the analyte.

The effect of high pressure on simple polymers like polyesters (PLA and PGA) and complex polymers (EC and HPMC) was explored by Raman spectroscopy. The evidence in Chapter 4 suggests that PLA undergoes a possible phase transition at 2.2 GPa. Both PLA and PGA went into a less ordered form at pressure points between 4 and 5 GPa. On the other hand, EC and HPMC exhibited a similar behaviour but at 2.70 and 2.92 GPa respectively.

EC and HPMC were used as formulation constituents using ibuprofen as a model drug (Chapter 5). The release pattern of ibuprofen from these formulations was mainly affected by the incorporation of PTM rather that the application of pressure. SEM images shown signs of deformation in EC by the PTM. Additionally, the release was affected by the polymer:API ratio.

The effect of pressure and PTM on the flowability of individual formulation components and formulation blends was also investigated (Chapter 6). The flow function coefficient of individual polymeric components has changed from easy flowing to free flowing. This change was observed by the addition of the PTM and further by the application of pressure (0.8 GPa). Neither the PTM nor the pressure has an effect on ibuprofen. In contrary, the flow function coefficient has decreased in the different formulation blends by adding the PTM. This effect was attributed potentially to solid bridges and particle mechanical interlocking between different components of the formulations induced by the PTM.

7.2 Limitations

Work presented in this thesis was challenged to some extent with limitations. These limitations include the time needed to successfully load samples in DAC. Attaining equal and gradual increments of pressure using DACs was also another challenge as simple turns of screws may increase the pressure to higher values. In contrary, trying to reduce the pressure may lead to depressurising the cell. In Chapter 3, it was difficult to reach exactly similar pressures when comparing the same sample with and without the addition of silver nanoparticles.

Further experiments could have been done for the formulations in Chapter 5, especially the high pressure one but the time required for a single formulation was 24 hours subjected that pressure was maintained as required. Such tests include tablet hardness test for HP formulations and uniformity of weight and content for tablets and capsules.

The powder flowability measurement of polymers exhibited some challenges as they may exhibit slip-stick behaviour during the shear stress test and this leads to invalidating the results.

7.3 Future directions

The application of SERS has been successful in improving *in-situ* Raman signalling but the reproducibility has been an issue. Other ways of adopting this technique can be tested in future to compare the level of enhancement. For example, the analyte can be mixed with the substrate before being loaded into a diamond anvil cell. This may improve the positioning of the substrate in relation to the analytes. SEM imaging of different batches of the nanoparticles may also give an insight about level of enhancement as the roughness of the surface of the substrate plays a role in the level of enhancement. Further investigations should be performed on single crystals of fluorescent polymers to exclude the effect of ball milling and grinding on the samples.

The high pressure experiments performed in this study has shown that the application of pressure has led to changes in Raman spectra of the studied samples at different pressure points. These changes are suggestive of phase transitions. It is worth testing a wider range of different classes of polymers and observing the changes within similar classes and between different classes.

The release pattern of ibuprofen from polymeric formulations was mainly affected by the incorporation of the PTM. This does not negate the effect of pressure on such systems. The polymeric platform can be prepared by hot melt extrusion as pellets. The model drug can then be dissolved in a suitable PTM that does not interact with formulation components and then forced into the pellets by use of pressure. This approach can be tested in thermally unstable drugs like peptides and proteins. Other polymers that have some degree of porosity are also good candidates in such experiments.

As discussed, the change in flowability of individual components was opposite to the formulation blends of similar components. One possible justification is that the formulation blends may have been affected by the mixing technique used. In future, the individual polymeric components should also be subjected to the RAM used in the blends. Moreover, the samples used should be subjected to more screening tests before and after the use of RAM. These tests include morphology and particle size.